The Thesis Committee for Clint Robert Woods
Certifies that this is the approved version of the following thesis:

Experimental Investigation of the Delamination Behavior of Curved Post-Tensioned Concrete Structures without Through-Thickness Reinforcement

APPROVED BY
SUPERVISING COMMITTEE:

Trevor Hrynyk, Supervisor

Oguzhan Bayrak, Co-Supervisor

Experimental Investigation of the Delamination Behavior of Curved Post-Tensioned Concrete Structures without Through-Thickness Reinforcement

by

Clint Robert Woods, B.S.Arch.E.

Thesis

Presented to the Faculty of the Graduate School of

The University of Texas at Austin

in Partial Fulfillment

of the Requirements

for the Degree of

Master of Science in Engineering

The University of Texas at Austin

December 2016

Dedication

To my family and friends for their endless love, support and good times.

Acknowledgements

Working on this research project and obtaining a graduate degree from the University of Texas at Austin has been one of the most challenging experiences of my life, but by far the most rewarding. I have learned lifelong lessons during my time here, and much of what was accomplished would not have been possible without the help of several individuals.

First, I would like to give a special thanks to my supervisors, Dr. Bayrak and Dr. Hrynyk, for all of their support, guidance and encouragement. Dr. Hrynyk introduced me to this project when he hired me on as an undergraduate research assistant, setting up the opportunity for me to continue my work as a graduate student. Dr. Bayrak has been a great mentor to me, and always provided great insights for this research project. Thank you, Dean Deschenes, for helping to get this project underway and being there to answer my questions. Dr. Bayrak and Dr. Hrynyk, thank you for your help in editing this document to improve its clarity and quality.

To the staff at the Ferguson Structural Engineering Laboratory, I appreciate all that you did for this project. David Braley made work entertaining with all of his hilarious stories and sly remarks about me doing something incorrectly. Though he was always giving me a hard time, I learned a great deal from him. Blake Stasney was always there to help solve problems and his vast knowledge of the lab was key to the success of this project. Dennis Fillip provided me with a lot of practical experience and much of what was fabricated for this project would not have been possible without his guidance. All three of them contributed to the success of this research with their training on the lab tools, and their operation of the cranes and forklifts. Thank you to Dr. Brown for scheduling all of our tasks, keeping the project organized and always asking if I broke something. I would like to thank Joel Arredondo and John Bacon for all their help with the electronics, wiring and instrument calibrations. John always joked about me making too much noise, so I am sure he is glad things will be a little quieter around the lab with me gone. A sincere thanks to Michelle Damvar, Deanna Mueller and Liz Clayton for all their administrative work and their organization of the lab events throughout the years.

Thanks to all of my fellow students at FSEL who helped me throughout the duration of this project. A big thanks is owed to Jongkwon Choi, who I worked with every day for the entirety of this project. This research truly could not have happened without all of his hard work and dedication. I really appreciate all that he taught me, the advice he shared with me and our friendship. Thank you, Dr. Yousefpour, for assisting with the setup of the data acquisition and answering my many questions. To all of the students who I worked with at FSEL, I want to thank you for all the assistance you offered for the concrete casts and other random tasks. The memories I have made working alongside all of you will remain with me for the rest of my life.

Finally, I want to thank my family and friends. My parents have provided me with love and support for all my endeavors in life, and I cannot thank them enough for all they have done. My brothers have always been there for me and I appreciate all that they have taught me throughout our years of growing up together. To my friends, thank you for the endless memories and for constantly pushing me to become a better man. Lastly, I want to thank my girlfriend, Ellen, for all that she has done for me throughout these last few years. Her endless love and support has helped me more than she could ever know.

Abstract

Experimental Investigation of the Delamination Behavior of Curved Post-Tensioned Concrete Structures without Through-Thickness Reinforcement

Clint Robert Woods, M.S.E.

The University of Texas at Austin, 2016

Supervisors: Trevor Hrynyk, Oguzhan Bayrak

The recent delamination failure of the concrete containment structure wall at the Crystal River Unit 3 Nuclear Power Plant has led to increased interest in the mechanical behavior of curved post-tensioned structures. Extensive investigations have been performed to identify the causes of the delamination failure, but no experimental research has focused on the behavior of curved post-tensioned structures. Analytical studies focused on the through-thickness stress development stemming from prestressing forces have been performed, yet there is no experimental data to verify the results. This research examines the behavior of curved post-tensioned structures and their delamination failures through the structural testing of two curved post-tensioned wall specimens.

Two 90° curved post-tensioned wall specimens were constructed and tested under monotonically increasing prestressing loads at the University of Texas at Austin. In an effort to gain insight into the size effect associated with delamination failures, the dimensions of the second specimen were doubled from the first. The specimens were

well-instrumented to ensure the delamination behavior was adequately captured. Using the output from load cells positioned at the live-end and dead-end of each curved wall specimen, the friction losses, forces, and stresses developed at various locations along the curved wall sections were determined. In order to directly compare the behavior of both specimens, the applied stresses were normalized with respect to the measured concrete compressive strength. The test results were used to determine the underlying mechanisms of the curved post-tensioned concrete structures, such as the size effect of delamination failure and initiation of delamination cracking.

The experimental results indicated an apparent size effect on the delamination resistances of the curved wall specimens, with a 32 % decrease in the normalized capacity from Specimen 1 to Specimen 2. In addition, the compressive stresses at the initiation of the delamination crack were $0.13f_c'$~$0.23f_c'$, which are significantly less than the allowable stress limit of 0.35fc' specified in ASME Boiler and Pressure Vessel Code (BPVC) Section III, Division 2 for the service load condition. Lastly, the measured friction losses were 38 %~43 % greater than the friction losses calculated based on ACI 343R-95.

Table of Contents

List of Tables x

List of Figures xii

Chapter 1: Introduction 1

1.1 Overview 1

1.2 Research Significance 3

Chapter 2: Experimental Program 4

2.1 Summary of Specimen Design and Geometry 4

2.2 Specimen Fabrication 10

2.3 Material Properties 15

2.4 Instrumentation 20

2.5 Test Setup and Loading Procedure 27

Chapter 3: Experimental Results 32

3.1 Test Observations 32

3.2 Friction Loss 38

3.3 Delamination Failure Capacity 41

3.4 Indication of Delamination 42

Chapter 4: Conclusions 54

Appendix A: Specimen Design and Fabrication 56

Appendix B: Material Testing Records 74

Appendix C: Experimental Results 101

References 113

List of Tables

Table 2-1: Potential Failure Modes of a Curved Post-Tensioned Concrete Structure 5

Table 2-2: Summarized Dimensions of the Test Specimens 6

Table 2-3: Summary of Concrete Mixture Proportions 16

Table 2-4: Summary of Concrete Material Tests...16

Table 2-5: Summary of Average Concrete Material Properties at 28 Days 17

Table 2-6: Summary of Average Concrete Material Properties at Test Day.........17

Table 2-7: Summary of Average Reinforcing Bar and Strand Properties 20

Table 3-1: Friction Coefficients for Post-Tensioning Tendons (ACI 343R-95)....39

Table A-1: Classification of Forces in Concrete Containments for Steel Reinforcing and Concrete Allowable Stresses (ASME BPVC Section III, Division 2) 57

Table A-2: Load Combinations and Load Factors (ASME BPVC Section III, Division 2) 58

Table B-1: Specimen 1 Live-End Anchor Block Concrete Compressive Strength Data 82

Table B-2: Specimen 1 Wall Section and Dead-End Block Concrete Compressive Strength Data 82

Table B-3: Specimen 2 Live-End Anchor Block Concrete Compressive Strength Data 83

Table B-4: Specimen 2 Wall Section Concrete Core Sample Compressive Strength Data 83

Table B-5: Specimen 2 Wall Section and Dead-End Anchor Block Air Cured Concrete Compressive Strength Data 84
Table B-6: Specimen 2 Wall Section and Dead-End Anchor Block Water Cured Concrete Compressive Strength Data 85
Table B-7: Specimen 1 Wall Section and Dead-End Anchor Block Concrete Modulus of Elasticity and Poisson's Ratio Data..87
Table B-8: Specimen 2 Wall Section and Dead-End Anchor Block Concrete Modulus of Elasticity and Poisson's Ratio Data..88
Table B-9: Specimen 1 Wall Section and Dead-End Anchor Block Concrete Splitting Tensile Strength Test Data...89
Table B-10: Specimen 2 Wall Section and Dead-End Anchor Block Concrete Splitting Tensile Strength Test Data 89
Table B-11: Specimen 1 Wall Section and Dead-End Anchor Block Concrete Modulus of Rupture Test Data...90
Table B-12: Specimen 2 Wall Section and Dead-End Anchor Block Concrete Modulus of Rupture Test Data...90
Table B-13: Specimen 1 Wall Section and Dead-End Anchor Block Concrete Direct Tension Test Data 90
Table B-14: Specimen 2 Wall Section and Dead-End Anchor Block Concrete Direct Tension Test Data 91
Table B-15: Specimen 1 Reinforcing Bar Tensile Testing Data 95
Table B-16: Specimen 2 Reinforcing Bar Tensile Testing Data 95

List of Figures

Figure 2-1: Reinforcement Details of the Curved Wall Test Specimens................7

Figure 2-2: Reinforcement Details of the Curved Wall Sections 8

Figure 2-3: Eccentricity of Ducts due to the Arrangement of Strands 9

Figure 2-4: Curved Wall Formwork Showing: (a) Outside Formwork for Specimen 1, (b) Assembled Inside Formwork and Outside Formwork Sections for Specimen 2...12

Figure 2-5: Threaded Rod Form Tie Inserted into Cellulose Tubing 13

Figure 2-6: Placement of the Teflon Sheets..13

Figure 2-7: Reinforcing Cage for the Curved Wall Section of Specimen 2 Showing: (a) Curved Wall Reinforcing Cage, (b) Dead-End Anchor Block Reinforcing Cage 15

Figure 2-8: Dog-Bone Direct Tension Specimen Showing: (a) Front View, (b) Side View, (c) Specimen Mold, (d)Testing Apparatus............................19

Figure 2-9: Details of Through-Thickness Instrumentations Showing: (a) Schematic of the Linear Potentiometer Setup, (b) Linear Potentiometer Attached to Specimen 1, (c) Schematic of the Linear Strain Conversion Transducer Setup, (d) LSCT Attached to Specimen 2..21

Figure 2-10: Polar Locations of the Instrumentations and Typical Sectional Locations of the Linear Potentiometers and Linear Strain Conversion Transducers 22

Figure 2-11: Strain Gauge Layout on Reinforcing Bars in the Curved Wall Sections 24

Figure 2-12: Layout of Embedded Strain Gauges at the 15° Location of Specimen 2 25
Figure 2-13: Concrete Surface Gauge Arrangement for the Top of Specimen 2 ..26
Figure 2-14: Test Setup for Specimen 1 Showing: (a) Live-End Setup, (b) Dead-End Setup, (c) Overall View of the Test Setup 28
Figure 2-15: Test Setup for Specimen 2 Showing: (a) Live-End Setup, (b) Dead-End Setup, (c) Overall View of the Test Setup 30
Figure 3-1: Failed Test Specimens Showing: (a) View from Top of Specimen 1, (b) View from Top of Specimen 2, (c) 15° Section of Specimen 1, (d) 8° Section of Specimen 2 33
Figure 3-2: Through-Thickness Expansion at the 15° Location of Specimen 1....35
Figure 3-3: Through-Thickness Expansion at the 15° Location of Specimen 2....35
Figure 3-4: Compressive Stress versus Average Strain of the Circumferential Reinforcing Bars at the 15° Location of Specimen 1 36
Figure 3-5: Compressive Stress versus Average Strain of the Circumferential Reinforcing Bars at the 15° Location of Specimen 2 37
Figure 3-6: Average Displacement of the Dead-End Anchor Block versus Live-End Load for Specimen 2 38
Figure 3-7: Measured Friction Losses for Specimen 2 40
Figure 3-8: Comparison of the Modified Friction Coefficient Based on the Measured Loads and the Friction Coefficient Based on ACI 343R-95............41
Figure 3-9: Size Effect on the Delamination Failure 42
Figure 3-10: Through-Thickness Expansions versus Normalized Compressive Stresses at the 15° Location of Specimen 1 44

Figure 3-11: Through-Thickness Expansions versus Normalized Compressive Stresses at the 45° Location of Specimen 1 44
Figure 3-12: Through-Thickness Expansions versus Normalized Compressive Stresses at the 75° Location of Specimen 1 45
Figure 3-13: Through-Thickness Expansions versus Normalized Compressive Stresses at the 15° Location of Specimen 2 46
Figure 3-14: Through-Thickness Expansions versus Normalized Compressive Stresses at the 45° Location of Specimen 2 46
Figure 3-15: Through-Thickness Expansions versus Normalized Compressive Stresses at the 75° Location of Specimen 2 47
Figure 3-16: Inside Face Vertical Strains versus Normalized Compressive Stresses at the 15° Location of Specimen 1..48
Figure 3-17: Inside Face Vertical Strains versus Normalized Compressive Stresses at the 45° Location of Specimen 1..48
Figure 3-18: Inside Face Vertical Strains versus Normalized Compressive Stresses at the 75° Location of Specimen 1..49
Figure 3-19: Inside Face Vertical Strains versus Normalized Compressive Stresses at the 15° Location of Specimen 2..50
Figure 3-20: Inside Face Vertical Strains versus Normalized Compressive Stresses at the 45° Location of Specimen 2..51
Figure 3-21: Inside Face Vertical Strains versus Normalized Compressive Stresses at the 75° Location of Specimen 2..51
Figure 3-22: Allowable Compression Stresses For Service Loads (ASME BPVC Section III, Division 2) 53

Figure A-1: Live-End Anchor Block Reinforcement Details for Specimen 1 Showing: (a) Top View, (b) Top View Rotated 90°, (c) View of Back Face, (d) Side View 59

Figure A-2: Dead-End Anchor Block Reinforcement Details for Specimen 1 Showing: (a) Top View, (b) Top View Rotated 90°, (c) View of Back Face, (d) Side View 60

Figure A-3: Live-End Anchor Block Reinforcement Details for Specimen 2 Showing: (a) Top View, (b) Top View Rotated 90°, (c) View of Back Face, (d) Side View 61

Figure A-4: Dead-End Anchor Block Reinforcement Details for Specimen 2 Showing: (a) Top View, (b) Top View Rotated 90°, (c) View of Back Face, (d) Side View 62

Figure A-5: Fabrication of Specimen 1 Live-End Anchor Block Showing: (a) Completed Reinforcing Cage, (b) Reinforcing Cage in Formwork, (c) Concrete Casting, (d) Completed Anchor Block 63

Figure A-6: Fabrication of Specimen 2 Live-End Anchor Block Showing: (a) Reinforcing Cage, (b) Reinforcing Cage in Formwork, (c) Formwork Completely Assembled (d) Concrete Casting, (e) Completed Anchor Block 64

Figure A-7: Fabrication of Curved Wall Formwork Showing: (a) Kerfed Plywood Sheathing with Grooves for Studs, (b) Drilling Holes for Form Ties, (c) Making Curved Plywood Studs, (d) Assembling Formwork, (e) Finished Outside Face Formwork for Specimen 1 (f) Finished Formwork for Specimen 2 65

Figure A-8: Specimen 1 Curved Wall and Dead-End Anchor Reinforcing Cage Fabrication Showing: (a) Placement of Live-End Anchor Block, (b) Placing Teflon Sheets, (c) Curved Wall Reinforcing Cage, (d) Dead-End Anchor Reinforcing Cage, (e) Completed Reinforcing Cage in Formwork 66

Figure A-9: Specimen 2 Curved Wall and Dead-End Anchor Reinforcing Cage Fabrication Showing: (a) Moving Live-End Anchor Block, (b) Placing Teflon Sheets, (c) Placement of Ducts, (d) Completed Curved Wall Reinforcing Cage, (e) Dead-End Anchor Reinforcing Cage, (f) Completed Reinforcing Cage in Formwork 67

Figure A-10: Concrete Casting Operations for Specimen 1 Showing: (a) Slump Test, (b) Placement of Concrete, (c) Internal Vibrating, (d) Finishing of Surface, (e) Curing of Specimen, (f) Completed Specimen 68

Figure A-11: Concrete Casting Operations for Specimen 2 Showing: (a) Slump Test, (b) Placement of Concrete, (c) Internal Vibrating, (d) Finishing of Surface, (e) Curing of Specimen, (f) Completed Specimen 69

Figure A-12: Typical Concrete Casting Operations for Material Test Specimens Showing: (a) Material Test Specimen Molds, (b) Cylinders, (c) Concrete Prisms, (d) Dog-Bone Specimens, (e) De-Molded Material Test Specimens 70

Figure A-13: Instruments Installed on Specimen 1 Showing: (a) Reinforcement Bar Strain Gauge, (b) Embedded Strain Gauge, (c) Surface Strain Gauge, (d) Linear Potentiometers for Through-Thickness Expansions, (e) NDI Optotrak Certus System Targets 71

Figure A-14: Instruments Installed on Specimen 2 Showing: (a) Reinforcement Bar Strain Gauge, (b) Embedded Strain Gauge, (c) Surface Strain Gauge, (d) LSCTs for Through-Thickness Expansions, (e) NDI Optotrak Certus System Targets, (f) Linear Potentiometer for Anchor Block Movement 72
Figure A-15: Structural Test Setup of Both Specimens Showing: (a) Inserting Strands, (b) Removing Slack from Strands, (c) Live-End Setup for Specimen 1, (d) Dead-End Setup for Specimen 1, (e) Live-End Setup for Specimen 2, (f) Dead-End Setup for Specimen 2 73
Figure B-1: Specimen 1 Live-End Anchor Block Batch Ticket 75
Figure B-2: Concrete Mixture Design Properties for Specimen 1 Wall Section and Dead-End Anchor Block 76
Figure B-3: Specimen 1 Wall Section and Dead-End Anchor Block Batch Ticket 77
Figure B-4: Specimen 2 Live-End Anchor Block Batch Ticket 78
Figure B-5: Concrete Mixture Design Properties for Specimen 2 Wall Section and Dead-End Anchor Block 79
Figure B-6: Specimen 2 Wall Section and Dead-End Anchor Block Batch Ticket 80
Figure B-7: Testing of Material Properties Showing: (a) Compressive Strength Test, (b) Modulus of Elasticity and Poisson's Ratio Test, (c) Splitting Tensile Strength Test, (d) Modulus of Rupture Test, (e) Direct Tension Test, (f) Reinforcing Bar Tension Test 81
Figure B-8: Specimen 1 Wall Section and Dead-End Anchor Block Concrete Compressive Strength Development 86

Figure B-9: Specimen 2 Wall Section and Dead-End Anchor Block Concrete Compressive Strength Development..86
Figure B-10: Typical Concrete Compressive Strength Test Stress versus Strain Plot 87
Figure B-11: Typical Concrete Direct Tension Test Stress versus Strain Plot......91
Figure B-12: Specimen 1 Steel Mill Certification Test Report for No. 3 Reinforcing Bars Used in the Curved Wall Section 92
Figure B-13: Specimen 1 Steel Mill Certification Test Report for No. 4 Reinforcing Bars Used in the Curved Wall Section 93
Figure B-14: Specimen 2 Steel Mill Certification Test Report for No. 4 Reinforcing Bars Used in the Curved Wall Section 94
Figure B-15: Typical Reinforcing Bar Tensile Test Stress versus Strain Plot 96
Figure B-16: Strand Mechanical Properties Data Report for Specimen 1.............97
Figure B-17: Strand Mechanical Properties Data Report for Specimen 2.............98
Figure B-18: Steel Mill Certification Test Report for Specimen 1 Ducts 99
Figure B-19: Steel Mill Certification Test Report for Specimen 2 Ducts 100
Figure C-1: Snapshots of the Delamination Failure of Specimen 1 at the 15° Location from the Front 102
Figure C-2: Snapshots of the Delamination Failure of Specimen 1 at the 15° Location from the Side...103
Figure C-3: Snapshots of the Delamination Failure of Specimen 2 at the 15° Location from the Front 104
Figure C-4: Snapshots of the Delamination Failure of Specimen 2 at the 15° Location from the Side...105

Figure C-5: Images of the Failed Test Specimens Showing: (a) Top of Specimen 1, (b) Back of Specimen 1, (c) Front of Specimen 1, (d) Top of Specimen 2, (e) Back of Specimen 2, (f) Front of Specimen 2 106

Figure C-6: Compressive Stress versus Average Strain of the Circumferential Rebar at the 45° Location of Specimen 1 107

Figure C-7: Compressive Stress versus Average Strain of the Circumferential Rebar at the 75° Location of Specimen 1 107

Figure C-8: Compressive Stress versus Average Strain of the Circumferential Rebar at the 45° Location of Specimen 2 108

Figure C-9: Compressive Stress versus Average Strain of the Circumferential Rebar at the 75° Location of Specimen 2 108

Figure C-10: Through-Thickness Strains versus Normalized Compressive Stresses at the 45° Location of Specimen 1 Measured by Embedded Strain Gauges 109

Figure C-11: Through-Thickness Strains versus Normalized Compressive Stresses at the 15° Location of Specimen 2 Measured by Embedded Strain Gauges 109

Figure C-12: Top Surface Through-Thickness Strains versus Normalized Compressive Stresses of Specimen 1 Measured by Surface Strain Gauges...110

Figure C-13: Average Top Surface Through-Thickness Strains versus Normalized Compressive Stresses of Specimen 2 Measured by Surface Strain Gauges...110

Figure C-14: NDI Optotrak Certus System Data Showing the Global Movement of Specimen 2 from the Top..111

Figure C-15: NDI Optotrak Certus System Data Showing the Global Movement of Specimen 2 from the Side 112

Chapter 1: Introduction

1.1 Overview

Concrete containment structures are commonly post-tensioned to resist hoop tension in the containment shell membrane induced by internal pressure. A circumferential tendon profile is typically the most effective and favorable alignment for the prestressing strands. A side effect from this arrangement, and the prestressing forces that are applied, is that the containment structure experiences through-thickness pressures along the circumferential line of prestressing. These pressures generate tensile stresses in the outer region of the curved containment structures. The through-thickness (radial) tension in the concrete may induce cracking along the line of prestressing and if the tensile stress is excessive, it can lead to a delamination failure of the structure.

In June of 1970, the delamination of the Turkey Point Unit 3 containment dome was discovered. The dome delamination occurred while 110 of the 165 tendons had been tensioned. From a thorough investigation of the delamination failure, it had been revealed that the main cause of the delamination failure was the combined action of inadequate concrete consolidation, unbalanced post-tensioning loads and rotating construction joints (Florida Power and Light Company, 1970). In April of 1976, surface cracks and voids were discovered in the dome of the Crystal River Nuclear Power Plant Unit 3. The dome had already been constructed and the tendons were fully tensioned. The primary causes of the delamination failure were radial tension forces from the prestressing combined with biaxial compression, and low direct tensile strength of the concrete resulting from low quality coarse aggregate (Ashar and Naus, 1983; Moreadith and Pages, 1983). In May of 1994, the delamination of the inner containment dome of the Kaiga Power Project, Unit-1 occurred after stressing 66 of the 183 prestressing strands during construction. Subsequently, the inside surface of the dome failed and collapsed. The primary cause of the delamination failure was determined to occur from the through-thickness tension induced by the prestressing strands combined with the compression of the membrane, which exceeded the tensile capacity of the concrete (Basu et al., 2001). In October of 2009, a delamination failure of the Crystal River Unit 3 containment structure wall was discovered. The failure occurred while creating an opening in the containment structure to replace an old steam generator. A substantial investigation revealed that the failure occurred due to a combination of an improper sequence of de-tensioning the prestressing strands and poor concrete quality. The delamination initiated from the tensile capacity of the concrete being exceeded as a result of the redistribution of stresses that occurred during the de-tensioning process (Progress Energy, 2010). It had been determined from the investigation that the delamination failure could not have been predicted based on the existing information at the time. Repairs were made to the areas affected by the delamination; however, in March of 2011, a second delamination occurred in an adjacent wall during the final stages of re-tensioning the tendons (Progress Energy, 2011). In February of 2013, it was decided that Crystal River Unit 3 would be decommissioned, rather than proceeding with further repairs (Penn, 2013).

The delamination failures of the containment structure domes and walls have led to extensive research being conducted to investigate the sources of the failures for each incident. Acharya and Menon (2003) provided theoretical and analytical approaches to estimate the through-thickness stress distribution owing to the circumferential prestressing forces. Another analytical study examined the through-thickness stress distribution induced by unbalanced moments stemming from tendon tensioning and detensioning (Bae, 2013). Other analytical studies have been focused on the distribution of through-thickness stresses for singly and doubly curved shells (Ragunath et al., 2001; Acharya and Menon, 2003).

Some experimental studies have been performed on the wall elements of containment structures and tendon breakout. Schultz, Julien, and Russell (1984) investigated the behavior of containment wall elements subjected to internal over-pressurization. The results of the investigation were used to confirm analytical models used to predict the strength and deformations of such wall elements. Other experimental research was performed to investigate tendon breakout failures in curved concrete box girders. Various duct arrangements were tested for box girders curved at approximately 16° angles to determine the tendon breakout capacity (Van Landuyt, 1991). However, none of the experimental research explicitly focused on the delamination behavior of curved post-tensioned structures. A few analytical studies attempted to explain the delamination phenomenon; however, it is still not well understood due to the lack of experimental data. This research program examines the delamination behavior of curved post-tensioned structures with monotonically increasing prestressing loads.

1.2 Research Significance

The delamination failures of several concrete containment structures at various nuclear power plants have led to significant interest in the delamination behavior of curved post-tensioned structures. Minor amounts of analytical research have been performed on curved post-tensioned structures; however, the delamination failure phenomenon is still not well understood. The results from this experimental investigation provides insights into the initiation of delamination cracking and the delamination failure of curved post-tensioned structures.

Chapter 2: Experimental Program

Two 90° curved wall specimens were constructed and tested under monotonically increasing prestressing loads at the Ferguson Structural Engineering Laboratory at the University of Texas at Austin. The specimens were designed to represent a quarter of a horizontal section of a concrete containment structure. Through-thickness (radial) reinforcement was not provided in the curved wall sections in order to observe the delamination behavior of concrete in curved post-tensioned structures. The following section includes a discussion on the details of the design, fabrication, material properties, instrumentation and test setup for the two curved wall specimens.

2.1 Summary of Specimen Design and Geometry

The test specimens were designed so that delamination would be the controlling failure mode under prestressing loads. Table 2-1 shows the possible failure modes for a curved post-tensioned concrete structure and the strategies that were used to mitigate them. The wall sections were designed based on the allowable stress design method according to the requirements under a service load condition of ASME Boiler and Pressure Vessel Code (BPVC) Section III, Division 2. The structures were only subjected to prestressing loads and the secondary effects, such as those caused by creep and shrinkage, were minimized by the unrestrained boundary condition provided over the main test area.

Table 2-1: Potential Failure Modes of a Curved Post-Tensioned Concrete Structure

Failure Mode	**Condition**	**Strategy**
Delamination	Allowed	No radial reinforcement
Anchorage	Not Allowed	STM design
Local Shear	Not Allowed	Even spaced ducts; allowable stress design
Global Shear	Unlikely	None
Local Bending	Not Allowed	Even spaced ducts; allowable stress design
Global Bending	Not Allowed	Duct offset
Concrete Crushing	Not Allowed	Strands rupture before concrete crushing
Buckling	Unlikely	None

The wall section for Specimen 1 was curved to a 90° angle at a 7 ft. radius, measured from the centerline of the duct. The height of the wall was 3 ft. and had a width of 6 in. Eight No. 3 circumferential reinforcing bars were spaced 4.5 in. on center for both the inside and outside surfaces, leading to a reinforcement ratio of 0.40 % for each surface. The vertical reinforcing bars were No. 4 bars spaced at 6.38 in. for the inside surface and 6.75 in. for the outside surface, leading to a reinforcement ratio of 0.50 %. It should be noted that the original the spacing of the vertical reinforcement for Specimen 1 was 12 in., producing a reinforcement ratio of 0.28 %. However, due to the width of the wall being 6 in., it was deemed more practical to reduce the spacing to the layout mentioned previously. Specimen 2 was curved at a radius of 14 ft., measured from the centerline of the duct. The height of Specimen 2 was 6 ft. and had a width of 12 in. Seventeen No. 4 circumferential reinforcing bars were spaced at 4.25 in. on each surface of the wall, producing a reinforcing ratio of 0.40 % for each surface. The vertical reinforcing bars were No. 4 bars spaced at 5.81 in. for the inside surface and 6.13 in. for the outside surface, leading to a reinforcing ratio of 0.28 %. The reinforcement layouts for both specimens met the ASME BPVC Section III, Division 2 minimum crack control reinforcement ratio of 0.20 % for each surface of the structure. Neither of the curved wall specimens had any through-thickness reinforcement, resulting in only the concrete resisting the radial tensile stresses produced by the prestressing loads. Table 2-2 and Figure 2-1 summarize the dimensions and details of the curved wall sections comprising both specimens.

Table 2-2: Summarized Dimensions of the Test Specimens

	Specimen 1	Specimen 2
Height, in.	36	72
Width, in.	6	12
Radius, in.	84	168
Circumferential Reinforcement Ratio, %	0.40	0.40
Vertical Reinforcement Ratio, %	0.50	0.28
Outer Diameter of Duct, in.	2	4
Number of Strands per Duct	4	19
Duct Offset, in.	0.25	0.75

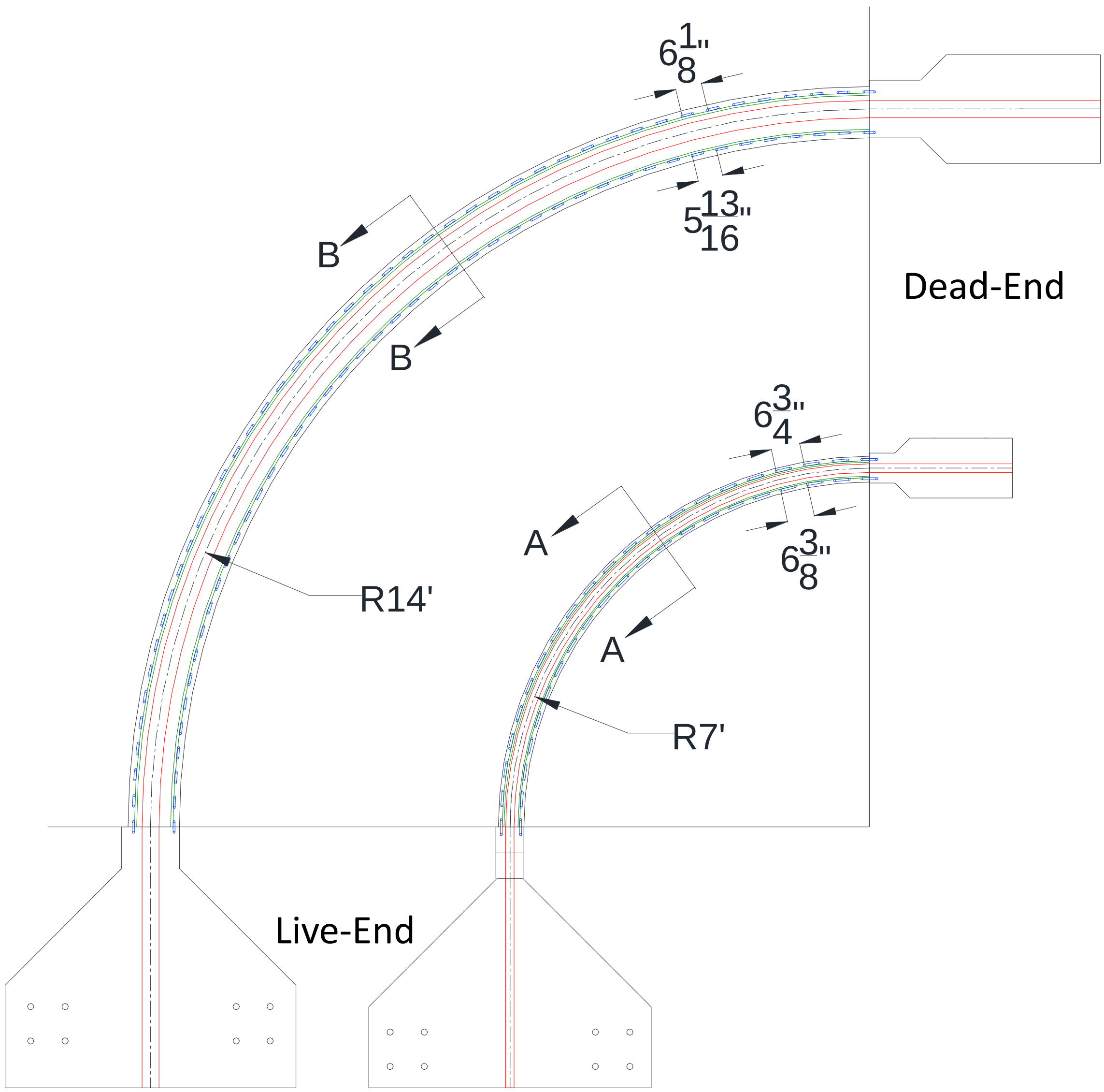

Figure 2-1: Reinforcement Details of the Curved Wall Test Specimens

Section cuts A-A and B-B display the reinforcement details of the curved wall sections. The details of the reinforcement for each section are depicted in Figure 2-2 on the following page.

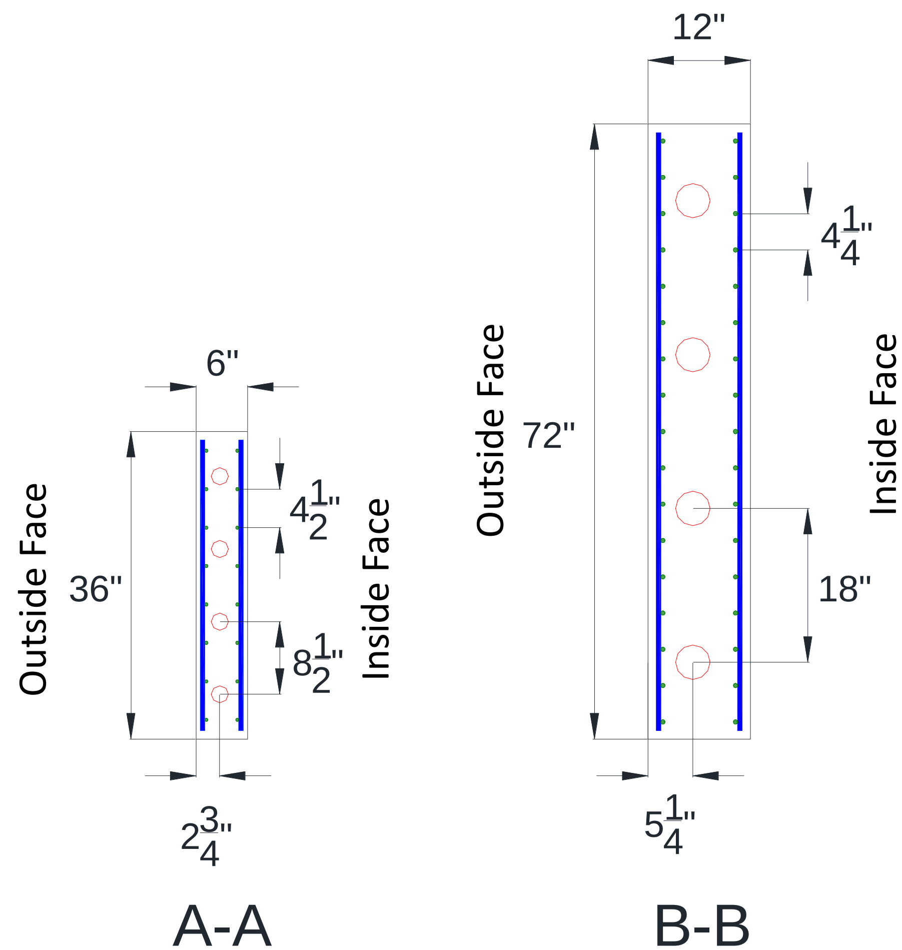

Figure 2-2: Reinforcement Details of the Curved Wall Sections

Each test specimen had four ducts evenly distributed over the height of the section and they were located in the center of the cross-section. Four 0.6-in. diameter strands were provided for each duct of Specimen 1 and nineteen 0.6-in. diameter strands were provided for each duct of Specimen 2. Therefore, an outside diameter of 2 in. and 4 in. was chosen for the ducts of Specimen 1 and 2, respectively. In order to minimize the bending generated by eccentrically located strands within the curved ducts, the duct locations were shifted 0.25 in. and 0.75 in. toward the outside surface of Specimen 1 and

2, respectively. These small offsets allowed for the centroid of the strands to be at the center of the curved wall section upon loading, as demonstrated in Figure 2-3.

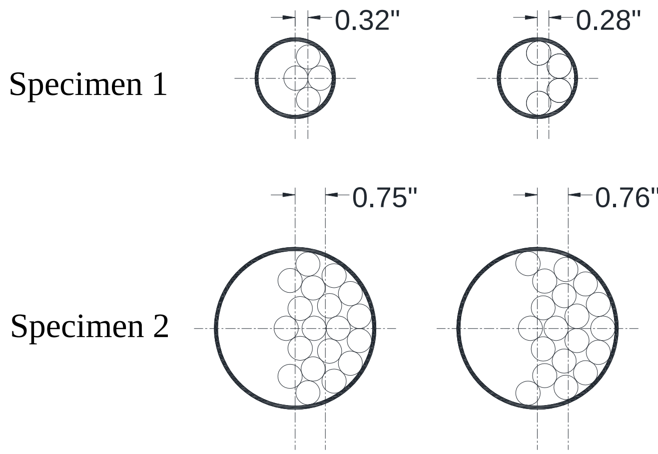

Figure 2-3: Eccentricity of Ducts due to the Arrangement of Strands

The live-end and dead-end anchor blocks were designed using the Strut-and-Tie method (STM) according to the specifications of ACI 318-14. The rupture strength of the prestressing strands was selected as a conservative design load for the STM design. Crack control reinforcement greater than 0.30 % was provided in all three directions, as needed, for both the live-end and dead-end anchor blocks. The circumferential reinforcement bars of the curved wall sections were spliced with the horizontal reinforcing bars in the live-end anchor block, and satisfied the development length requirements of reinforcement in compression and the splice length requirements of ACI 318-14. Details of the reinforcement layout for both the live-end and dead-end anchor blocks for each specimen can be found in Appendix A.

The anchorage devices for both Specimen 1 and Specimen 2 were provided by VSL. Custom made anchorage devices were fabricated by VSL for use in Specimen 1.

VSL Type ECI 6-19 anchorage devices were used for the post-tensioning system of Specimen 2.

2.2 Specimen Fabrication

The fabrication of the test specimens was done on a wooden platform and consisted of a two phase process. The first phase was the construction of the live-end anchor block. Once the live-end anchor block was completed, it was moved to the desired location on the laboratory floor. When the anchor block was in position, it was tied down to the strong floor using eight 1-in. diameter threaded rods. Each threaded rod was tensioned to a force of 30 kips, creating a total tie down force of 240 kips. The live-end anchor block was used as the primary reference point for the second phase of the fabrication process. The second phase of fabrication was building the curved wall section and the dead-end anchor block. Using the position of the live-end anchor as a reference, the center point of the curve was determined. With this reference, the start and end point of the curved wall section was located and used to create the 90° curve that was desired. The curved wall section and dead-end anchor block were cast in concrete together, so there was only a cold joint between the face of the live-end anchor block and the start of the curved wall.

Due to the unique geometry of the curved walls and the anchor blocks, wooden formwork was constructed for the fabrication of the specimens. The formwork was designed using ACI SP-4, and the hydrostatic pressure of wet concrete was used to determine the loads carried by each member of the formwork. For the formwork of the anchor blocks, 3/4 in. plywood was used as the sheathing material, and 2x4 studs were adequately spaced to ensure moment, shear and a deflection limit of 1/360 of the span were met.

The reinforcing cage for the live-end anchor block was constructed first. The stirrups were placed and positioned using wood blocks to ensure proper spacing. Then the horizontal reinforcing bars used for crack control were placed and tied. Finally, the horizontal reinforcing bars being used to splice the live-end anchor block with the curved wall section were placed and tied. Holes were drilled in the formwork to allow the horizontal reinforcing bars to be spliced and to ensure an adequate development length of the reinforcing bars, as specified in ACI 318-14 for lap splices in compression. Holes were also drilled in the formwork to assist with the placement of the ducts and allow for the ducts to be spliced as well. Eight 1.5-in. diameter PVC pipes were placed in the live-end anchor blocks in order to provide through-thickness holes to tie them down to the laboratory floor, as mentioned earlier.

The concrete was placed in the live-end anchor block formwork using a 2 cubic yard concrete bucket and the overhead crane in the laboratory. Internal vibrators were used to ensure that the concrete was properly consolidated. After vibration, the top surfaces of the live-end anchor blocks were finished with trowels and covered with plastic sheeting to cure the concrete. Once the live-end anchor block was complete, the construction of the curved wall section and dead-end anchor block could begin.

To make the curved formwork for the wall sections, special measures were taken to ensure accurate construction. The studs for the curved formwork were made of two layers of 3/4 in. plywood. Using a wood router mounted on a rotating track, the plywood studs were cut into curved pieces at the required radii. To get the plywood sheathing to bend to the desired radius, it was kerfed at a 1/2 in. depth at a spacing of 2 in. and 3 in. for Specimen 1 and Specimen 2, respectively. Rabbets and dados were routed into the sheathing to insert and bond the curved studs to the sheathing itself. The curved forms for Specimen 1 were continuous for each face of the wall, however, the curved forms for

Specimen 2 were built in three sections for ease of construction. A thin layer of laminate sheeting was bonded to the curved formwork for Specimen 2 so that they could be reused for multiple casts. Figure 2-4 shows the curved wall forms for each specimen.

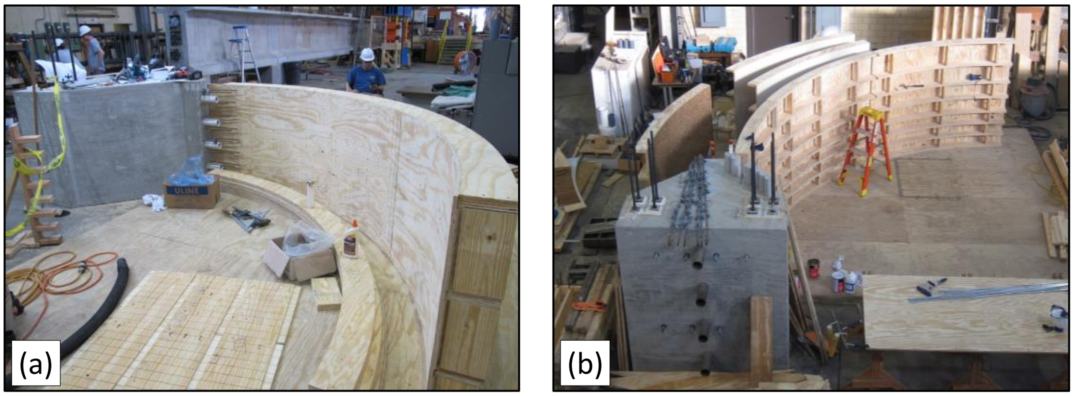

Figure 2-4: Curved Wall Formwork Showing: (a) Outside Formwork for Specimen 1, (b) Assembled Inside Formwork and Outside Formwork Sections for Specimen 2

7/16-in. diameter threaded rods were used as form ties for the wall sections to prevent bursting failure of the formwork from the large lateral pressures during the concrete casting. Since the curved wall specimens were intended to have no through-thickness reinforcement, the threaded rods were encased in clear cellulose tubes (outer diameter 0.625 in. and inner diameter 0.50 in.) so that they could be removed after casting and before testing, as seen in Figure 2-5. The tubes had good impact resistance in order to withstand the falling concrete during casting, but had poor tensile properties so they would not provide any form of through-thickness reinforcement for the curved wall specimens. 4x4 lumber was used as wales for the formwork, and holes were drilled in them for the form ties.

Figure 2-5: Threaded Rod Form Tie Inserted into Cellulose Tubing

Prior to the assembly of the reinforcing bar cage for the curved wall section and the dead-end anchor block, two layers of Teflon sheet were placed on the wooden platform to create a frictionless surface for the test specimens to move on during testing, as shown in Figure 2-6. The bottom layer of Teflon sheet was epoxied to the wood platform so it would not move during the concrete casting and testing of the specimens.

Figure 2-6: Placement of the Teflon Sheets

The circumferential reinforcing bars for the inside face of the curved wall were spliced with the live-end anchor block and placed using wood spacers to ensure accurate construction. Then the vertical reinforcing bars were placed and tied to the circumferential reinforcing bars on the inside face of the curved walls. Next the steel ducts were placed in the curved wall sections and spliced with the live-end anchor block. The location of the ducts was critical to the overall behavior of the test specimens, therefore, metal bolsters were positioned between the circumferential reinforcing bars and the ducts to ensure accurate placement. For Specimen 1, 3/4 in. bolsters were used along with 1/8 in. wood pieces to create the desired spacing of 7/8 in. between the ducts and the inside face circumferential reinforcing bars. For Specimen 2, 2.75 in. metal bolsters were positioned between the circumferential reinforcing bars on the inside face and the ducts. After placing the ducts, the circumferential and vertical reinforcing bars for the outside face were placed and tied. 1 in. reinforcing bar spacer wheels were attached to the circumferential reinforcing bars at regular intervals to ensure a concrete clear cover of 0.5 in. was attained for Specimen 1. 1 in. reinforcing bar spacer wheels were attached to the vertical reinforcing bars at regular intervals to make certain the concrete clear cover of 1 in. was achieved for Specimen 2. Reinforcing bars were tied at each intersection so that there would be minimal movement of the reinforcing bars during casting. The complete reinforcing cage for the curved wall section and dead-end anchor block of Specimen 2 is shown in Figure 2-7. The reinforcing cage for the dead-end anchor block was assembled upon completion of the curved wall reinforcing cage. The ducts were spliced with the trumpets of the bearing plates using heat shrink wrap provided by the manufacturer. In order to increase the bearing capacity of the concrete in the local zone area, spiral reinforcement was provided around the trumpets and bearing plates.

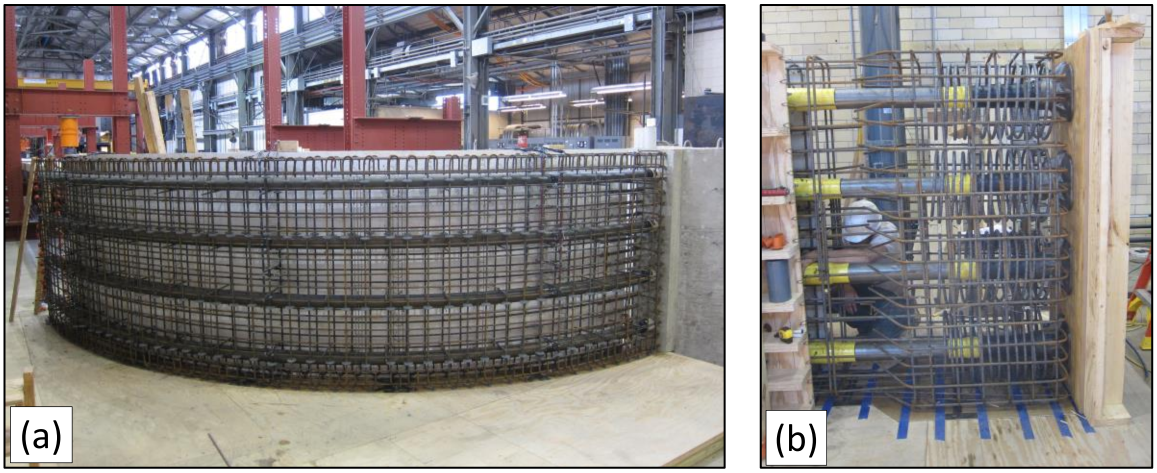

Figure 2-7: Reinforcing Cage for the Curved Wall Section of Specimen 2 Showing: (a) Curved Wall Reinforcing Cage, (b) Dead-End Anchor Block Reinforcing Cage

The concrete was placed in the formwork using a 2 cubic yard concrete bucket and the overhead crane in the laboratory. Internal vibrators were used to ensure that the concrete was properly consolidated. After vibration, the top surfaces of the specimens were finished with trowels and covered with plastic sheeting to cure the concrete. The formwork for Specimen 1 was removed approximately 28 days after casting and 5 days after casting for Specimen 2.

2.3 Material Properties

Concrete mixtures with design strengths of 3,000 and 3,500 psi were selected for Specimen 1 and Specimen 2, respectively. The concrete mixtures contained Type I cement, 25-30 % class F fly ash, and river gravel with a maximum nominal coarse aggregate size of 3/8 in. This size of coarse aggregate was chosen because of the tight spacing of the reinforcing cage of Specimen 1 and was used again in Specimen 2 for consistency. The details of the mixture proportions per cubic yard are shown in Table 2-3 for each specimen.

Table 2-3: Summary of Concrete Mixture Proportions

Material	**Specimen 1**	**Specimen 2**
Cement, lb./yd^3	318	362
Class F Fly Ash, lb./yd^3	106	155
Sand, lb./yd^3	1468	1301
3/8 in. Coarse Aggregate, lb./yd^3	1800	1850
Water, gal./yd^3	30	31
High Range Water Reducer, oz./yd^3	16.96	25.85
Retarder, oz./yd^3	-	5.17

To characterize the mechanical properties of the concretes, material testing was conducted to measure the compressive strength, modulus of elasticity, Poisson's ratio, splitting tensile strength, modulus of rupture, and direct tensile strength, which are summarized in Table 2-4. For each of the material tests conducted, a minimum of three specimens were tested to ensure that the reported values were accurate. All material test specimens, testing procedures, and reported values for each test were in accordance with ASTM, except for the direct tensile strength, which has no standardized test method.

Table 2-4: Summary of Concrete Material Tests

Material Test	Specimen Shape	Dimensions (in.)	ASTM Standard
Compressive Strength	Cylinder	4 x 8	ASTM C39
Modulus of Elasticity	Cylinder	4 x 8	ASTM C469
Poisson's Ratio	Cylinder	4 x 8	ASTM C469
Splitting Tensile Strength	Cylinder	4 x 8	ASTM C496
Modulus of Rupture	Prism	6 x 6 x 24	ASTM C78
Direct Tension	Dog-Bone	See Figure 2-8	N/A

The results of the measured concrete mechanical properties are summarized in Table 2-5 and Table 2-6 for the 28 day strength and test day strength, respectively. It should be noted that for Specimen 2 there was a drop in the compressive strength of the concrete from the 28 day strength and the test day strength, therefore core samples were taken from Specimen 2 after the structural test to verify the compressive strength of the concrete. The measured value of the core samples' compressive strength is shown in Table 2-6 and was used for subsequent calculations involving Specimen 2.

Table 2-5: Summary of Average Concrete Material Properties at 28 Days

Specimen ID	Specimen 1	Specimen 2
Compressive strength, f_c', ksi	1.73	4.65
Modulus of elasticity, E_c, ksi	3,963	4,596
Poisson's ratio, ν	N/A	0.214
Modulus of rupture, f_r, psi	N/A	671
Splitting tensile strength, f_{sp}, psi	226	534
Direct tensile strength, f_t', psi	N/A	427

* Water cured specimens were used for the material testing at 28 days

Table 2-6: Summary of Average Concrete Material Properties at Test Day

Specimen ID (age in days)	Specimen 1 (126)	Specimen 2 (133)
Compressive strength, f_c', ksi	3.01	6.82*
Modulus of elasticity, E_c, ksi	3,576	4,911
Poisson's ratio, ν	0.175	0.197
Modulus of rupture, f_r, psi	639	826
Splitting tensile strength, f_{sp}, psi	385	492
Direct tensile strength, f_t', psi	230	441

*Compressive strength measured from concrete cores obtained after the structural test

To measure the direct tensile properties of the concrete, dog-bone shaped specimens were selected (refer to Figure 2-8). Four 3/8-in. diameter threaded rods were embedded into each end of the dog-bone specimens so that they could later be mounted to clevises that would be gripped by the testing machine. To increase the capacity of the anchorage, nuts were attached to each end of the embedded threaded rods. The clevises used for the dog-bone tests contained ball joint rod ends to allow the specimens to rotate freely during testing. MTS 810 material testing system with 22 kips capacity was used to perform the direct tension test. The displacements of the dog-bone specimens were measured with four linear strain conversion transducers (LSCTs) at 16 in. and 8 in. gauge lengths. These displacements were used to calculate the average strain of each test. The test speed was maintained at a rate of 0.0025-0.005 in./min. until failure. The dimensions and testing apparatus for the dog-bone specimens are shown in Figure 2-8.

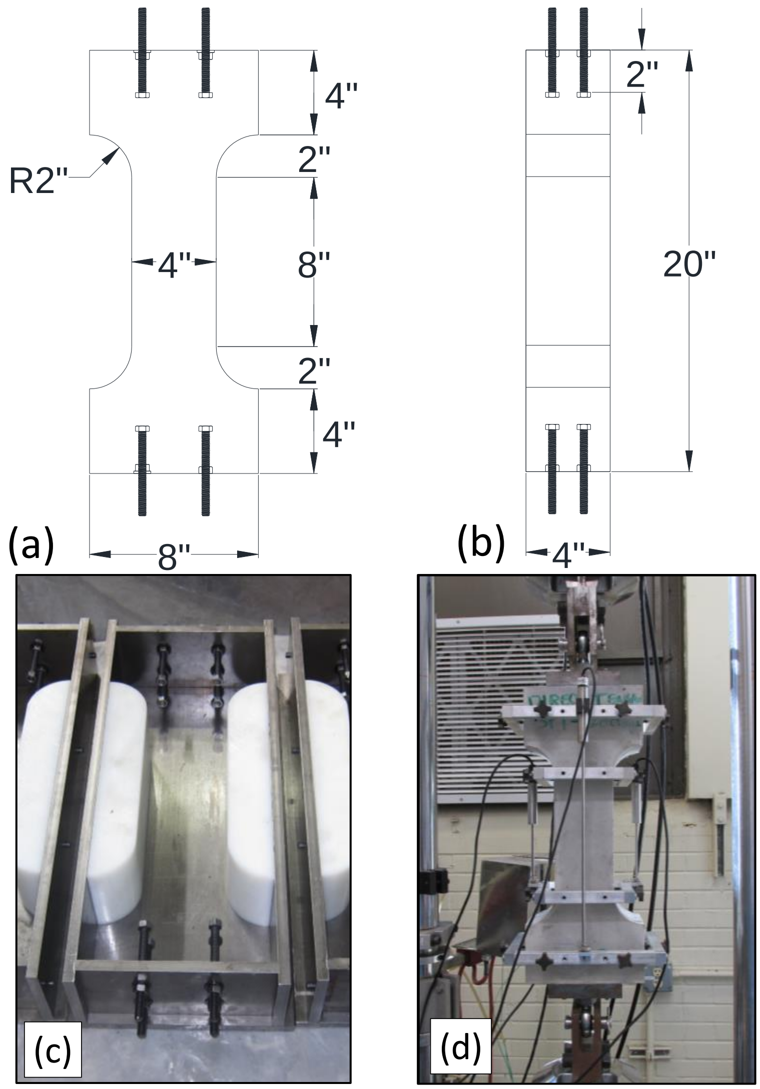

Figure 2-8: Dog-Bone Direct Tension Specimen Showing: (a) Front View, (b) Side View, (c) Specimen Mold, (d) Testing Apparatus

Reinforcing bars for each specimen were specified as Grade 60 deformed steel bars, satisfying the requirements of ASTM A615. A minimum of three samples of both the vertical and horizontal reinforcing bars used in the curved wall sections were tested in accordance with ASTM A370. The results of the reinforcing bars tensile tests are shown in Table 2-7. The mechanical properties of the Grade 270 seven-wire 0.6-in. diameter low relaxation strands meeting the requirements of ASTM A416 were provided by the manufacturer and are also summarized in Table 2-7.

Table 2-7: Summary of Average Reinforcing Bar and Strand Properties

<table>
<tr><td colspan="2">Specimen ID</td><td colspan="2">Specimen 1</td><td>Specimen 2</td></tr>
<tr><td rowspan="4">Reinforcing Bars</td><td>Bar Size</td><td>No. 3</td><td>No. 4</td><td>No. 4</td></tr>
<tr><td>Yield stress, f_y, ksi</td><td>67.3</td><td>73.9</td><td>60.7</td></tr>
<tr><td>Tensile strength, f_u, ksi</td><td>109.2</td><td>100.3</td><td>96.4</td></tr>
<tr><td>Modulus of Elasticity, E_s, ksi</td><td>30,641</td><td>29,339</td><td>28,627</td></tr>
<tr><td rowspan="2">0.6-in. strand</td><td>Tensile Strength, f_u, ksi</td><td colspan="2">283</td><td>285</td></tr>
<tr><td>Modulus of Elasticity, E_s, ksi</td><td colspan="2">28,300</td><td>29,000</td></tr>
</table>

Steel tubes with 14 gauge thickness (0.083 in.) meeting the requirements of ASTM A513 were used for the duct material for both specimens. This was chosen because the design curvature tolerance required for both specimens could be easily achieved by a process of bending steel tubes. The outer diameter of the ducts for Specimen 1 was 2 in. and the outer diameter of the ducts for Specimen 2 was 4 in. The steel ducts were bent by a local steel fabricator to a 90° angle at a radius of 7 ft. for Specimen 1 and a 14 ft. radius for Specimen 2.

2.4 Instrumentation

To capture the behavior of the specimens throughout the structural testing, each specimen was heavily instrumented with various measuring devices. The instruments were typically installed at key polar coordinates, 15°, 45°, and 75° locations, along the curved wall section. The live-end and dead-end anchor block movement of each specimen was measured during the structural tests using linear potentiometers. Three linear potentiometers were used to measure the movement of the live-end anchor block for Specimen 1. For Specimen 2, the movements of the live-end and dead-end anchor blocks were measured using six linear potentiometers for each. Through-thickness (radial) expansions were directly measured using 15 linear potentiometers for Specimen 1 and 16 linear strain conversion transducers (LSCTs) for Specimen 2. These devices were able to measure the through-thickness expansions by passing through the cellulose tubes that were embedded into the curved wall sections, as shown in Figure 2-9. The linear potentiometers were connected to rigid metal pipe straps mounted on the inside face of the curved wall with metal wire. The LSCTs were connected to aluminum rods with heat shrink wrap and coupling nuts, so that when Specimen 2 failed, the rod would disconnect and the instrumentation would not get damaged.

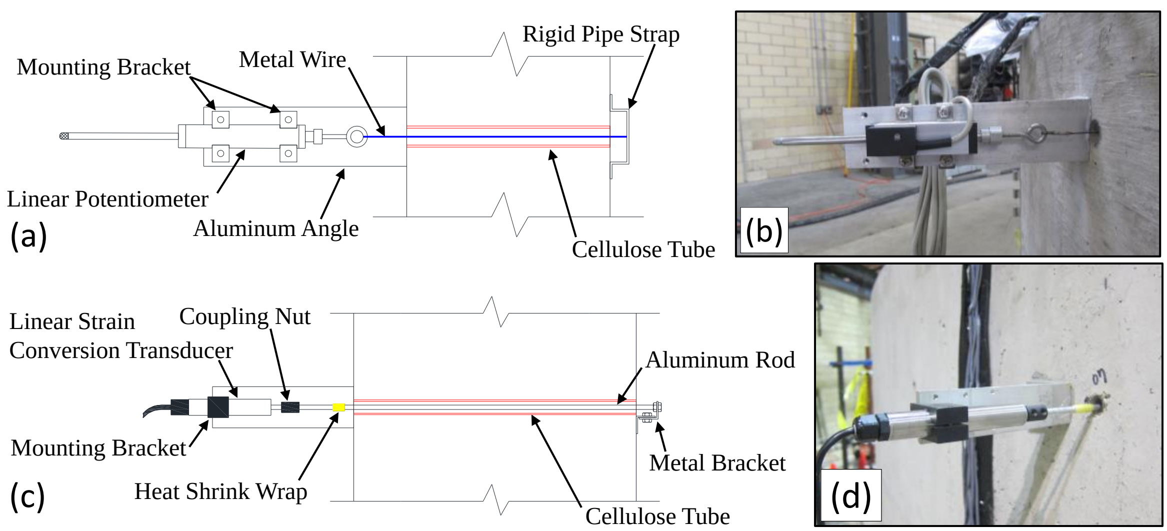

Figure 2-9: Details of Through-Thickness Instrumentations Showing: (a) Schematic of the Linear Potentiometer Setup, (b) Linear Potentiometer Attached to Specimen 1, (c) Schematic of the Linear Strain Conversion Transducer Setup, (d) LSCT Attached to Specimen 2

The linear potentiometers and LSCTs measured displacements near the locations of the ducts and at the middle of the wall sections. For Specimen 2, an additional LSCT was placed between the top two ducts at the 15° location. The polar locations of the instrumentations and the sectional locations of the linear potentiometers and LSCTs are presented in Figure 2-10.

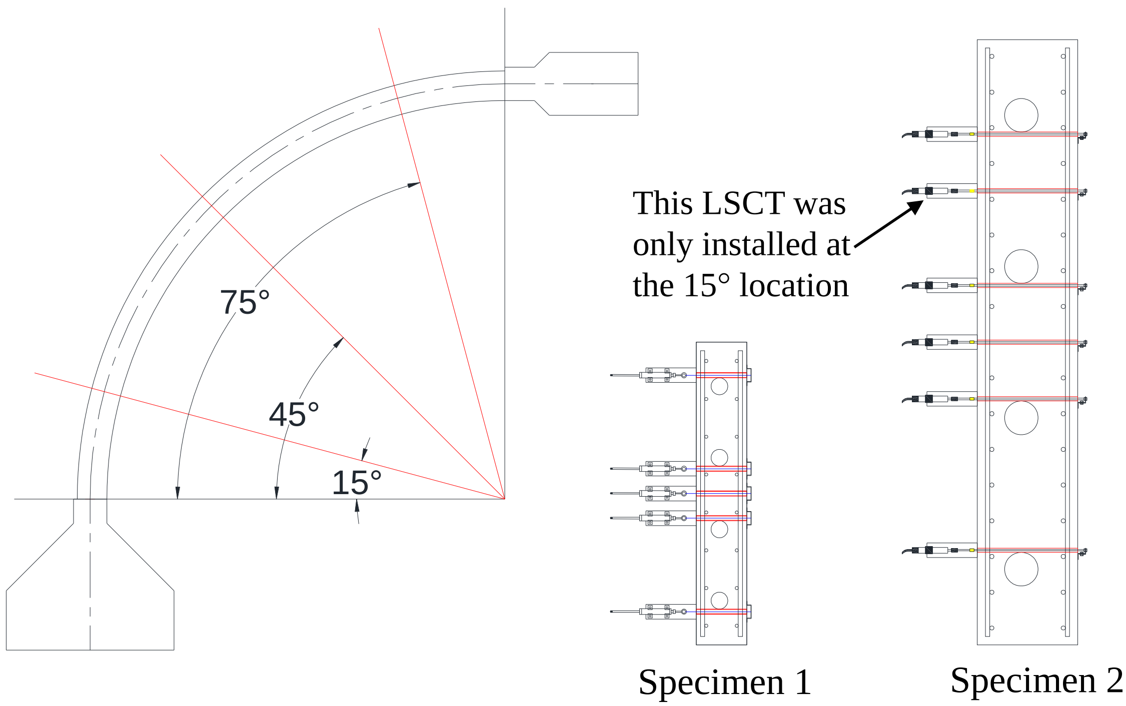

Figure 2-10: Polar Locations of the Instrumentations and Typical Sectional Locations of the Linear Potentiometers and Linear Strain Conversion Transducers

Four loads cells were positioned at both the live-end and dead-end anchor blocks to measure the load applied at both ends of each tendon group during the structural tests. The load outputs from each of the load cells were used to calculate the actual forces and stresses developed at each location of the curved wall. The arrangement of the load cells for each test specimen are provided in Section 2.5 and the layout of the load cells can be seen in Figure 2-14 and Figure 2-15 for Specimen 1 and Specimen 2, respectively.

The circumferential and vertical reinforcing bars for the inside and outside faces of each test specimen were instrumented with strain gauges (FLA-3 or FLA-5) at the 15°, 45°, and 75° locations. Most of the strain gauges were attached on the reinforcing bars near the duct locations, where the sectional maximum moments were expected to occur due to the prestressing force. The locations of the strain gauges attached to the reinforcing bars can be seen in Figure 2-11.

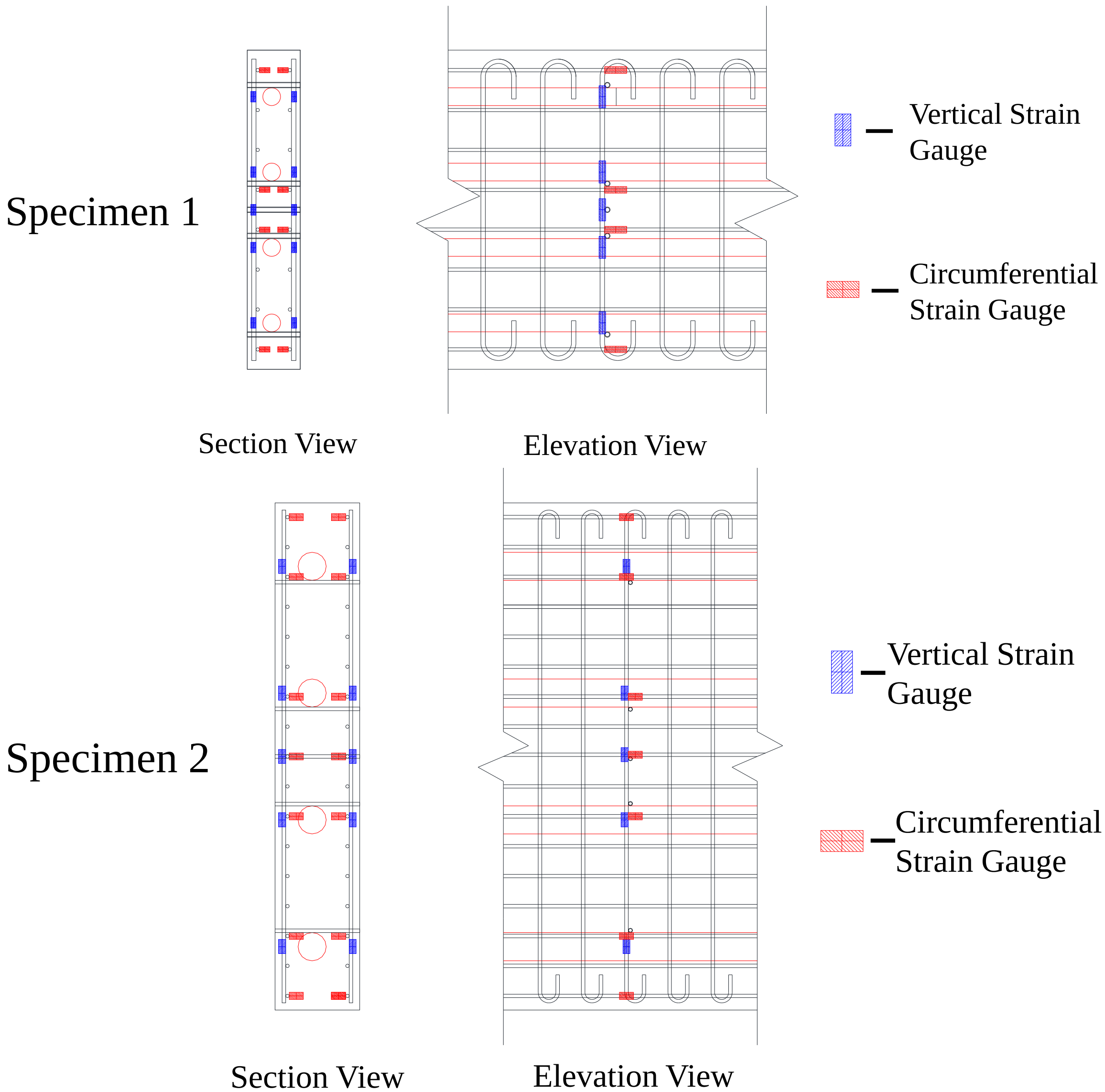

Figure 2-11: Strain Gauge Layout on Reinforcing Bars in the Curved Wall Sections

Several embedded concrete strain gauges (PLFM-60) were instrumented in both test specimens. Two embedded strain gauges were installed in Specimen 1 to measure through-thickness strains at the 45° location. One gauge was placed at the mid height of the section and the other was place just beneath the second duct from the top. Each embedded strain gauge was attached at the center of the wall to a cellulose tube, so that it would be stationary during the concrete cast. Thirty-six embedded strain gauges were installed in Specimen 2 and distributed among the 15°, 45°, and 75° locations; however, most were concentrated at the 15° location. For Specimen 2, embedded strain gauges were arranged to measure strains in the radial direction, as well as the circumferential direction. Similar to Specimen 1, the embedded strain gauges in Specimen 2 were attached to the cellulose tubes so that they were stationary during the concrete cast. Details of the embedded strain gauges at the 15° location for Specimen 2 can be seen in Figure 2-12.

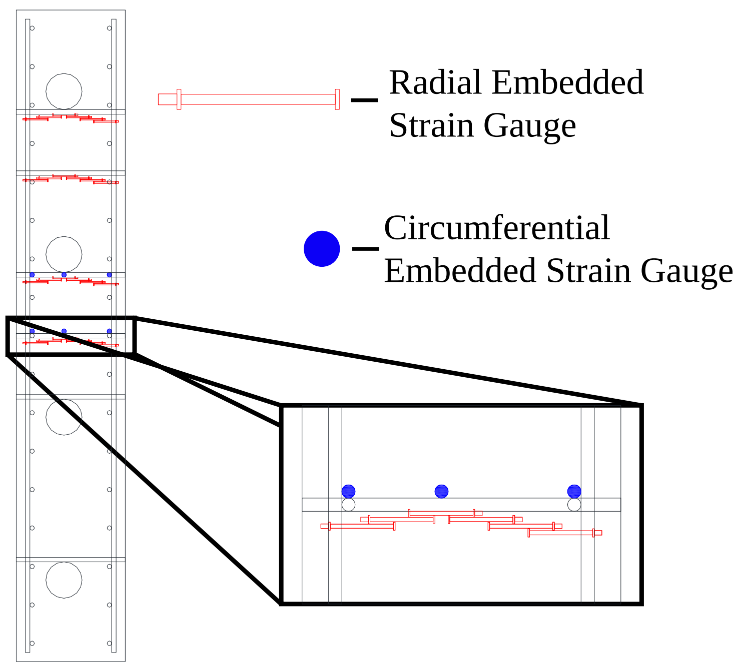

Figure 2-12: Layout of Embedded Strain Gauges at the 15° Location of Specimen 2

Concrete surface strain gauges (PL-60-11) were also used on the top surfaces of both specimens. One surface strain gauge was installed at each of the 15°, 45°, and 75° locations for Specimen 1. Six surface gauges were installed on the top surface at each of the 15°, 45°, and 75° locations of Specimen 2, and they were arranged in a staggered fashion so that the entire width of the wall was measured, which can be seen in Figure 2-13. Surface gauges were also installed on the inside and outside surfaces of the wall section of Specimen 2 at mid height at the 15°, 45°, and 75° locations. Additional surface gauges were installed just below the second duct from the top at the 15° location, one on the inside and outside surface.

Figure 2-13: Concrete Surface Gauge Arrangement for the Top of Specimen 2

NDI Optotrak Certus system was used to measure the overall movement of the test specimens during the structural tests. The system uses targets that emit infrared signals to a camera which tracks the movement of the targets using a 3-D coordinate system. For Specimen 1, the targets were placed on top of the wall, and covered the entire curved wall section. The targets were placed on either edge of the wall and spaced 5 in. apart. For Specimen 2, targets were placed both on top and on the inside surface of the curved wall section. The targets on top of the wall were placed on either edge and spaced 12 in. apart, starting at the 0° location and continuing to approximately the 57° location. The targets on the inside surface of the curved wall section were spaced 18 in. apart along the length of the wall and were spaced 9 in. apart over the height of the wall. The targets on the inside surface began at the 0° location and continued to approximately the 43° location.

2.5 TEST SETUP AND LOADING PROCEDURE

For both test specimens, the live-end anchor block was tied down to the laboratory strong floor with approximately 240 kips of force. To minimize friction between the base of the test specimen and the wood platform surface, two layers of Teflon sheets were placed under the curved wall and dead-end anchor block. These boundary conditions created a statically-determinate condition with a fixed-free boundary for both specimens.

For Specimen 1, four 60-ton center-hole hydraulic rams and four 500 kip center-hole load cells were placed around the ducts at the live-end anchor block. Steel bearing plates measuring 1 in. x 8 in x 8 in. with a 2 in. diameter hole in the center were placed between the rams and the live-end block. A tension ring with a tapered hole was placed between each of the rams and load cells to reduce the spacing of the strands to fit in the 2 in. diameter of the ducts. Steel spacers measuring 1 in. x 5.5 in. x 5.5 in. with a 2.5 in. diameter hole in the center were placed between the anchor heads and the loads cells at both the live-end and dead-end anchor blocks for easy removal of the test setup after the structural test. Four 500 kip center-hole load cells were also placed at the dead-end anchor block in order to measure the loads from the dead-end anchor block.

Four 0.6-in. diameter seven-wire strands were placed in each of the ducts of Specimen 1. The slack was removed from each of the strands at the live-end anchor block prior to the structural test to ensure uniform tensioning of the strands and to secure the ram stroke. 1 kip of force was applied to each strand using a monostrand stressing jack for the slack removal. Load was applied to Specimen 1 by the hydraulic rams pushing the anchor heads away from the live-end anchor block. Each tendon group was stressed at the same rate of load using a hydraulic manifold system, so the prestressing loads applied to each individual tendon group were equal during the structural test. Graphic images, as well as a picture, of the test setup for Specimen 1 can be seen in Figure 2-14.

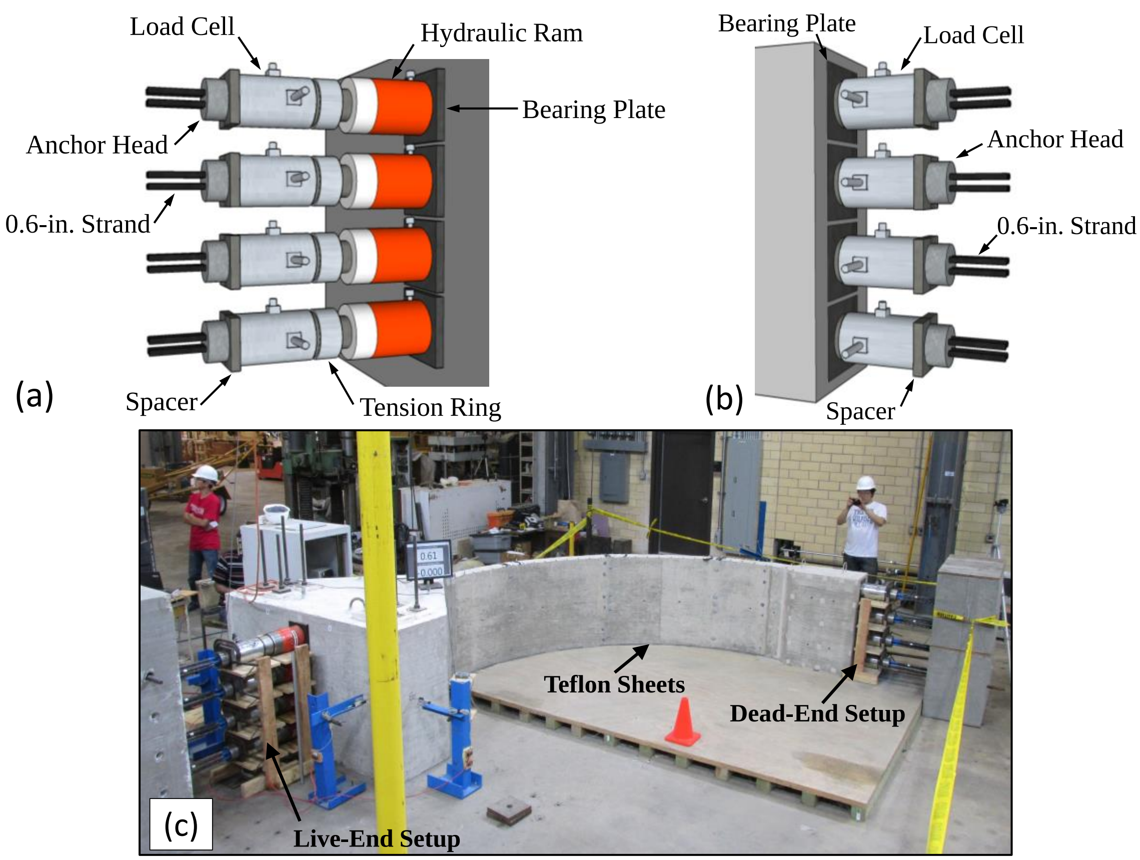

Figure 2-14: Test Setup for Specimen 1 Showing: (a) Live-End Setup, (b) Dead-End Setup, (c) Overall View of the Test Setup

The test setup for Specimen 2 was modified from Specimen 1 due to the increase in size and load demand. A 10 in. x 48 in. x 96 in. steel plate with four machined holes at the duct locations was used as a stressing plate. The stressing plate was supported by two 8 in x 8 in. x 1 in. L-shaped steel angles that were 66 in. in length. Eight 3/8 in. x 3 in. steel flat bars that were 8 ft. in length connected the angles and the stressing plate for lateral support. The stressing plate was placed on a 2 in. x 92 in. x 72 in. steel bottom plate. Teflon sheets were epoxied to the angles on the stressing plate and the bottom plate so that the friction between the stressing plate and bottom plate was minimized. Steel flat bars were welded to the stressing plate in order to hold the four 1000 kip center-hole load cells and the four anchor heads. Four machined spherical washers that were 12 in. in diameter and 3-in. thick with a 6.25-in. diameter center-hole were placed between each of the anchor heads and the load cells to eliminate an eccentric loading condition upon loading. Four 400-ton hydraulic rams were placed between the live-end anchor block and the stressing plate. Bearing plates measuring 51 in. x 15 in. x 1 in. were placed between the rams and the live-end anchor block. Both the rams and the bearing plates were mounted to the live-end anchor block using 3/4 in. threaded rods that were embedded into the live-end anchor block. Four 1000 kip center-hole load cells, four anchor heads, and four spherical washers were also placed at the dead-end anchor block in order to measure the applied loads from both ends of the test specimen.

Nineteen 0.6-in. diameter seven-wire strands were inserted into each of the ducts of Specimen 2. The slack was removed from each of the strands from both the live-end and the dead-end anchor blocks prior to the structural test to ensure uniform tensioning of the strands and to secure the ram stroke. 1 kip of force was applied to each strand using a 12-ton center-hole ram and a 0.6-in. diameter monostrand chuck to remove the slack. Once all the strands had their slack removed, the pressure was released from the 400-ton rams so that there was no load on Specimen 2 prior to the structural test. Load was applied to Specimen 2 from the 400-ton rams pushing the stressing plate away from the live-end anchor block and tensioning the strands. All four of the rams were connected to the same hydraulic manifold to ensure an equal distribution of pressure, therefore an equal load, was applied to each ram during the structural test. The load outputs measured from each load cell showed approximately uniform distribution of the load on each tendon group.

It should be noted that two 250-ton hydraulic rams were inserted between the 400-ton rams in case the 400-ton rams reached their maximum capacity prior to the delamination failure of Specimen 2. However, the 250-ton rams were not used during the structural testing of Specimen 2 and therefore can be disregarded. Figure 2-15 shows graphic images and a photograph of the test setup for Specimen 2.

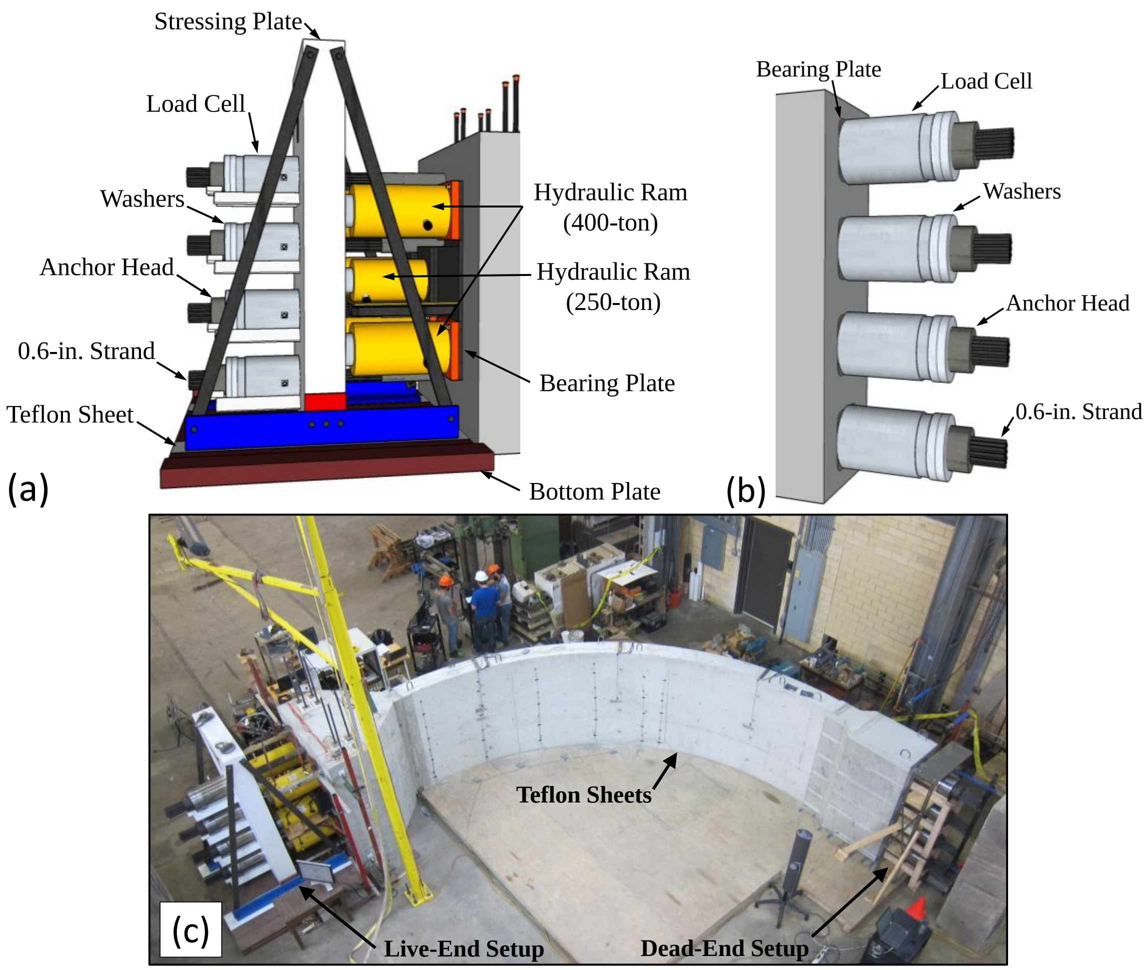

Figure 2-15: Test Setup for Specimen 2 Showing: (a) Live-End Setup, (b) Dead-End Setup, (c) Overall View of the Test Setup

Both of the curved wall specimens were structurally tested under monotonically increasing prestressing loads, therefore stoppages during the loading sequences were kept to a minimum. Each specimen was loaded slowly to ensure that all aspects of the specimen response could be captured by the instrumentation. Specimen 1 was loaded at an average rate of 125 lb./sec., and gradually increased to an average load rate of 360 lb./sec. The load was applied in 50 kip increments up to a load level of 350 kips. At each load increment, the load was briefly held to inspect the specimen and to take pictures. Once the 350 kip load was surpassed, the specimen was loaded up to the delamination failure. Specimen 2 was tested in the same manner as Specimen 1. Specimen 2 was loaded at an average rate of 200 lb./sec., and gradually increased to an average load rate of 410 lb./sec. The load was applied in 100 kip increments up to 1000 kips. After surpassing 1000 kips, the load was applied in 200 kip increments up to 2000 kips. Upon reaching each load stage increment, the specimen was briefly inspected and pictures were taken. After surpassing 2000 kips, Specimen 2 was loaded up to the delamination failure.

Chapter 3: Experimental Results

3.1 Test Observations

In the following discussion, the delamination failure is examined using the compressive stresses in the concrete from the prestressing load as related to the strength of the concrete. The delamination failure of both test specimens was very sudden and was explosive in nature. From inspection of the video recordings for the structural tests of the specimens, it was concluded that the delamination failures initiated approximately at the 15° locations of the wall sections. The delamination failures occurred in this region of the test specimens and propagated throughout the rest of the structures. This location of the failure was anticipated due to the large friction losses experienced by the strands over the length of the structure. For Specimen 1, the delamination crack extended from the 0° location to approximately the 68° location of the wall section. The delamination crack of Specimen 2 extended from the 0° location to approximately the 78° location. Figure 3-1 shows images of the failed test specimens.

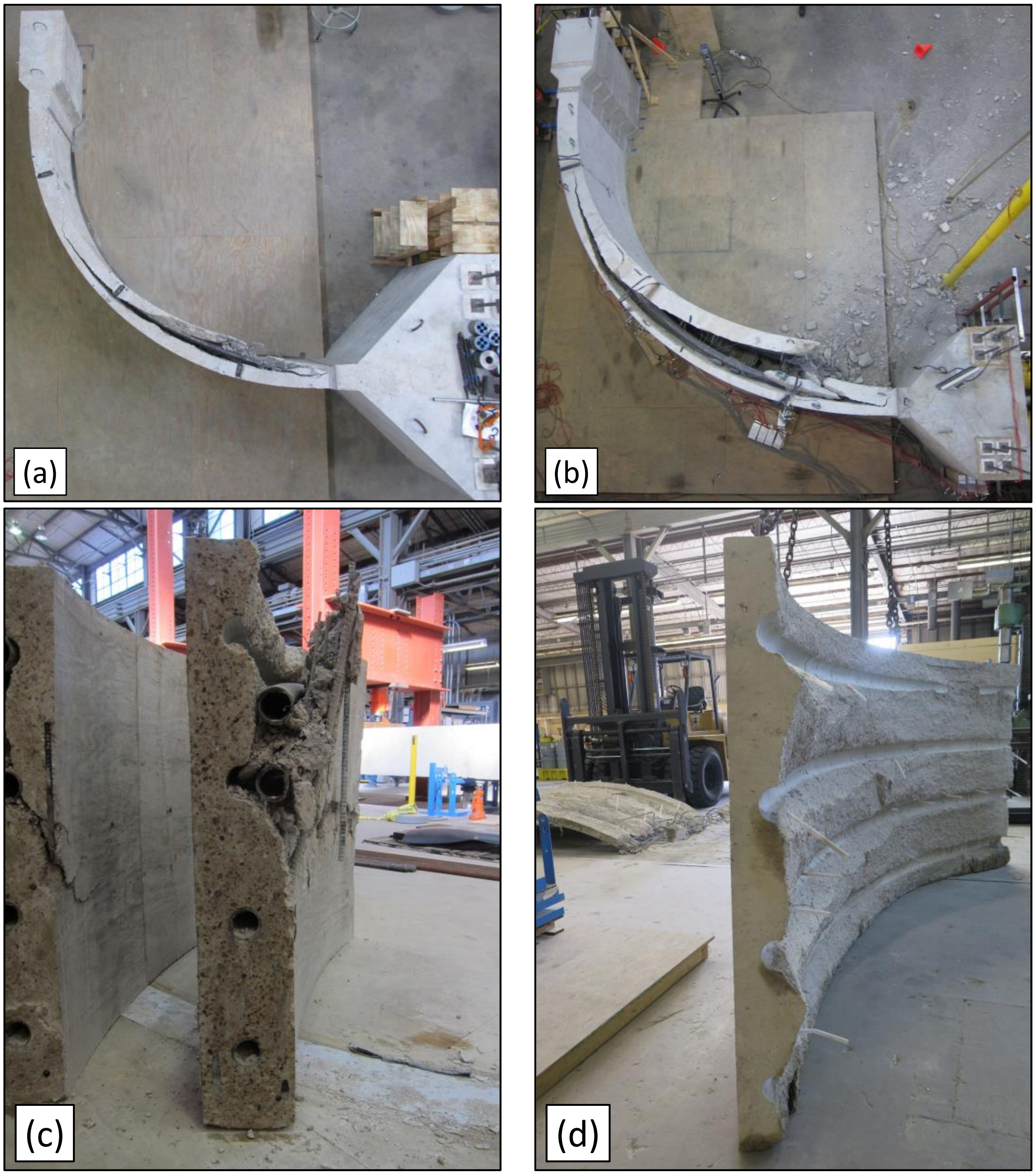

Figure 3-1: Failed Test Specimens Showing: (a) View from Top of Specimen 1, (b) View from Top of Specimen 2, (c) 15° Section of Specimen 1, (d) 8° Section of Specimen 2

For both specimens, the delamination crack started at the top duct and then spread toward the bottom duct. A possible cause for this progressive delamination crack development is the variation in the density of the concrete comprising the curved wall sections. It is believed that when the concrete was cast, the internal vibration may have induced water and paste migration towards the top surface, typical of concrete placement. Therefore, the concrete at the top of the specimens may have been slightly weaker than that at the bottom surface of the test specimens. Another suspected cause for the failure of the walls section to occur in this order was the different boundary conditions provided at the top and bottom surfaces of the curved wall specimens. Although two layers of Teflon sheets were placed under the curved wall sections to minimize friction of the wall section in the horizontal direction, the rotational movement was somewhat restricted. The rotational movement at the bottom of the curved wall sections was restrained by the self-weight of the structure above; however, the top of the curved wall section was unrestrained. These hypotheses on the failure of the test specimens can be supported through the examination of the delamination measurements taken at the 15° location. For both specimens, the through-thickness expansions at the top duct were found to be predominant throughout the duration of the structural tests, which is shown in Figure 3-2 and Figure 3-3. Given that the prestressing load was similar at each duct, the previously mentioned failure hypotheses were deemed plausible.

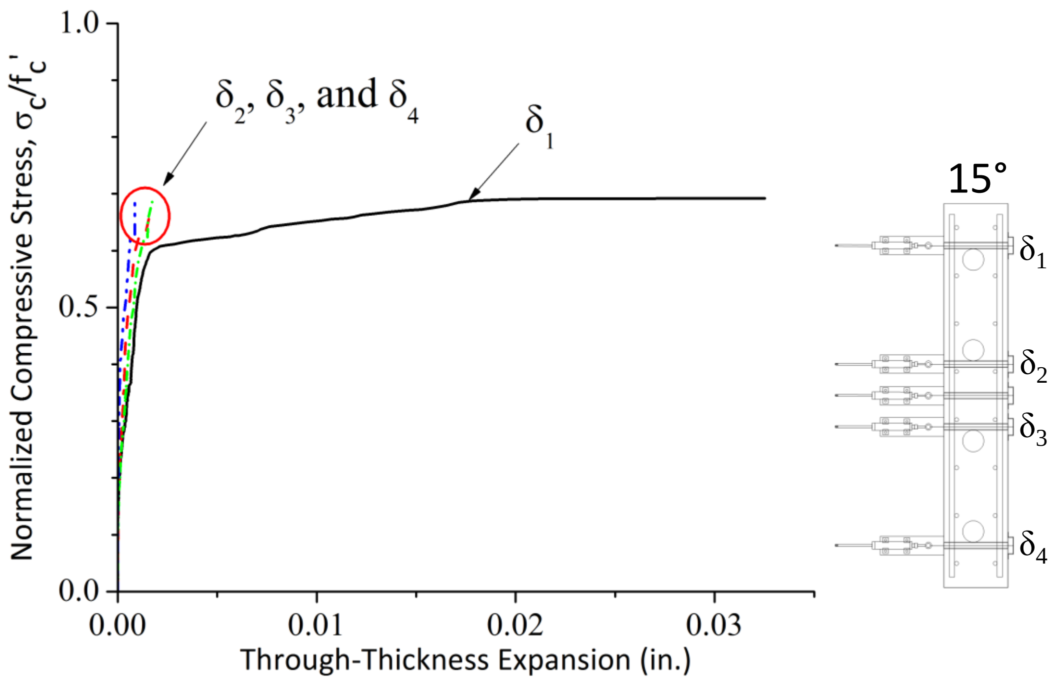

Figure 3-2: Through-Thickness Expansion at the 15° Location of Specimen 1

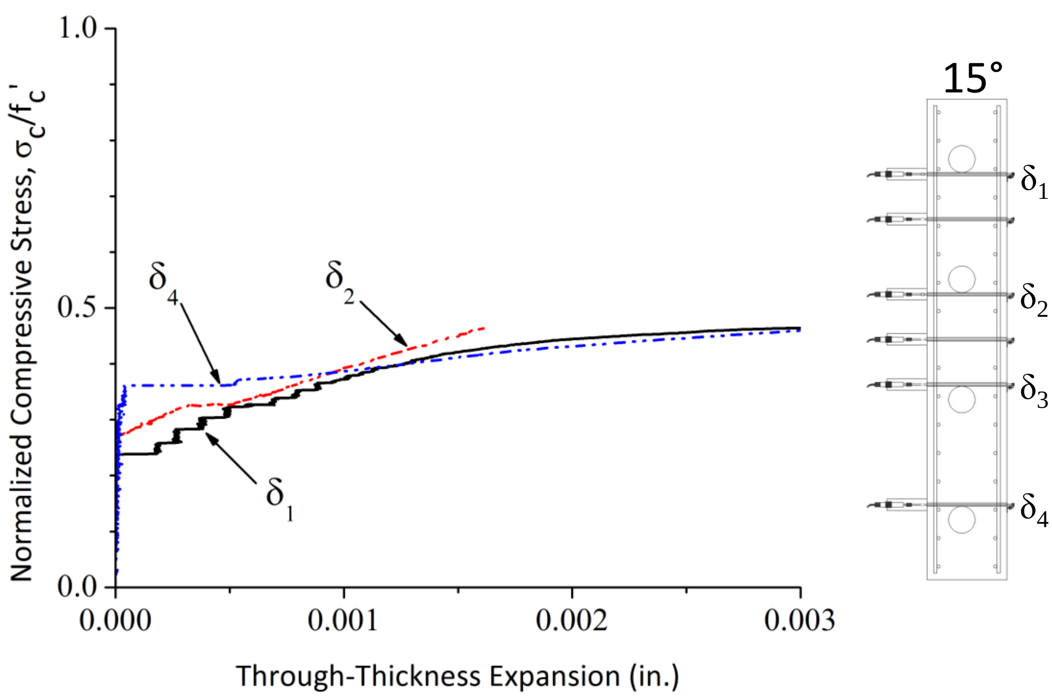

Figure 3-3: Through-Thickness Expansion at the 15° Location of Specimen 2

Another observation from the structural testing of the curved wall sections was the effectiveness of the duct offset. The ducts were offset towards the outer surface of the wall sections to minimize the out-of-plane bending of the structure owing from eccentrically located strands within a curved duct, as discussed in section 2.1. Figure 3-4 and Figure 3-5 display the average strains of the circumferential reinforcing bars versus the compressive stress at the 15° location for Specimen 1 and Specimen 2, respectively. It can be seen that the circumferential strain readings for the inside and outside surfaces were similar for both specimens, implying that the wall sections did not experience any significant degree of bending.

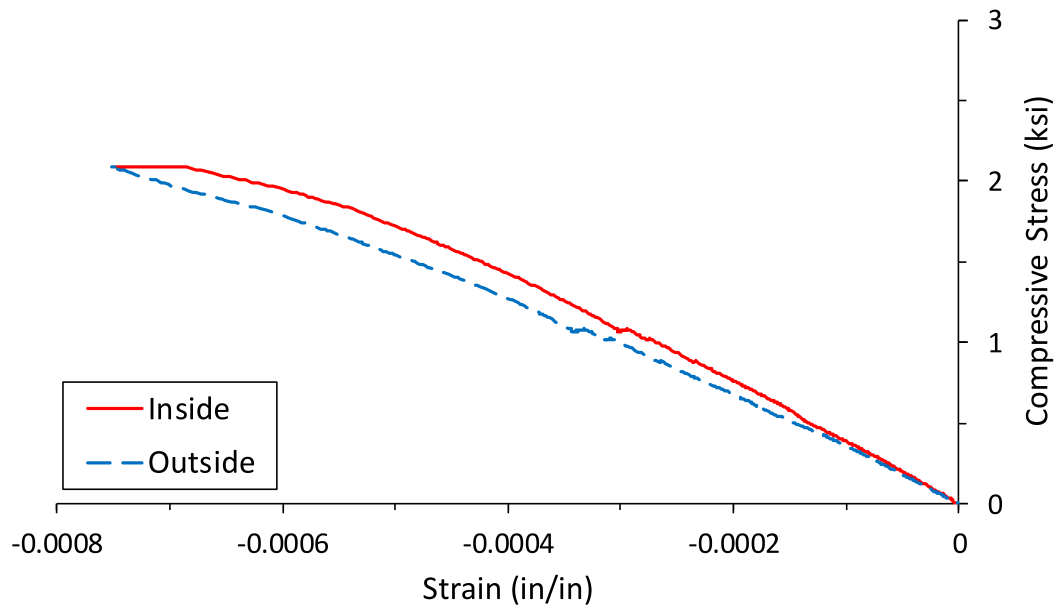

Figure 3-4: Compressive Stress versus Average Strain of the Circumferential Reinforcing Bars at the 15° Location of Specimen 1

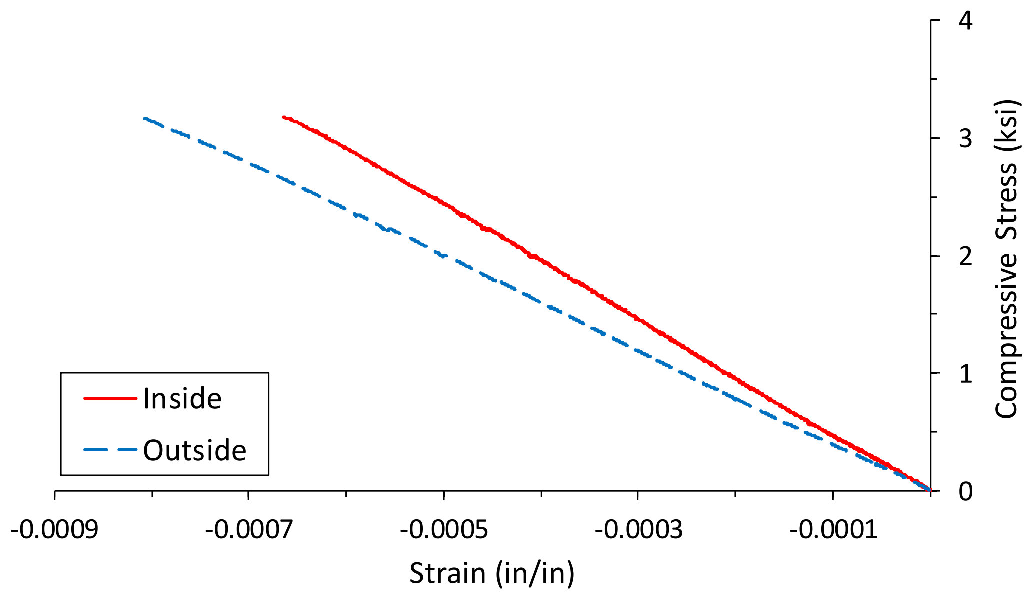

Figure 3-5: Compressive Stress versus Average Strain of the Circumferential Reinforcing Bars at the 15° Location of Specimen 2

After the structural test of Specimen 1, it was decided to attach linear potentiometers to the dead-end block of Specimen 2 in order to measure its movement during testing. The linear potentiometers were attached to the top and bottom of the dead-end block at three locations. The displacement readings, displayed in Figure 3-6, also showed that the dead-end anchor block shrank along the line of prestressing and the out-of-plane bending was minimal. The NDI Optotrak Certus system data for Specimen 2, shown in Appendix C, also revealed that the specimen did not experience much bending. Therefore, offsetting the ducts was effective in minimizing the out-of-plane bending and the specimens behaved as intended.

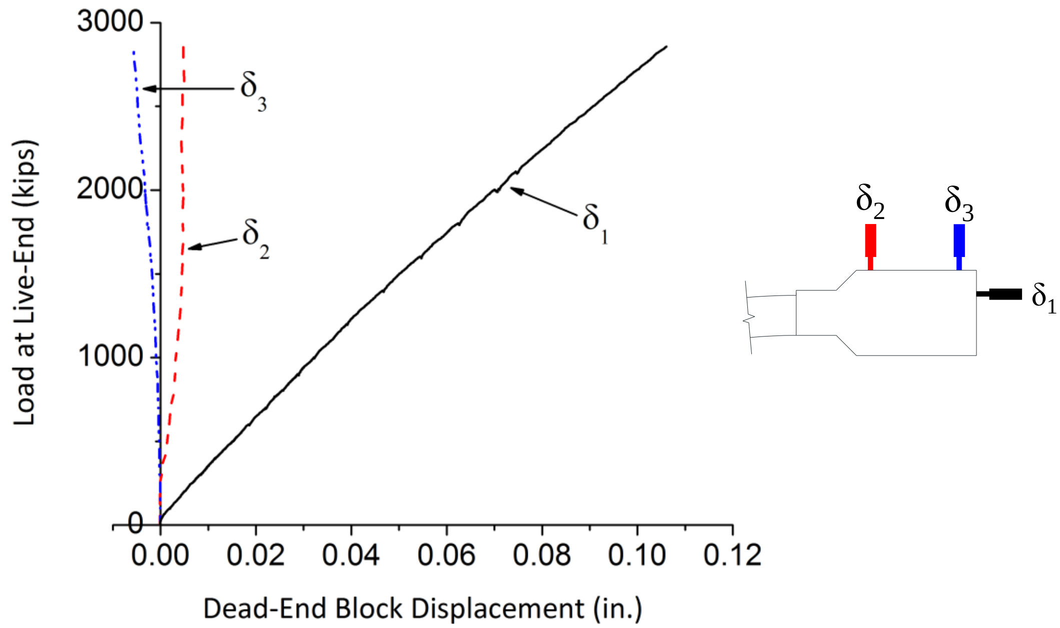

Figure 3-6: Average Displacement of the Dead-End Anchor Block versus Live-End Load for Specimen 2

3.2 Friction Loss

To determine the applied compressive stresses at any location along the specimens, friction losses must be taken into account. The large angle change of the test specimens results in large losses of load due to friction. The friction losses for each curved wall specimen were estimated using the friction loss equation presented in ACI 343R-95.

$$f_f = f_{po}\left(1 - e^{-(Kl+\mu\alpha)}\right) \qquad \text{Equation 3-1 (ACI 343R-95)}$$

Where: f_f = stress due to friction loss

f_{po} = stress at the jacking end

K = wobble coefficient

μ = curvature coefficient

l = length of duct

α = total angular change of prestressing profile in radians

The coefficients of wobble and curvature are dependent on the duct material and the type of tendons used for prestressing. The coefficients presented in ACI 343R-95 are shown in Table 3-1, highlighted are the coefficients that applied to the curved wall specimens.

Table 3-1: Friction Coefficients for Post-Tensioning Tendons (ACI 343R-95)

Types of tendons and sheathing	Wobble coefficient, K, per ft.	Curvature coefficient, μ
Tendons in flexible metal sheathing		
- wires	0.0010-0.0015	0.15-0.25
- 7-wire strands	0.0005-0.0020	0.15-0.25
- high-strength bars	0.0001-0.0006	0.08-0.30
Tendons in rigid and semi-rigid galvanized		
- 7-wire strands	0.0002	0.15-0.25
Pregreased tendons		
- Wires and 7-wire strands	0.0003-0.0020	0.05-0.15
Mastic-coated tendons		
- Wires and 7-wire strands	0.0010-0.0020	0.05-0.15

The wobble coefficient was assumed as 0.0002 per ft. and the curvature coefficient was assumed as 0.25 to give a conservative estimate of the friction losses. Based on the equation presented in ACI 343R-95, the friction losses were calculated to be approximately 33 % for both specimens. It should be noted that the wobble coefficient increased the friction losses less than 1 %, therefore it was ignored for subsequent calculations. Due to the large friction losses, the delamination failure occurred close to the live-end anchor block where the load was greater. Using the loads measured by the load cells at both the live-end and dead-end, there was an average friction loss of 46.8 % for Specimen 1 and 45.2 % for Specimen 2. These values represent 43 % and 38 % larger friction losses for Specimens 1 and 2, respectively, than that calculated from the ACI 343R-95 code. This implies that a modification of the friction coefficients presented in the code equation may be necessary for large angle structures. Figure 3-7 below shows the measured loads from the live-end and dead-end versus the strand elongation of Specimen 2. The elongation of the strands for Specimen 1 was not measured, therefore a plot of load versus strand elongation could not be provided.

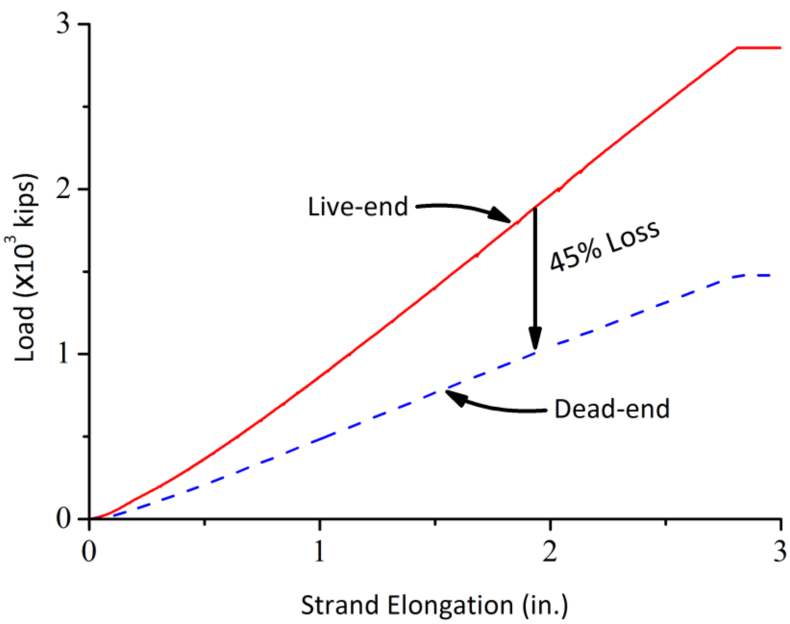

Figure 3-7: Measured Friction Losses for Specimen 2

Using the friction loss equation presented in the ACI 343R-95 code and the loads measured from the structural tests, modified friction coefficients of μ=0.40 and μ=0.38 for Specimens 1 and 2, respectively, were calculated. The modified friction coefficients are used for all discussions in Chapter 3 to calculate the prestressing load at given angles for both structures. Figure 3-8 compares the friction loss coefficients presented in the ACI 343R-95 code versus the modified coefficients throughout the curvature of the wall sections.

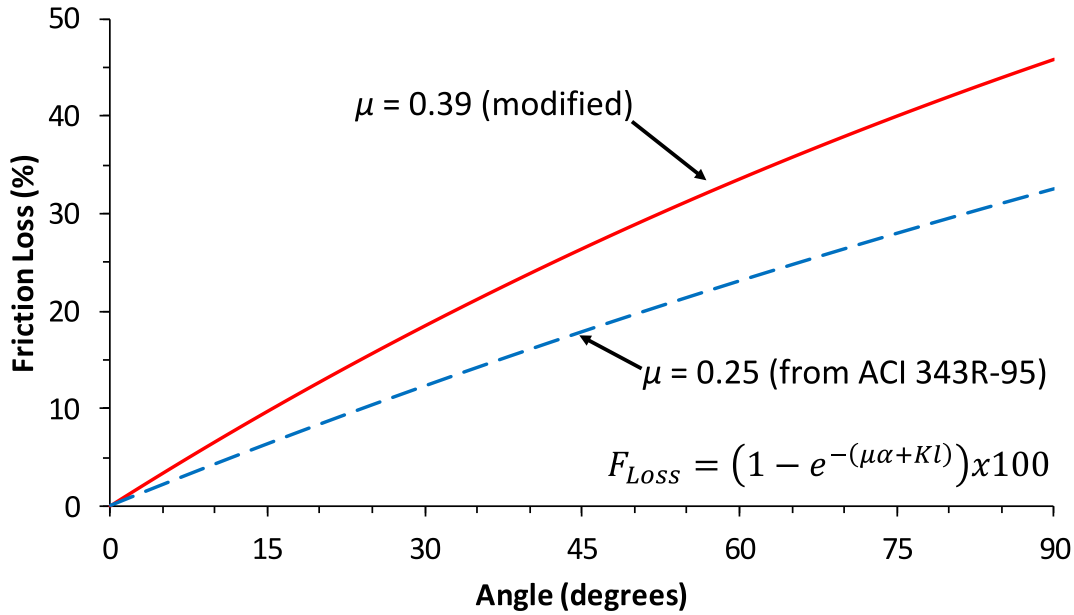

*The wobble coefficient, K, was not used in this calculation of friction losses

Figure 3-8: Comparison of the Modified Friction Coefficient Based on the Measured Loads and the Friction Coefficient Based on ACI 343R-95

3.3 Delamination Failure Capacity

In order to directly compare the delamination failure capacities of both test specimens, the failure loads were normalized in terms of their respective concrete strengths. It should be noted that only the instrumentation at the duct locations were used for this discussion. Other measurements recorded during the structural tests can be found in Appendix C. Some instrumentations did not function properly during the structural tests and their results were omitted from this discussion.

The failure load at the 15° location was 424 kips for Specimen 1 and 2585 kips for Specimen 2. These loads were divided by the gross sectional area of each specimen to calculate the compressive stresses at delamination failure. The compressive stresses at failure, $\sigma_{failure}$, for Specimen 1 and Specimen 2 were 2.08 ksi and 3.18 ksi, respectively, corresponding to failure at 69 % and 47 % of the compressive strength. Figure 3-9 compares the normalized compressive stresses of each specimen with their respective dimensions. It should be noted that since the normalized compressive stresses of Specimen 1 were higher than Specimen 2, the through-thickness expansion of Specimen 1 was more affected by the Poisson's effect.

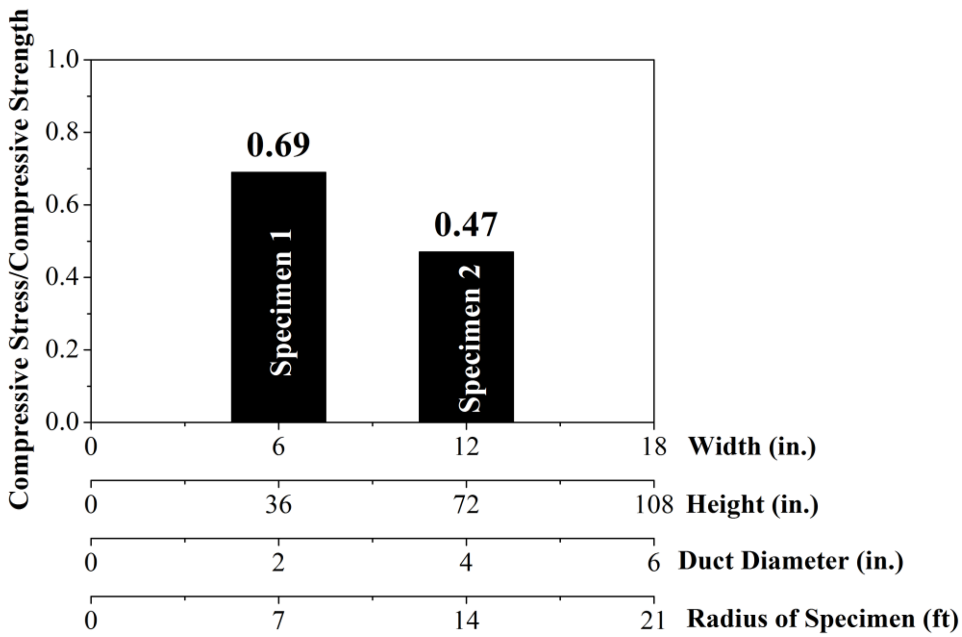

Figure 3-9: Size Effect on the Delamination Failure

3.4 INDICATION OF DELAMINATION

An indicator of an ensuing delamination failure is the initiation of the first delamination crack. In an attempt to identify the initiation of the delamination crack, direct and indirect instrument measurements were used for the test specimens. Through-thickness expansions were directly measured using linear potentiometers and linear strain conversion transducers (LSCTs). An indirect method for determining the initiation of the delamination crack was through the vertical strain gauges instrumented on the inside face of both specimens.

Another method to identify the onset of delamination cracks would be the inspection of horizontal surface cracks; however, the inspection of surface cracks during the testing of the curved wall specimens was considered too dangerous to carry-out due to the large prestressing forces that were applied and the explosive nature of the delamination failures. Therefore, vertical reinforcement strains were used to indirectly measure the delamination cracks.

Prior to the initiation of the delamination crack, it is suspected that the through-thickness expansion was too small to be measured by the linear potentiometers and LSCTs. Though once the delamination crack formed, apparent expansions were measured by the instruments. At 19 % of the failure load of Specimen 1, the through-thickness measurements at the top three ducts simultaneously showed significant expansions, as seen in Figure 3-10 through Figure 3-12, indicating the formation of a delamination crack. At approximately 28 % of the failure load, the bottom duct showed the initiation of delamination cracking at the 15° location. At approximately 87 % of the failure load, there was another increase in the measured through-thickness deformations and the slope of the measurements begins to flatten out. This was a good indicator that the ultimate delamination failure was about to occur.

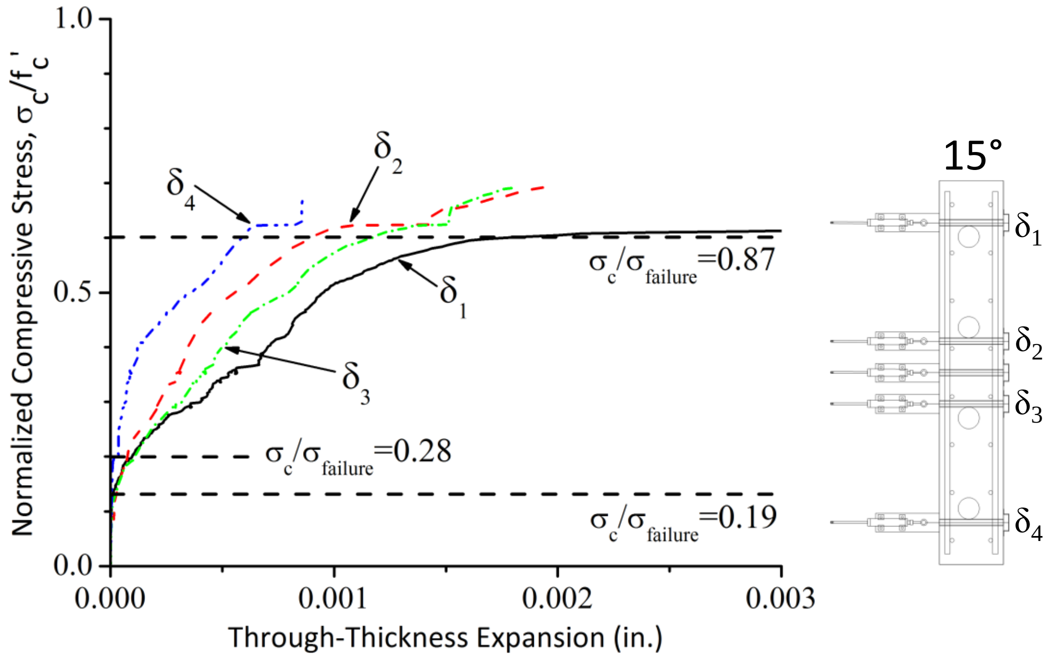

Figure 3-10: Through-Thickness Expansions versus Normalized Compressive Stresses at the 15° Location of Specimen 1

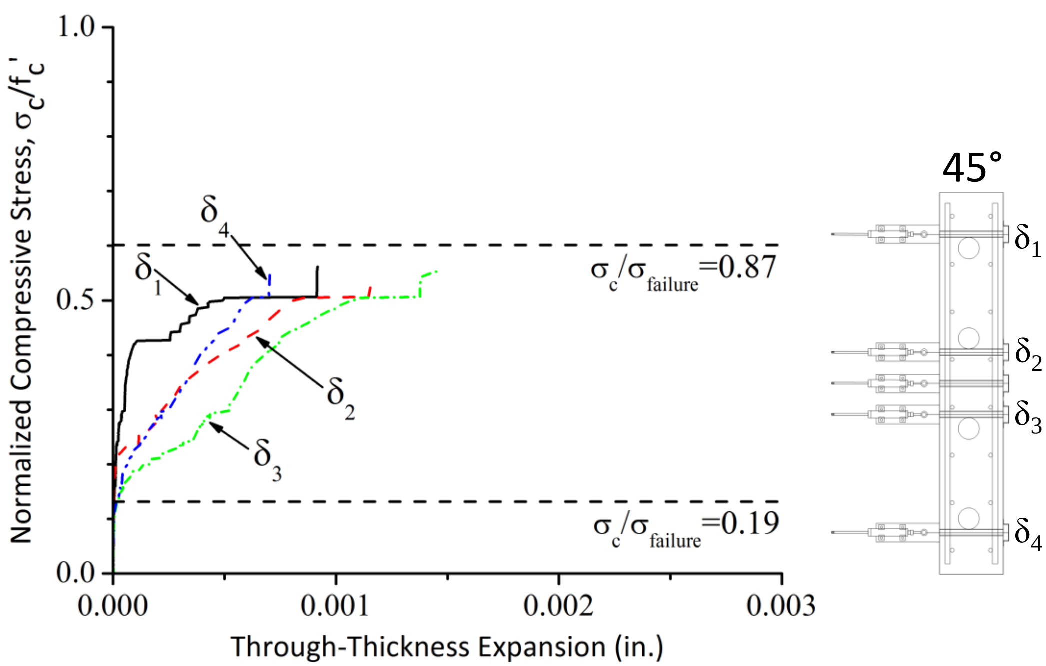

Figure 3-11: Through-Thickness Expansions versus Normalized Compressive Stresses at the 45° Location of Specimen 1

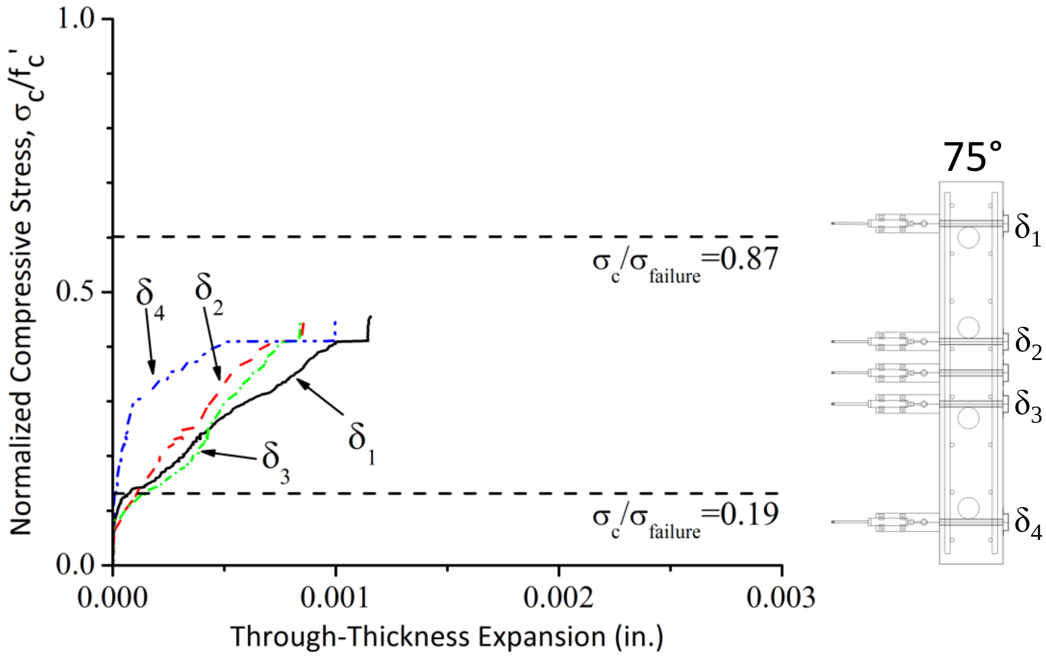

Figure 3-12: Through-Thickness Expansions versus Normalized Compressive Stresses at the 75° Location of Specimen 1

For Specimen 2, a similar trend is also seen in the through-thickness expansion measurements, shown in Figure 3-13 through Figure 3-15. The delamination crack initiated at the top duct at 50 % of the failure load. The second duct from the top and the bottom duct showed increased deformations at approximately 60 % and 78 % of the failure load, respectively. The LSCT at the 15° location of the third duct did not function properly during the structural test of Specimen 2 and therefore its results were not reported. Similar to Specimen 1, there was another increase in the through-thickness deformations at approximately 87 % of the failure load of Specimen 2, indicating that the ultimate delamination failure would occur soon. It should be noted that the initiation of delamination cracking occurred at a lower normalized stress for Specimen 1 than for Specimen 2.

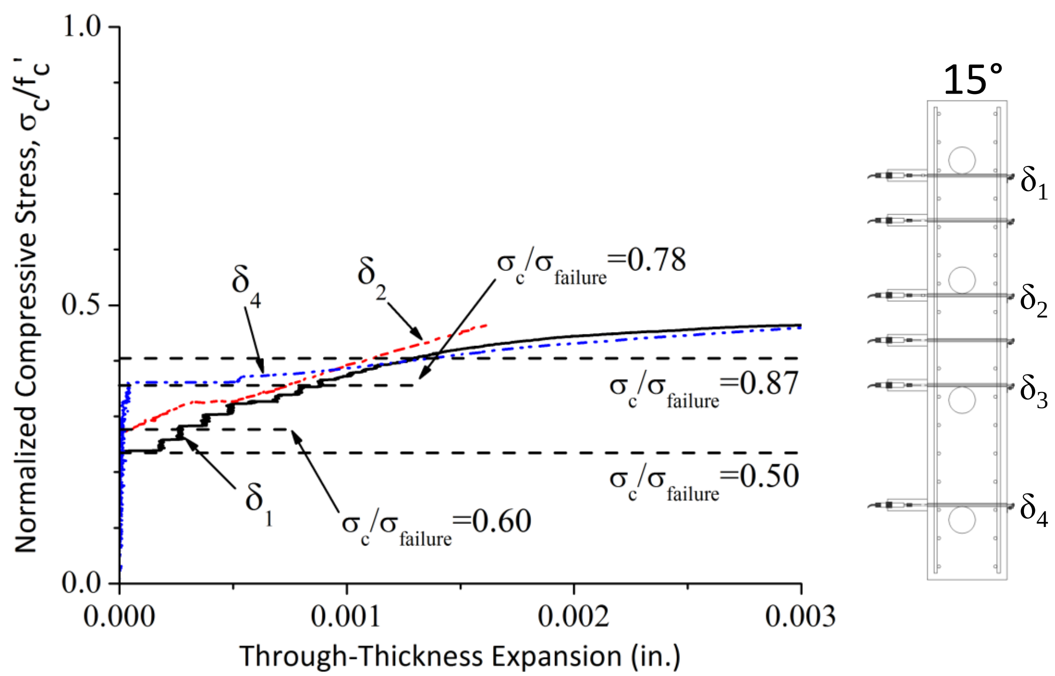

Figure 3-13: Through-Thickness Expansions versus Normalized Compressive Stresses at the 15° Location of Specimen 2

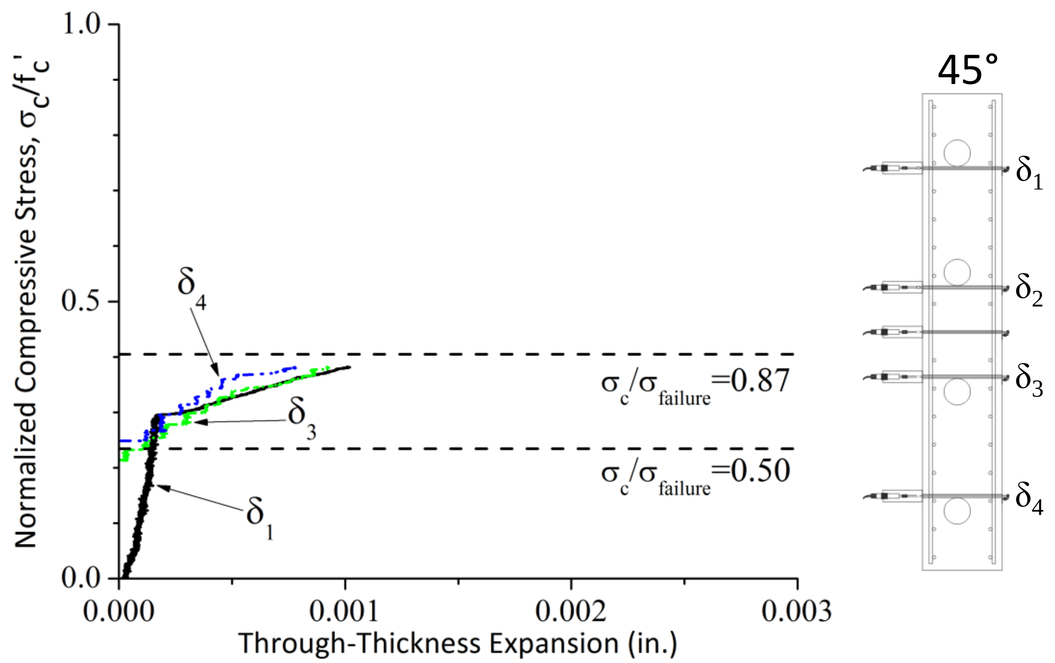

Figure 3-14: Through-Thickness Expansions versus Normalized Compressive Stresses at the 45° Location of Specimen 2

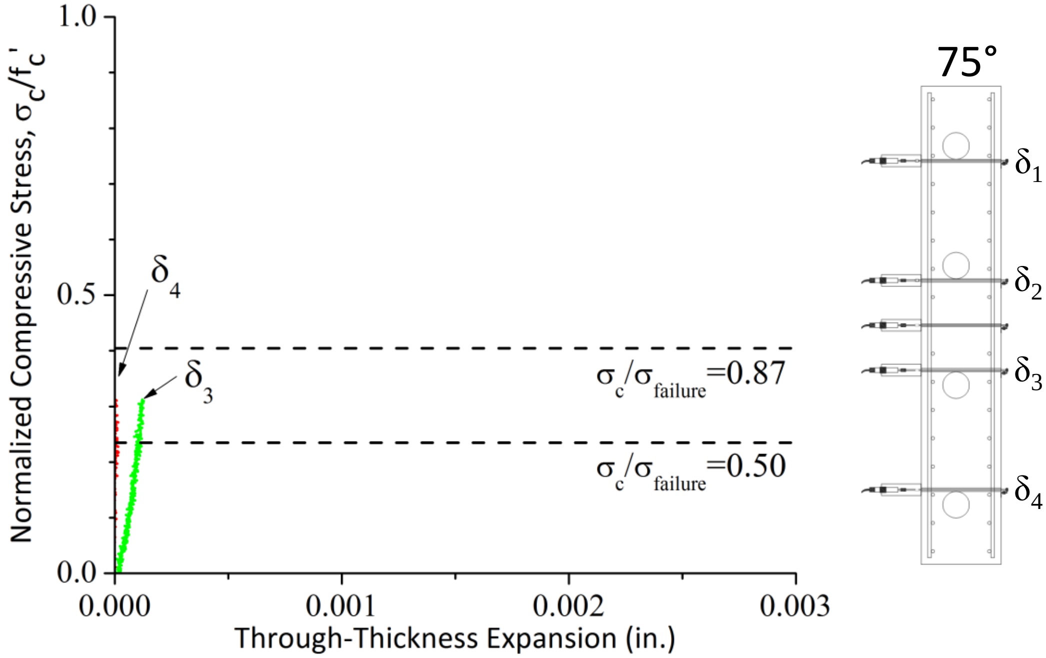

Figure 3-15: Through-Thickness Expansions versus Normalized Compressive Stresses at the 75° Location of Specimen 2

The vertical strain measurements on the inside face also showed good correlation with the through-thickness expansion data. Initially the vertical strains showed linear responses and then had a gradual change in slope, which can be seen in Figure 3-16 through Figure 3-18. This change in slope of the vertical strain readings can be associated with the initiation of the delamination crack. For Specimen 1, the vertical strains showed a linear trend up to approximately 32 % of the failure load. At around 87 % of the failure load, the slope of the vertical strain gauge at the 15° location of the top duct begins to flatten out. This flattening of the slope occurred at the same load level as the through-thickness expansion data, therefore both measurements coincide with the indication of the ensuing delamination failure.

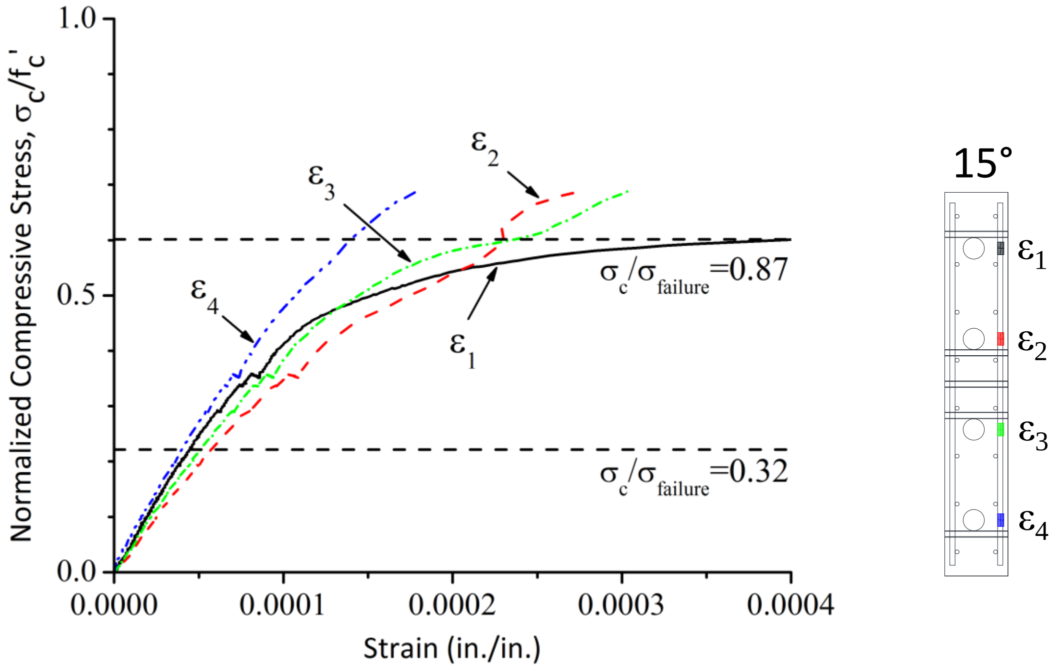

Figure 3-16: Inside Face Vertical Strains versus Normalized Compressive Stresses at the 15° Location of Specimen 1

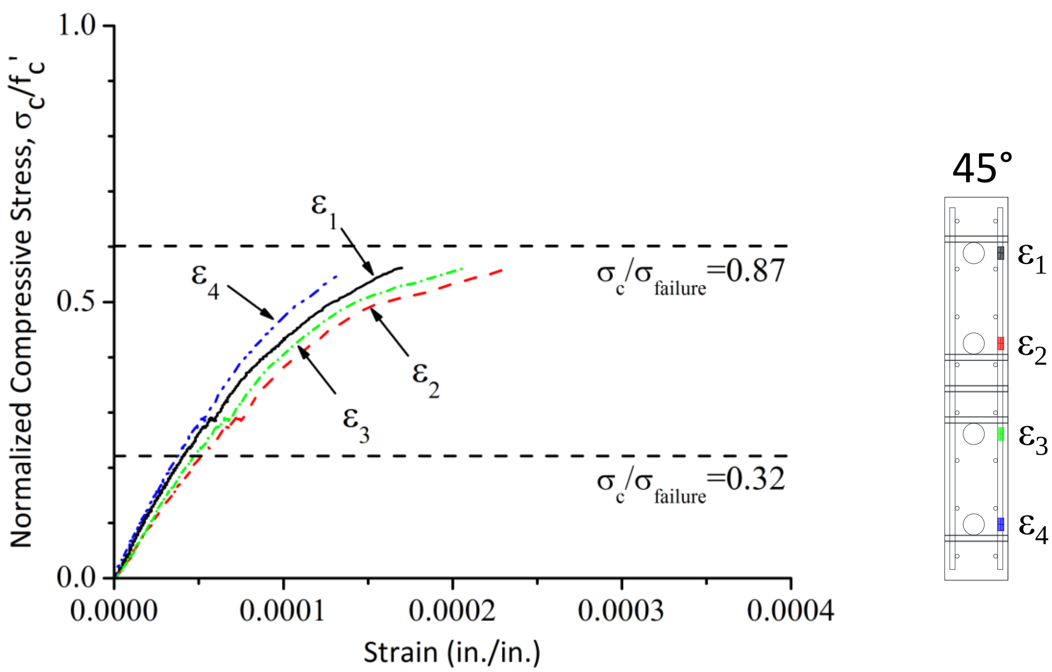

Figure 3-17: Inside Face Vertical Strains versus Normalized Compressive Stresses at the 45° Location of Specimen 1

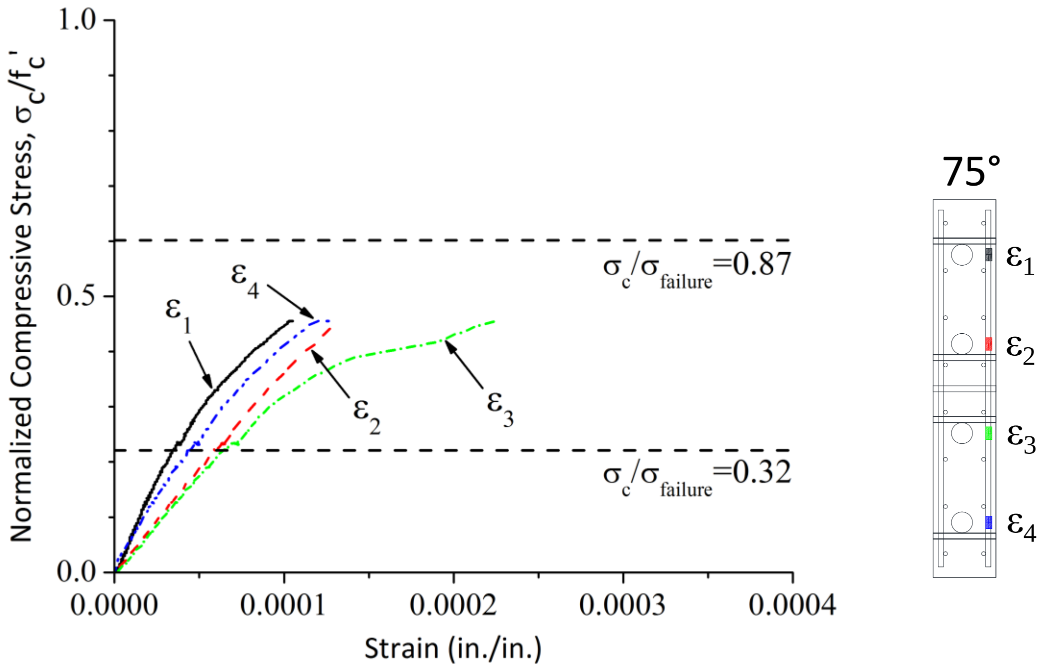

Figure 3-18: Inside Face Vertical Strains versus Normalized Compressive Stresses at the 75° Location of Specimen 1

Similar trends in the vertical strain measurements are seen for Specimen 2, and are shown in Figure 3-19 through Figure 3-21. The slopes of the vertical strain gauges showed linear responses up to 50 % of the failure load. This change in slope occurs at the same load level as the initial increase in the through-thickness expansions measured for Specimen 2, which are displayed in Figure 3-13 and Figure 3-14. It also should be noted that for the second duct and the bottom duct the vertical strain does not show much change from the initial near-linear response until approximately 60 % and 78 % of the failure load, which is also what is seen in the through-thickness expansion data shown in Figure 3-13. Therefore, it can be suggested that the change in slope of the vertical strains indicate the initiation of the delamination crack. At around 87 % of the failure load, the slopes of the vertical strains begin to flatten out, indicating the approaching delamination failure of Specimen 2. Again, this coincides with the same load level that the through-thickness expansion data demonstrated a leveling out of the slope.

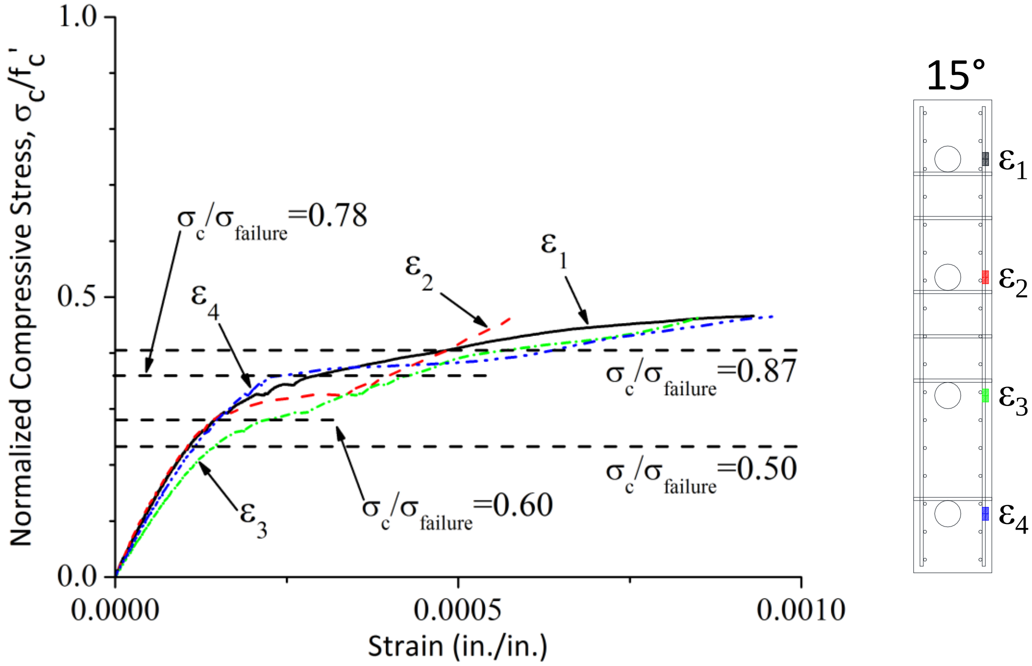

Figure 3-19: Inside Face Vertical Strains versus Normalized Compressive Stresses at the 15° Location of Specimen 2

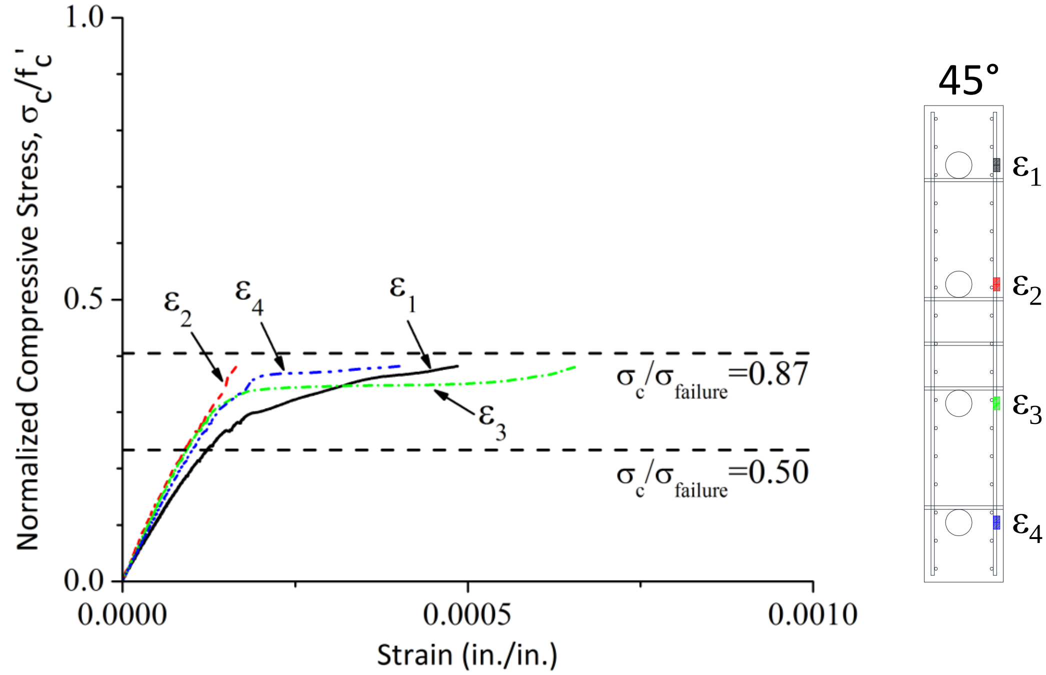

Figure 3-20: Inside Face Vertical Strains versus Normalized Compressive Stresses at the 45° Location of Specimen 2

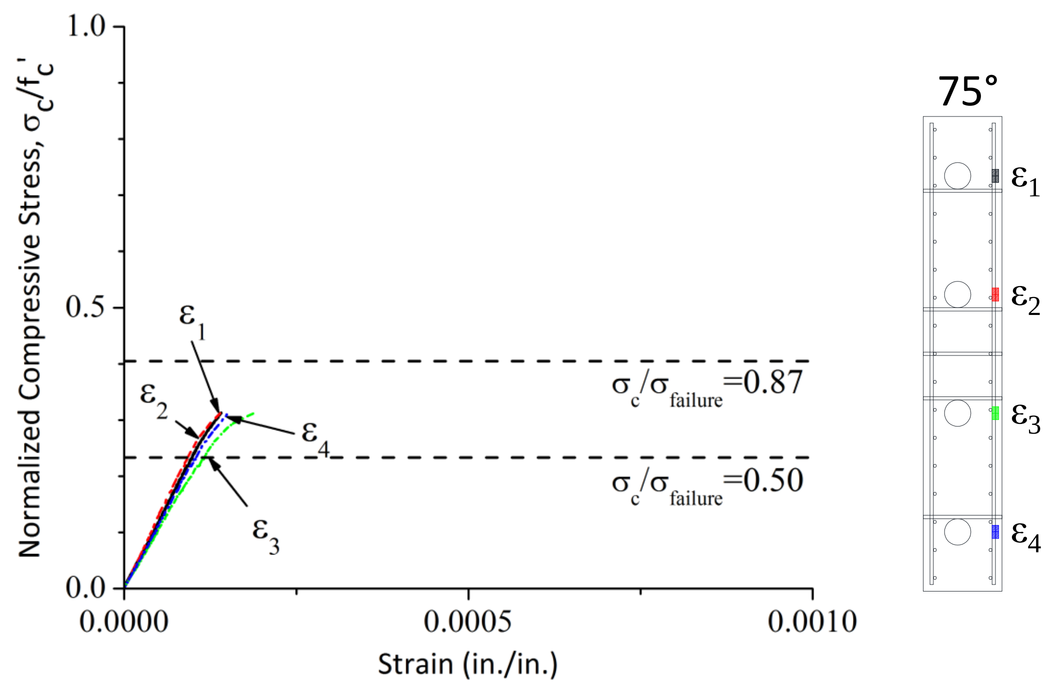

Figure 3-21: Inside Face Vertical Strains versus Normalized Compressive Stresses at the 75° Location of Specimen 2

As can be seen in Figure 3-10 through Figure 3-21, the through-thickness expansions and the vertical strains both exhibited three stages of response under the prestressing loads. Within the first stage of the response, the concrete was intact without signs of the formation of a delamination crack. In this region of the response, the through-thickness expansions and vertical strains displayed near linear trends. Once the initiation of the delamination crack occurred, the measured through-thickness expansions showed increases in the deformations and the vertical strains changed slope gradually. Within the final stage of the curved wall section response the delamination crack was increasing in width, shown by the flattening out of the slopes, up to the ultimate delamination failure of the specimen.

As shown in Figure 3-10 through Figure 3-15, the initiation of the delamination crack occurred at 19 % and 50 % of the failure loads for Specimens 1 and 2, respectively. These loads correspond to $0.13f_c$' for Specimen 1 and $0.23f_c$' for Specimen 2, respectively. The loading condition of the test specimens for this testing program is classified as a service load condition under the primary membrane without bending category. From Figure 3-22, it can be seen that the allowable compressive stress for the loading condition described is $0.35f_c$'. This level of compressive stress is significantly greater than the stress corresponding to the initiation of delamination cracking for both of the curved wall specimens that were tested.

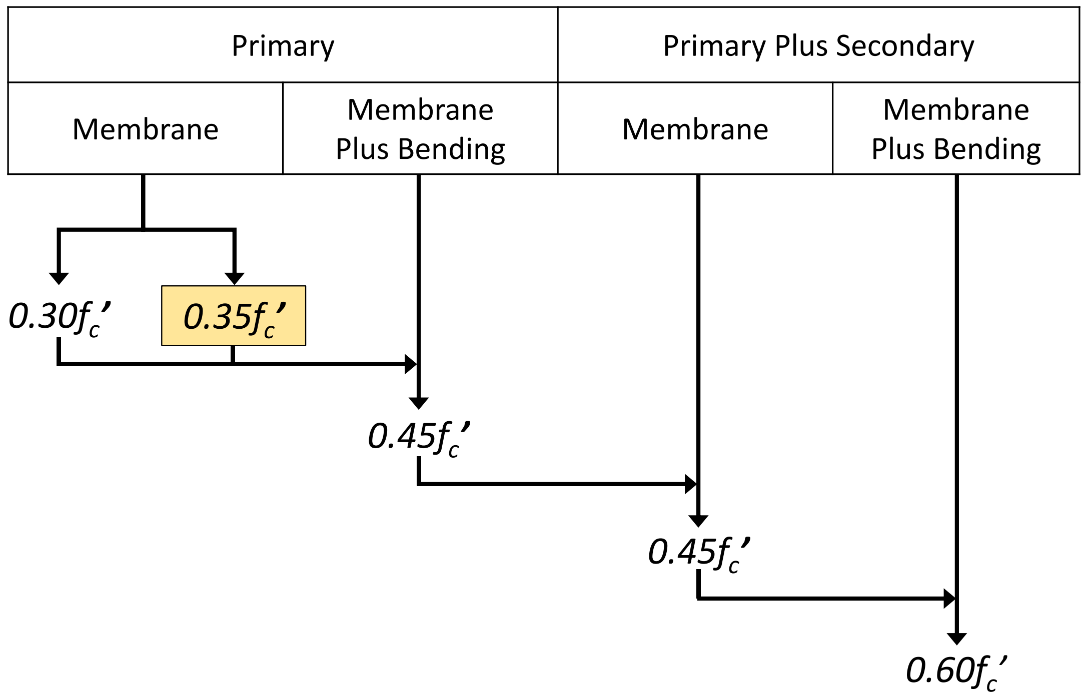

Figure 3-22: Allowable Compression Stresses For Service Loads (ASME BPVC Section III, Division 2)

Chapter 4: Conclusions

Two curved post-tensioned wall specimens were constructed and tested under monotonically increasing prestressing loads. Neither of the specimens contained through-thickness reinforcement in order to observe the behavior of concrete under these loading conditions. Based on the results obtained from this test program, the following conclusions can be made:

- The delamination failure capacity based on the normalized compressive strength decreased as the size of the curved post-tension wall specimen increased. The compressive stress at failure was 69 % and 47 % of the concrete compressive strength of Specimen 1 and 2, respectively. This shows a 32 % decrease in the normalized capacity from Specimen 1 to Specimen 2.
- The initiation of delamination cracks and their growth were measured by monitoring through-thickness expansions and vertical reinforcement strain measurements. Based on the results, the delamination cracks initiated at compressive stress levels of $0.13f_c'$~$0.23f_c'$, which are significantly lower than the allowable stress limit of $0.35f_c'$ that is provided in ASME BPVC Section III, Division 2 for service load conditions.
- The friction losses measured for the two test specimens measured 45~47 %. These losses are considerably larger than the losses calculated using the friction coefficients provided in ACI 343R-95. Therefore, it may be necessary to modify the friction coefficients for post-tensioned ducts with large angle changes.

Although the current test program has provided substantial insights into the behavior of curved post-tensioned concrete structures, there are many variables that should be investigated in order to gain a better understanding of the underlying mechanics of curved post-tensioned concrete structures. Some examples include increasing the width of the wall while maintaining the radius of the curvature, changing the spacing of the ducts, or incorporating through-thickness reinforcement. There is a clear need of more testing on specimens of this nature in order to gain a true understanding of how curved post-tensioned walls behave under prestressing loads.

Appendix A: Specimen Design and Fabrication

Appendix A provides additional details on the design and fabrication of the two curved wall specimens presented in this thesis. The information is presented as follows:

- Design tables from ASME BPVC Section III, Division 2 used for the load classification and design of the curved wall specimens.
- Detailed drawings of the reinforcement layout for the live-end and dead-end anchor block for Specimens 1 and 2.
- Images of the fabrication process for Specimens 1 and 2, including the reinforcement cages, formwork construction and concrete casting.
- Images of the instrumentation for Specimens 1 and 2.
- Images of the test setup for Specimens 1 and 2.

The curved wall specimens were designed using ASME BPVC Section III, Division 2. The curved wall sections are classified under the primary membrane since the prestressing loads were the only loads applied to the structures, which can be seen in Table A-1. Secondary loads, such as those caused by creep and shrinkage, were minimized by the unrestrained boundary condition provided over the main test area. The two wall specimens fall under the service load category for construction loads, refer to Table A-2. The allowable stresses for service loads are shown in Chapter 3, Figure 3-22. Bending in the membrane was minimized through offsetting the ducts, therefore the allowable stresses for the curved wall sections are $0.35f_c'$.

Table A-1: Classification of Forces in Concrete Containments for Steel Reinforcing and Concrete Allowable Stresses (ASME BPVC Section III, Division 2)

Location	Origin of Loads	Type of Force	Classification
Regions away from discontinuities	External (includes prestressing)	Membrane Bending Shear	Primary Primary Primary
	Volume changes effects such as creep, shrinkage and thermal strains	Membrane Bending Shear	Secondary Secondary Primary
Regions at and near gross changes in shell geometry	External (includes prestressing)	Membrane Bending Shear	Primary Primary Primary
	Volume changes effects such as creep, shrinkage and thermal strains	Membrane Bending Shear	Secondary Secondary Primary
Regions near large openings	External (includes prestressing)	Membrane Bending Shear	Primary Primary Primary
	Volume changes effects such as creep, shrinkage and thermal strains	Membrane Bending Shear	Secondary Secondary Primary

Table A-2: Load Combinations and Load Factors (ASME BPVC Section III, Division 2)

Category	D	L	F	P_t	G	P_a	T_t	T_o	T_a	E_o	E_{ss}	W	W_t	R_o	R_a	R_r	P_v	H_a
Service																		
Test	1.0	1.0	1.0	1.0	…	…	1.0	…	…	…	…	…	…	…	…	…	…	…
Construction	1.0	1.0	1.0	…	…	…	…	1.0	…	…	…	1.0	…	…	…	…	…	…
Normal	1.0	1.0	1.0	…	1.0	…	…	1.0	…	…	…	…	…	1.0	…	…	1.0	…
Factored																		
Severe environmental	1.0	1.3	1.0	…	1.0	…	…	1.0	…	1.5	…	…	…	1.0	…	…	1.0	…
	1.0	1.3	1.0	…	1.0	…	…	1.0	…	…	…	1.5	…	1.0	…	…	1.0	…
Extreme environmental	1.0	1.0	1.0	…	1.0	…	…	1.0	…	…	1.0	…	…	1.0	…	…	1.0	…
	1.0	1.0	1.0	…	1.0	…	…	1.0	…	…	…	…	1.0	1.0	…	…	1.0	…
Abnormal	1.0	1.0	1.0	…	1.0	1.5	…	…	1.0	…	…	…	…	…	1.0	…	…	…
	1.0	1.0	1.0	…	1.0	1.0	…	…	1.0	…	…	…	…	…	1.25	…	…	…
	1.0	1.0	1.0	…	1.25	1.25	…	…	1.0	…	…	…	…	…	1.0	…	…	…
Abnormal/severe environmental	1.0	1.0	1.0	…	1.0	1.25	…	…	1.0	1.25	…	…	…	…	1.0	…	…	…
	1.0	1.0	1.0	…	1.0	1.25	…	…	1.0	…	…	1.25	…	…	1.0	…	…	…
	1.0	1.0	1.0	…	1.0	…	…	1.0	…	1.0	…	…	…	…	…	…	…	1.0
	1.0	1.0	1.0	…	1.0	…	…	1.0	…	…	…	1.0	…	…	…	…	…	1.0
Abnormal/extreme environmental	1.0	1.0	1.0	…	1.0	1.0	…	…	1.0	…	1.0	…	…	…	1.0	1.0	…	…

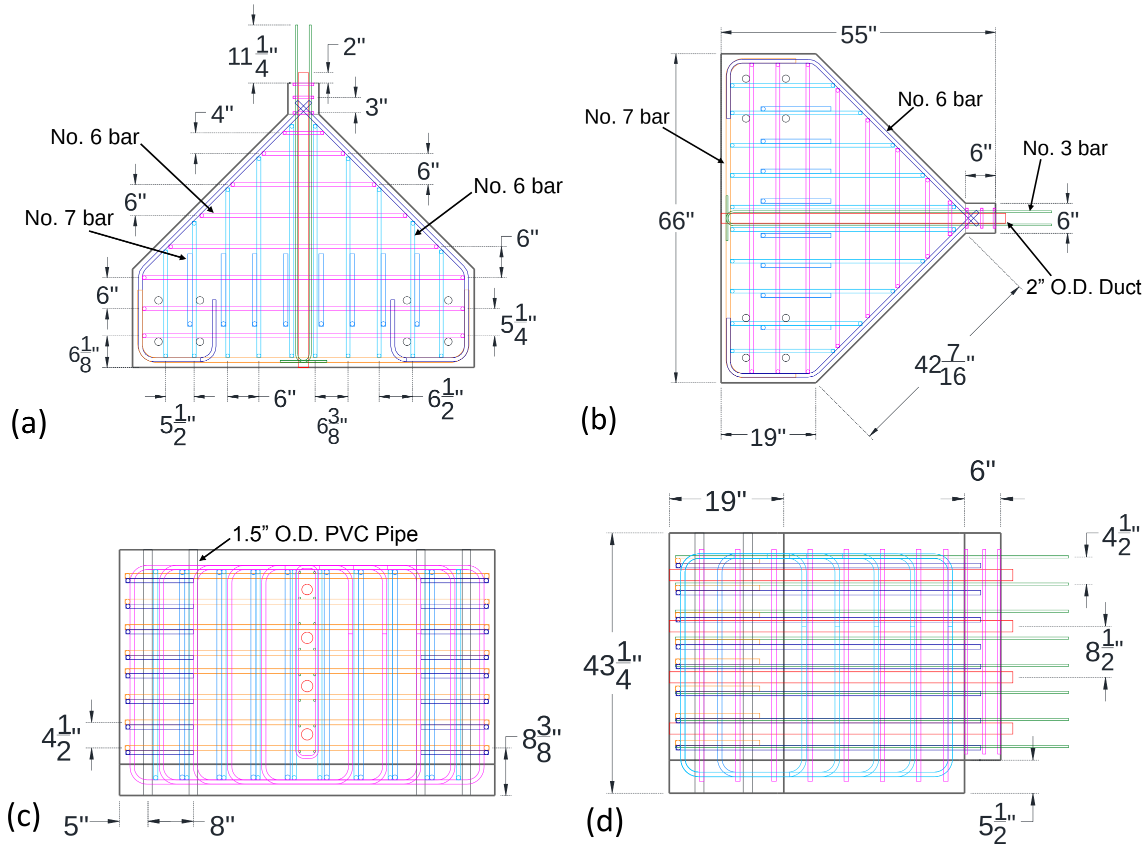

Figure A-1: Live-End Anchor Block Reinforcement Details for Specimen 1 Showing: (a) Top View, (b) Top View Rotated 90°, (c) View of Back Face, (d) Side View

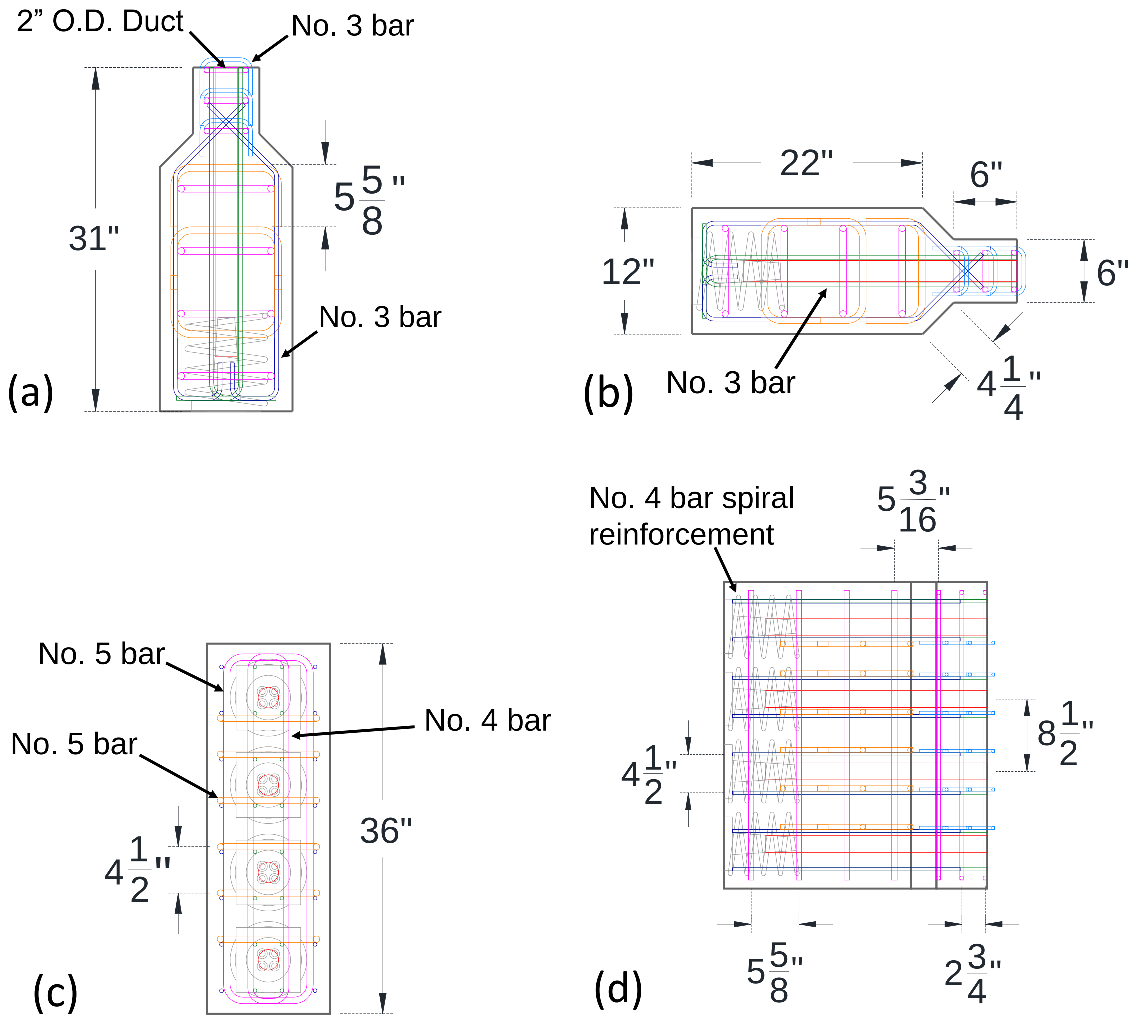

Figure A-2: Dead-End Anchor Block Reinforcement Details for Specimen 1 Showing: (a) Top View, (b) Top View Rotated 90°, (c) View of Back Face, (d) Side View

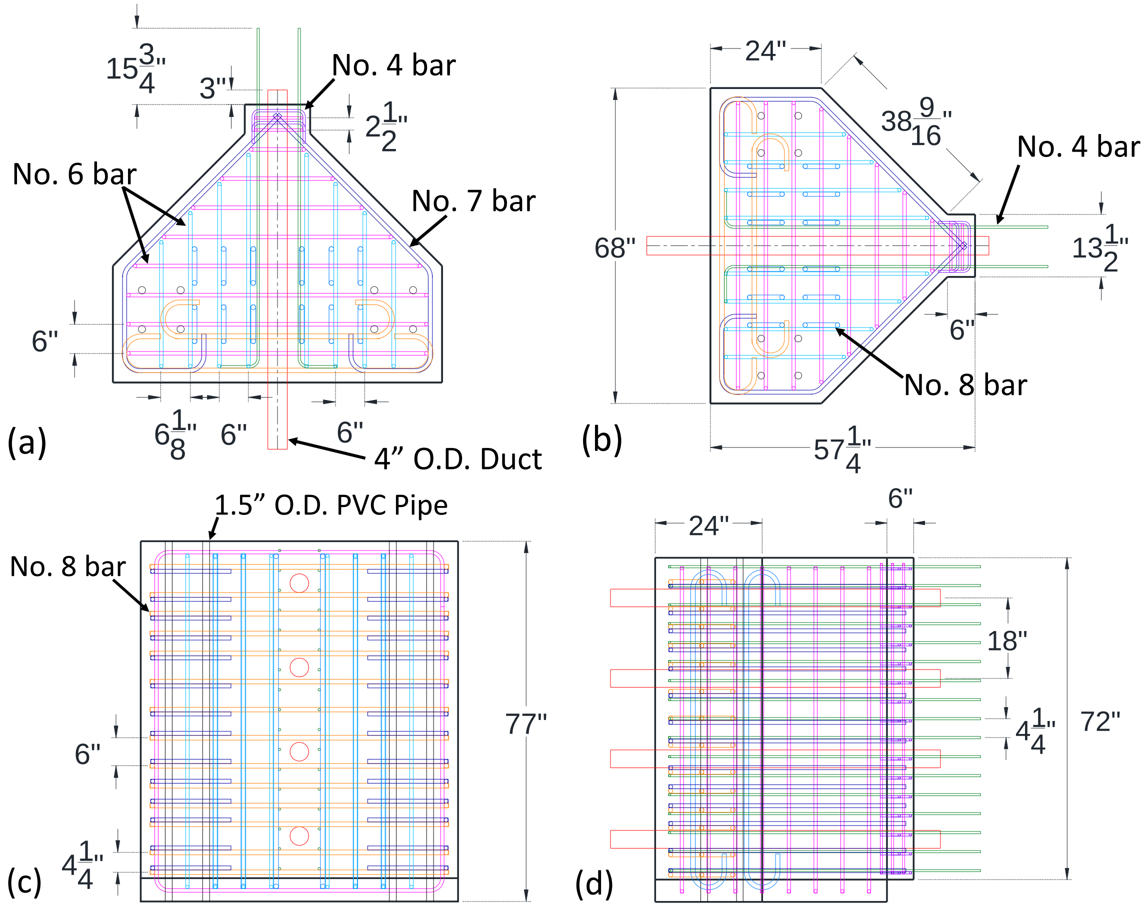

Figure A-3: Live-End Anchor Block Reinforcement Details for Specimen 2 Showing: (a) Top View, (b) Top View Rotated 90°, (c) View of Back Face, (d) Side View

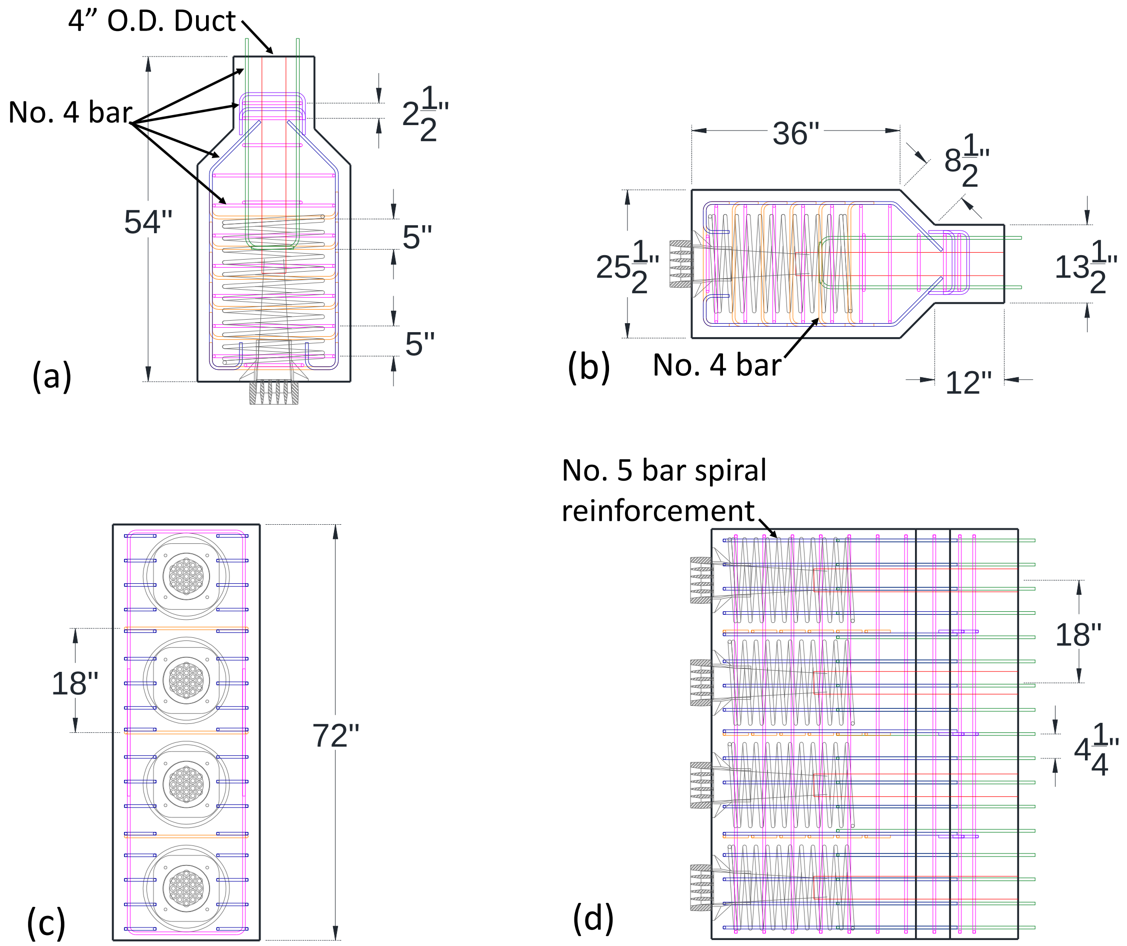

Figure A-4: Dead-End Anchor Block Reinforcement Details for Specimen 2 Showing: (a) Top View, (b) Top View Rotated 90°, (c) View of Back Face, (d) Side View

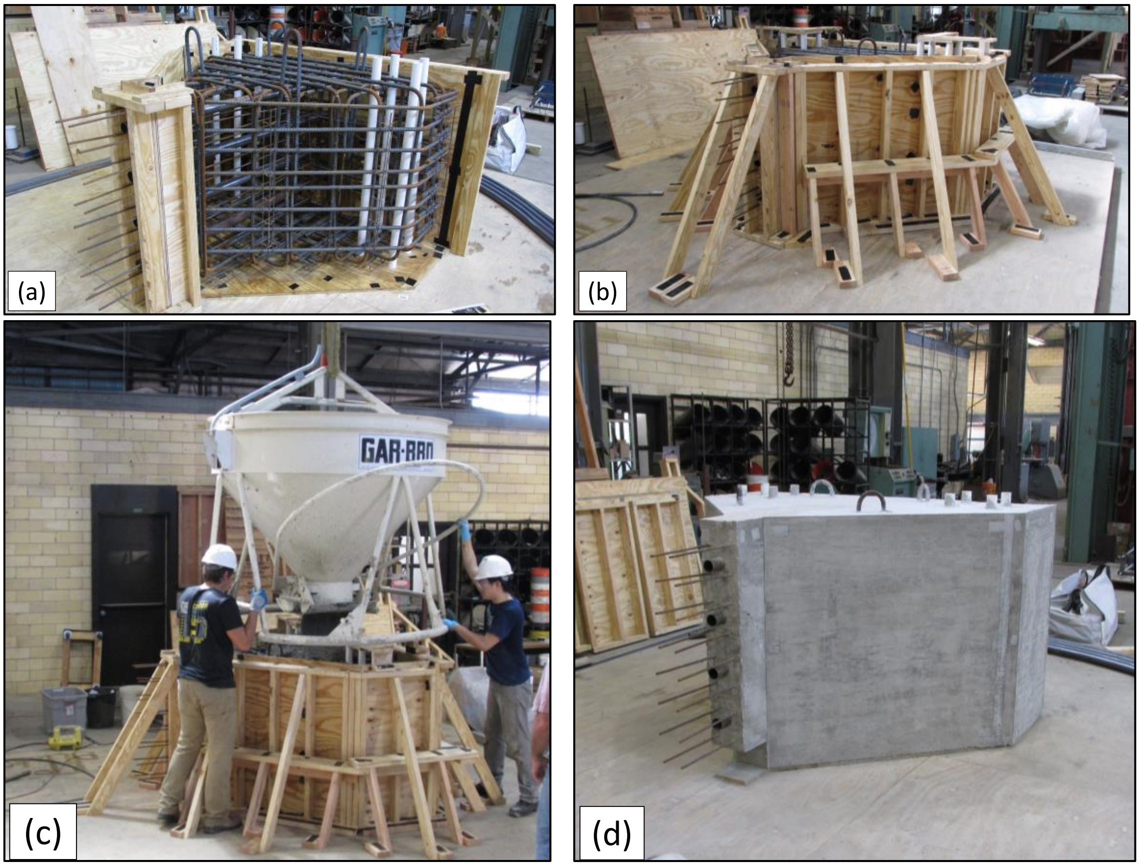

Figure A-5: Fabrication of Specimen 1 Live-End Anchor Block Showing: (a) Completed Reinforcing Cage, (b) Reinforcing Cage in Formwork, (c) Concrete Casting, (d) Completed Anchor Block

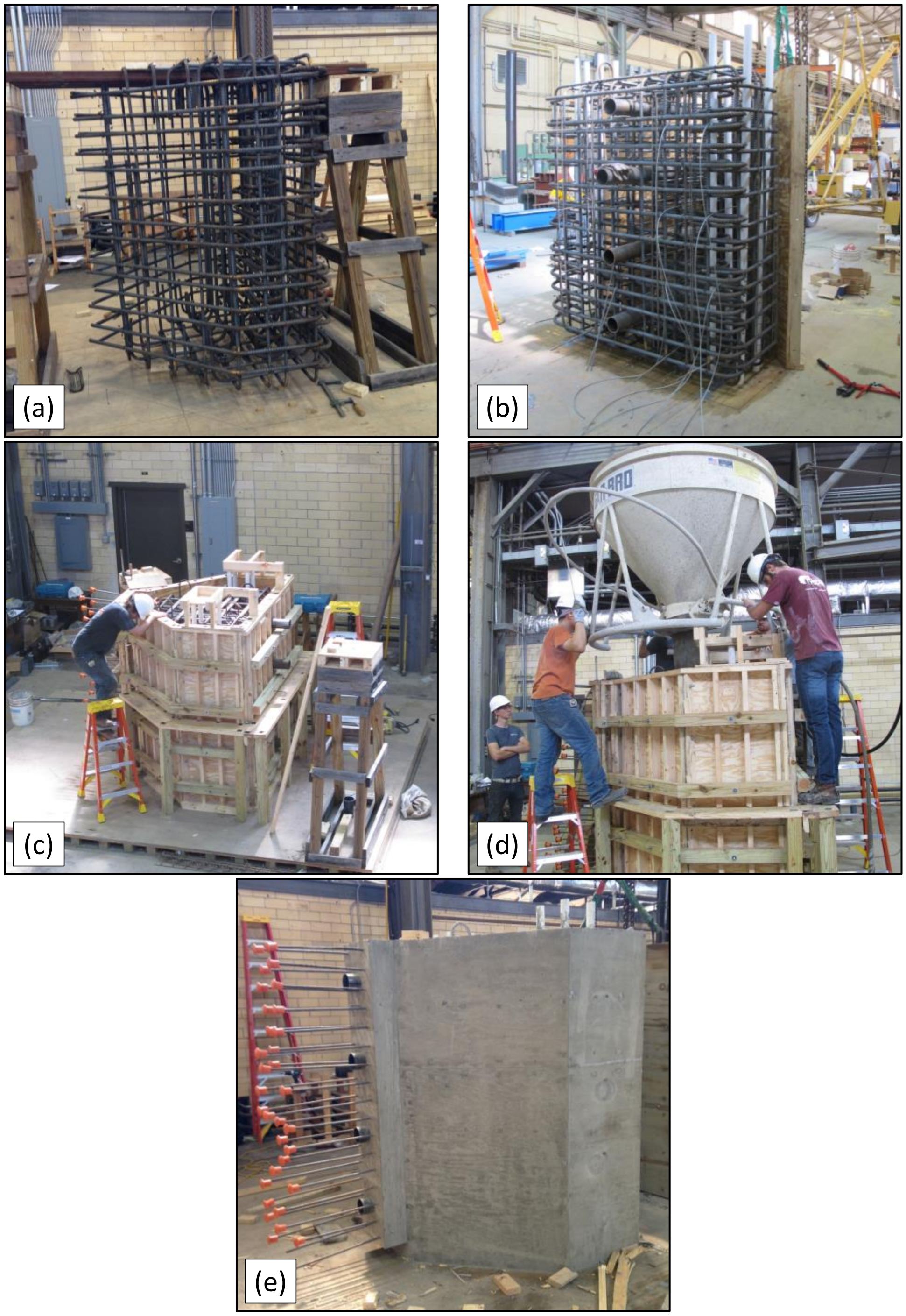

Figure A-6: Fabrication of Specimen 2 Live-End Anchor Block Showing: (a) Reinforcing Cage, (b) Reinforcing Cage in Formwork, (c) Formwork Completely Assembled (d) Concrete Casting, (e) Completed Anchor Block

Figure A-7: Fabrication of Curved Wall Formwork Showing: (a) Kerfed Plywood Sheathing with Grooves for Studs, (b) Drilling Holes for Form Ties, (c) Making Curved Plywood Studs, (d) Assembling Formwork, (e) Finished Outside Face Formwork for Specimen 1 (f) Finished Formwork for Specimen 2

Figure A-8: Specimen 1 Curved Wall and Dead-End Anchor Reinforcing Cage Fabrication Showing: (a) Placement of Live-End Anchor Block, (b) Placing Teflon Sheets, (c) Curved Wall Reinforcing Cage, (d) Dead-End Anchor Reinforcing Cage, (e) Completed Reinforcing Cage in Formwork

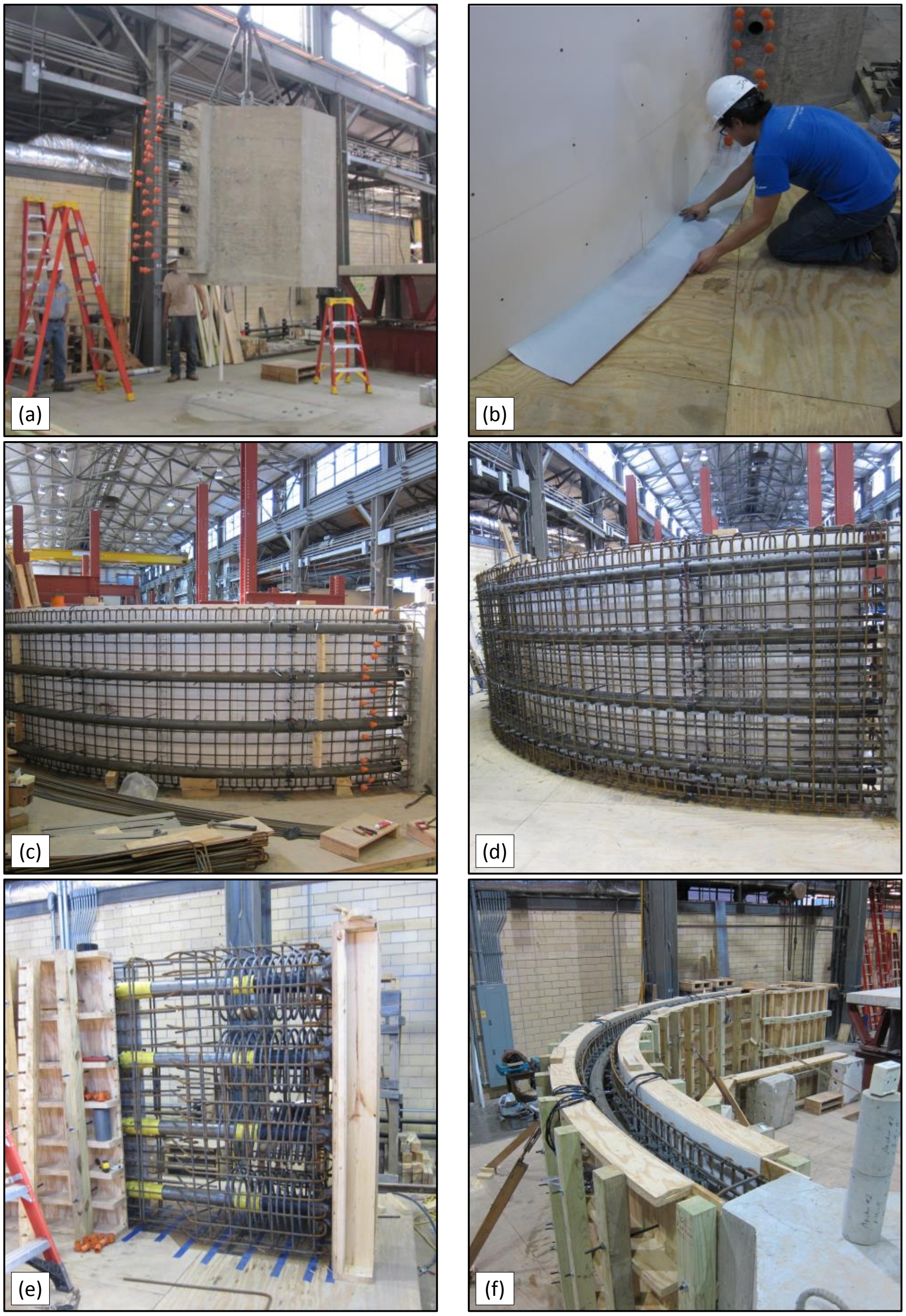

Figure A-9: Specimen 2 Curved Wall and Dead-End Anchor Reinforcing Cage Fabrication Showing: (a) Moving Live-End Anchor Block, (b) Placing Teflon Sheets, (c) Placement of Ducts, (d) Completed Curved Wall Reinforcing Cage, (e) Dead-End Anchor Reinforcing Cage, (f) Completed Reinforcing Cage in Formwork

Figure A-10: Concrete Casting Operations for Specimen 1 Showing: (a) Slump Test, (b) Placement of Concrete, (c) Internal Vibrating, (d) Finishing of Surface, (e) Curing of Specimen, (f) Completed Specimen

Figure A-11: Concrete Casting Operations for Specimen 2 Showing: (a) Slump Test, (b) Placement of Concrete, (c) Internal Vibrating, (d) Finishing of Surface, (e) Curing of Specimen, (f) Completed Specimen

Figure A-12: Typical Concrete Casting Operations for Material Test Specimens Showing: (a) Material Test Specimen Molds, (b) Cylinders, (c) Concrete Prisms, (d) Dog-Bone Specimens, (e) De-Molded Material Test Specimens

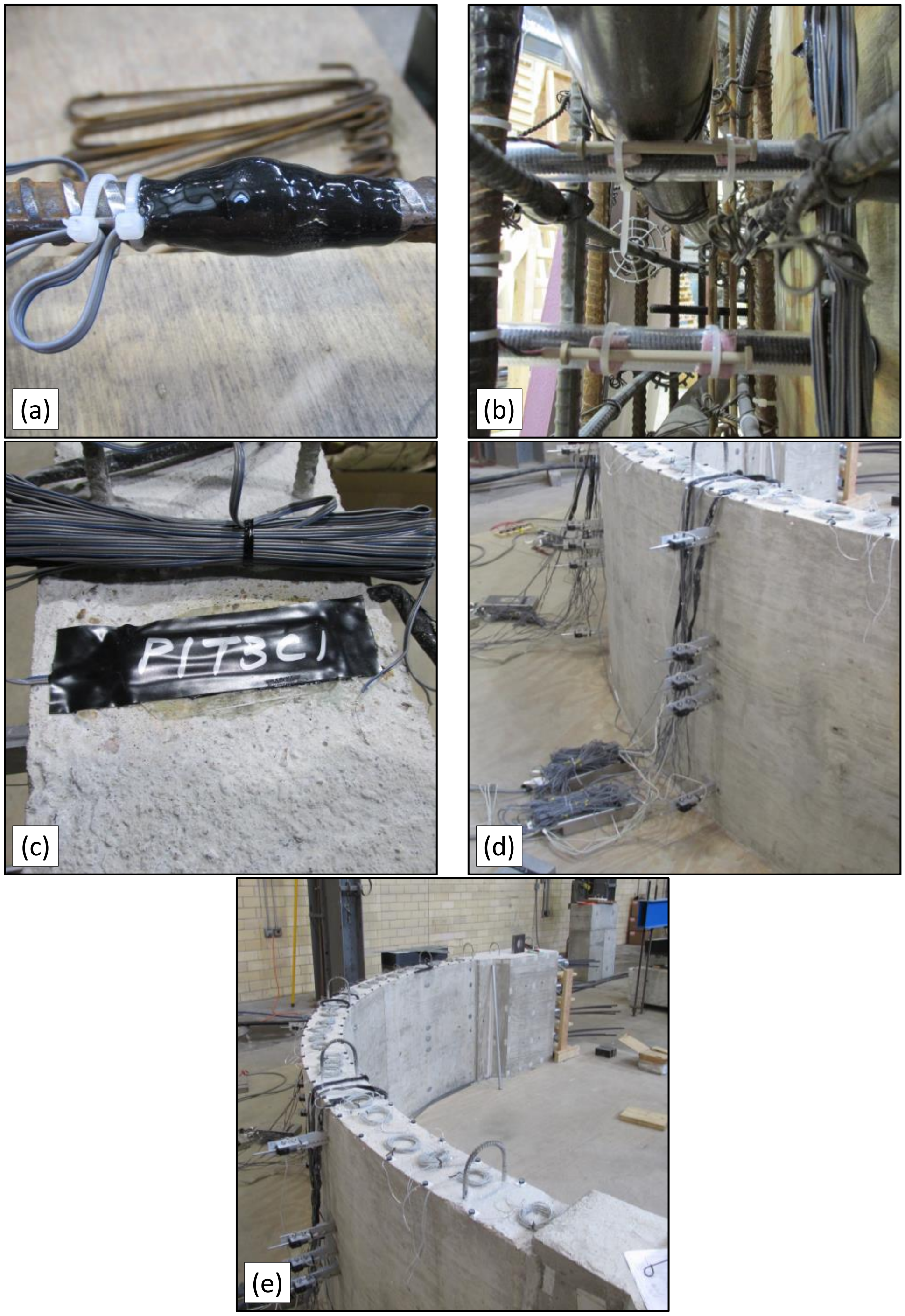

Figure A-13: Instruments Installed on Specimen 1 Showing: (a) Reinforcement Bar Strain Gauge, (b) Embedded Strain Gauge, (c) Surface Strain Gauge, (d) Linear Potentiometers for Through-Thickness Expansions, (e) NDI Optotrak Certus System Targets

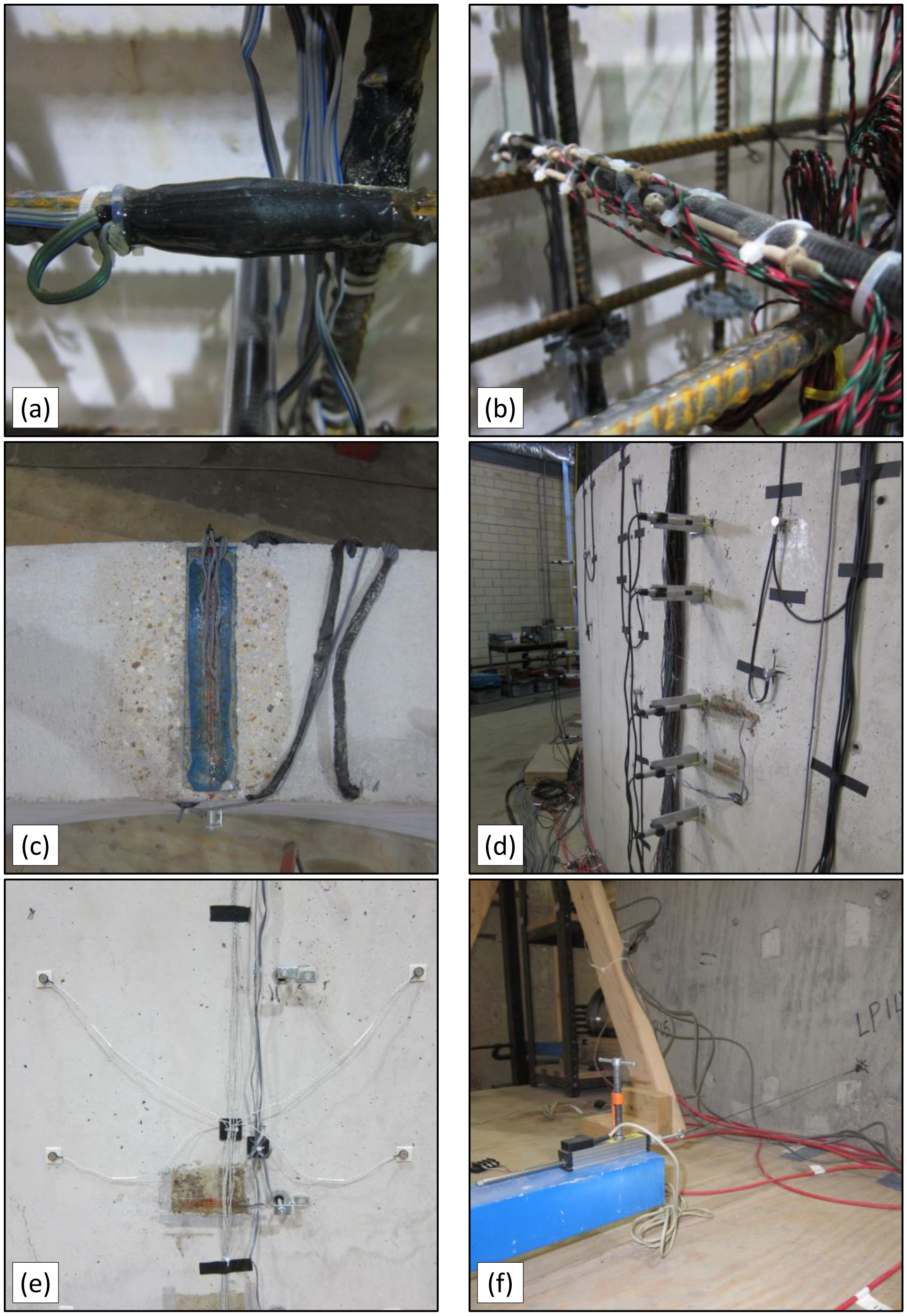

Figure A-14: Instruments Installed on Specimen 2 Showing: (a) Reinforcement Bar Strain Gauge, (b) Embedded Strain Gauge, (c) Surface Strain Gauge, (d) LSCTs for Through-Thickness Expansions, (e) NDI Optotrak Certus System Targets, (f) Linear Potentiometer for Anchor Block Movement

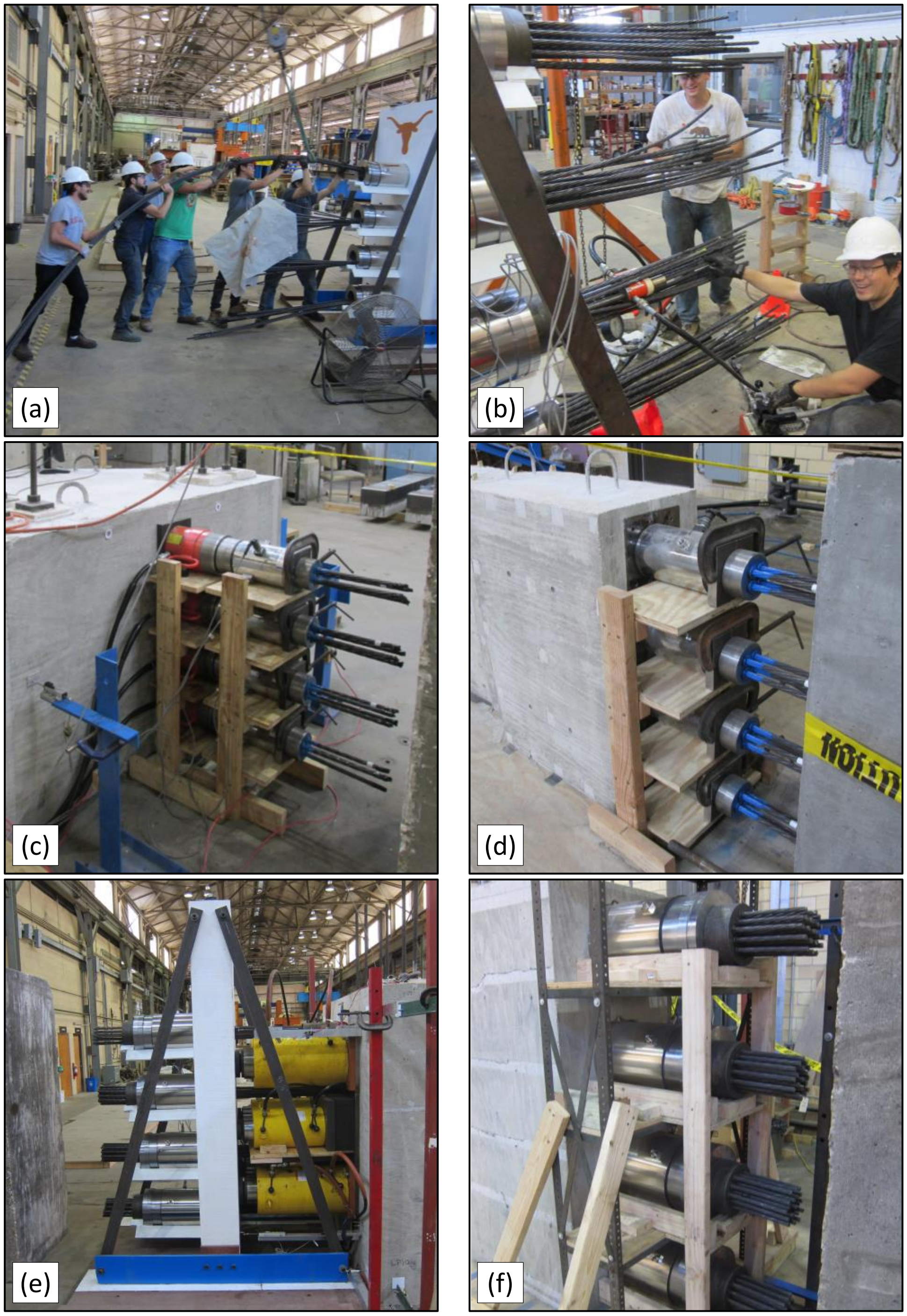

Figure A-15: Structural Test Setup of Both Specimens Showing: (a) Inserting Strands, (b) Removing Slack from Strands, (c) Live-End Setup for Specimen 1, (d) Dead-End Setup for Specimen 1, (e) Live-End Setup for Specimen 2, (f) Dead-End Setup for Specimen 2

Appendix B: Material Testing Records

Appendix B presents the results of the materials testing for both concrete and steel. All concrete material properties were calculated using the measured dimensions of the material test specimens. The information is presented as follows:

- Concrete mixture designs and batch tickets for the live-end anchor block, curved wall section and dead-end anchor block for both specimens.
- Images of the material tests.
- Concrete compressive strength data for the live-end anchor block, curved wall section and dead-end anchor block for both specimens.
- Concrete elastic modulus and Poisson's Ratio data for the curved wall section and dead-end anchor block for both specimens.
- Concrete splitting tensile strength data for the curved wall section and dead-end anchor block for both specimens.
- Concrete modulus of rupture data for the curved wall section and dead-end anchor block for both specimens.
- Concrete direct tension data for the curved wall section and dead-end anchor block for both specimens.
- Steel mill certification test reports for the reinforcing bars for both specimens.
- Reinforcing bar tensile test data for the curved wall section for both specimens
- 0.6-in. strand mechanical properties data provided by the manufacturer for both specimens.
- Steel mill certification test reports for the duct material for both specimens.

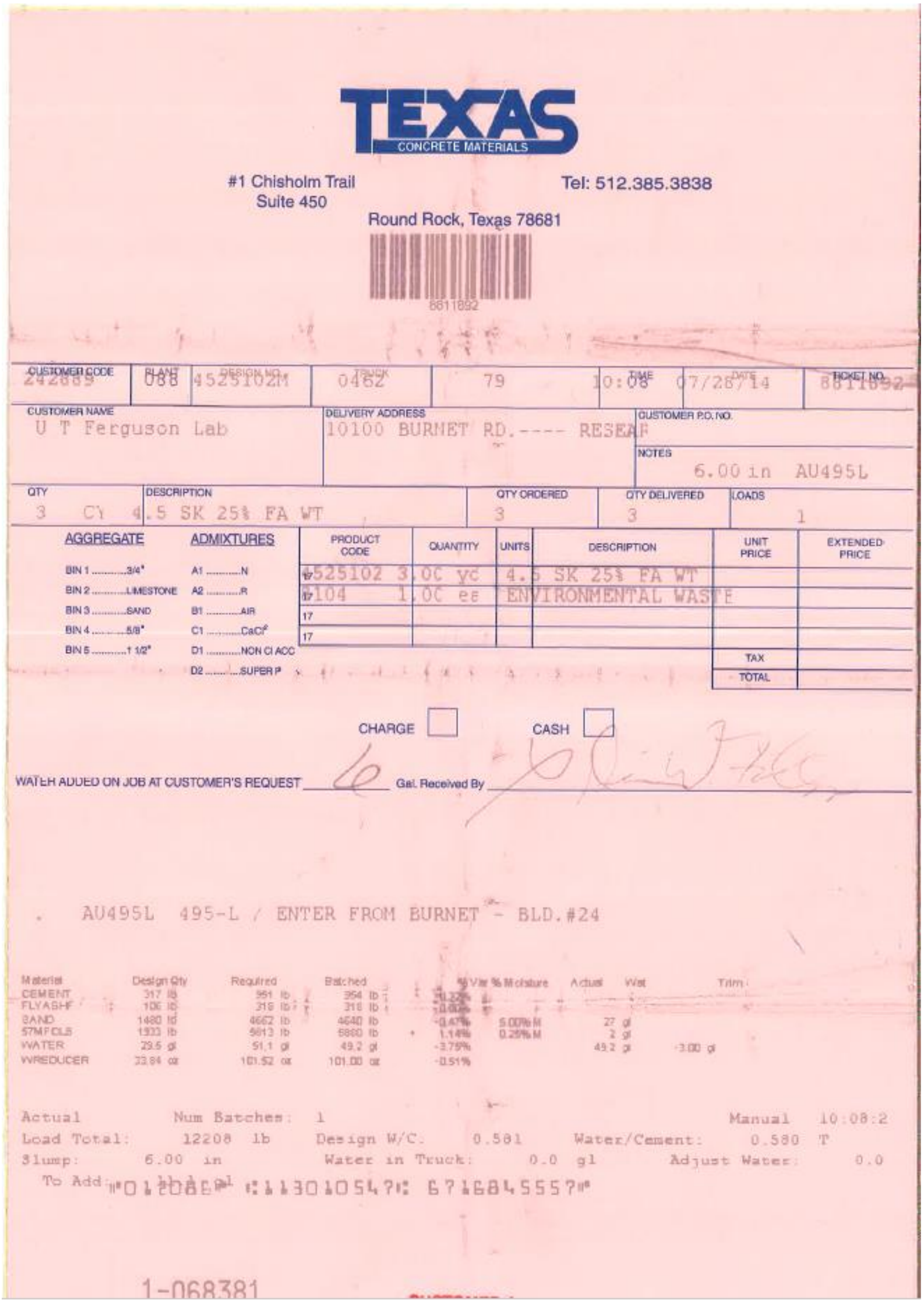

TEXAS CONCRETE MATERIALS

#1 Chisholm Trail
Suite 450

Tel: 512.385.3838

Round Rock, Texas 78681

8611892

CUSTOMER CODE	PLANT	DESIGN NO.	TRUCK		TIME	DATE	TICKET NO.
242889	088	4525102M	0462	79	10:08	07/28/14	8611892

CUSTOMER NAME: U T Ferguson Lab

DELIVERY ADDRESS: 10100 BURNET RD.---- RESEAR

CUSTOMER P.O. NO.

NOTES: 6.00 in AU495L

QTY	DESCRIPTION	QTY ORDERED	QTY DELIVERED	LOADS
3 CY	4.5 SK 25% FA WT	3	3	1

AGGREGATE	ADMIXTURES
BIN 1 ....3/4"	A1 ....N
BIN 2 ....LIMESTONE	A2 ....R
BIN 3 ....SAND	B1 ....AIR
BIN 4 ....5/8"	C1 ....CaCl²
BIN 5 ....1 1/2"	D1 ....NON Cl ACC
	D2 ....SUPER P

PRODUCT CODE	QUANTITY	UNITS	DESCRIPTION	UNIT PRICE	EXTENDED PRICE
4525102	3.00	yd	4.5 SK 25% FA WT		
8104	1.00	ea	ENVIRONMENTAL WASTE		
17					
17					
				TAX	
				TOTAL	

CHARGE ☐ CASH ☐

WATER ADDED ON JOB AT CUSTOMER'S REQUEST 6 Gal. Received By

AU495L 495-L / ENTER FROM BURNET - BLD.#24

Material	Design Qty	Required	Batched	% Var	% Moisture	Actual	Wat	Trim
CEMENT	317 lb	951 lb	954 lb	1.22%				
FLYASHF	106 lb	318 lb	318 lb	0.00%				
SAND	1480 lb	4662 lb	4640 lb	-0.47%	5.00% M	27 gl		
57MFCLS	1933 lb	5813 lb	5880 lb	1.14%	0.25% M	2 gl		
WATER	29.5 gl	51.1 gl	49.2 gl	-3.75%		49.2 gl		-3.00 gl
WREDUCER	33.84 oz	101.52 oz	101.00 oz	-0.51%				

Actual Num Batches: 1 Manual 10:08:2
Load Total: 12208 lb Design W/C: 0.581 Water/Cement: 0.580 T
Slump: 6.00 in Water in Truck: 0.0 gl Adjust Water: 0.0
To Add

1-068381

Figure B-1: Specimen 1 Live-End Anchor Block Batch Ticket

4525381

Date : 12/15/2014
Mix Code : 4525381 Description : **4.5 SK 25% FA 3/8" PG**

Revision Number : 85 Creation Date : 15 Dec 2014 Customer :
Plant : BOLM ROAD Created By : cthomas2 Project :

Specifications

Consistence Class : 5.0 Air, % : 2
Strength Class : 2500 Max W/C : 0.59 Max Agg Size : 3/8

Material Type	Material Code	Description	Supplier Source	Design Quantity	Specific Gravity	Volume ft3
Cement	CEMENT	CEMENT	ALAMO CEMENT CO-SANANTON	318 lb	3.15	1.62
Fly Ash	FLYASHF	FLYASH CLASS F - C618	BORAL-ROCKDALE	106 lb	2.30	0.74
Fine Aggregate	SAND	SAND	AUSTIN AGGREGATES-AUSTIN	1468 lb	2.62	8.98
Coarse Aggregate	381RR	#8 - 3/8" RIVER ROCK ASTM C33	AUSTIN AGGREGATES-AUSTIN	1800 lb	2.60	11.09
Water	WATER	WATER	CITY-WATER	30.0 gal	1.00	4.01
Admixture	HRWR	HRWR	SIKA ADMIXTURES-DALLAS	4.0 /cwt	1.10	0.02
			Yield	**3944 lb**		**27.00**

Design Properties

Density : 146.1 lb/ft3 Grading Specification : ASTM C 33 #8
Cement Content : 424 lb Actual Dmax : 0.375 mm

Prepared By :

Corben Thomas

Page 1

Figure B-2: Concrete Mixture Design Properties for Specimen 1 Wall Section and Dead-End Anchor Block

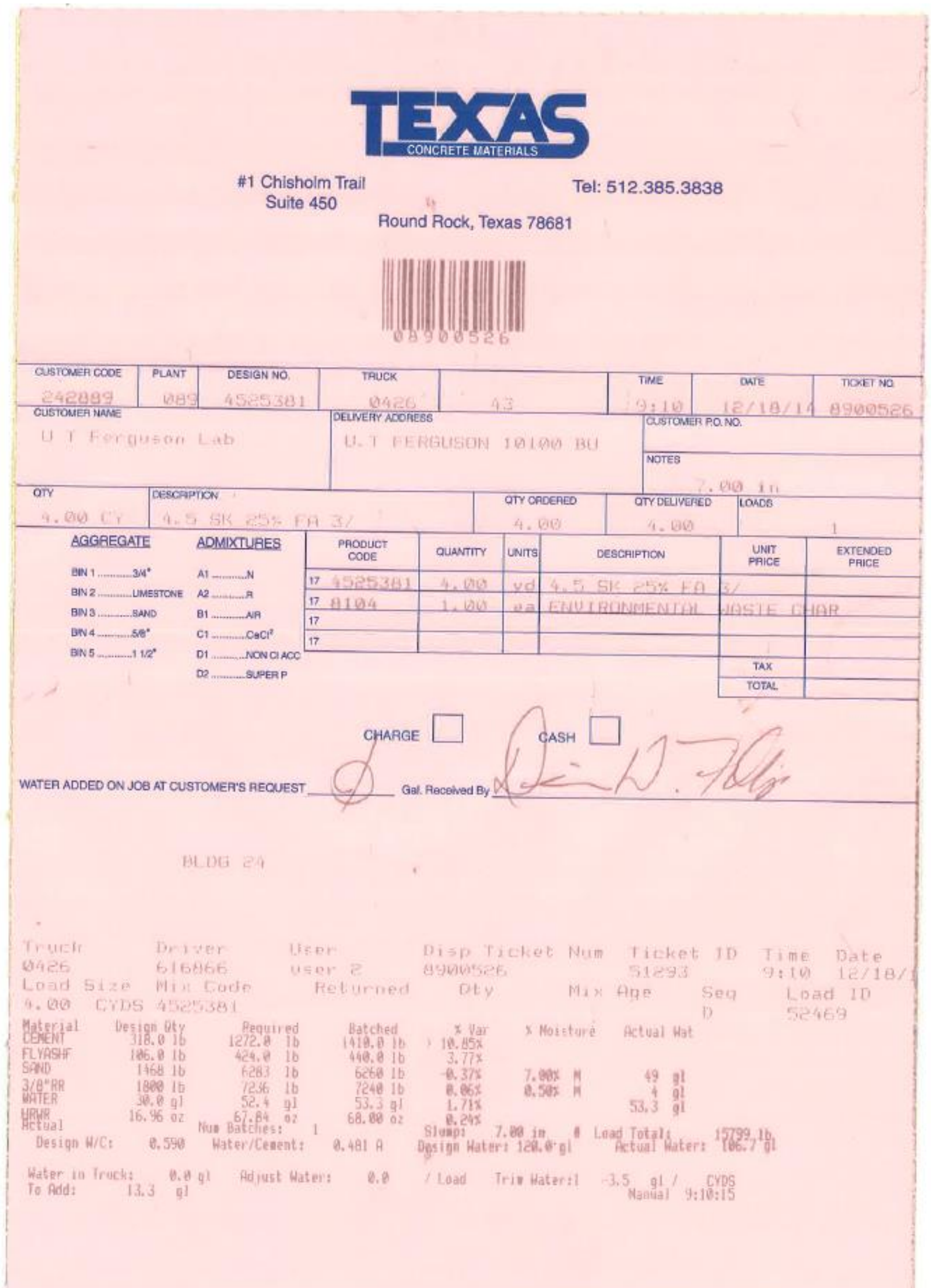

TEXAS CONCRETE MATERIALS

#1 Chisholm Trail
Suite 450
Round Rock, Texas 78681
Tel: 512.385.3838

08900526

CUSTOMER CODE	PLANT	DESIGN NO.	TRUCK		TIME	DATE	TICKET NO.
242889	089	4525381	0426	43	9:10	12/18/14	8900526

CUSTOMER NAME: U T Ferguson Lab
DELIVERY ADDRESS: U.T FERGUSON 10100 BU
CUSTOMER P.O. NO.:
NOTES: 7.00 in

QTY	DESCRIPTION	QTY ORDERED	QTY DELIVERED	LOADS
4.00 CY	4.5 SK 25% FA 3/	4.00	4.00	1

AGGREGATE	ADMIXTURES
BIN 1 ......3/4"	A1 ......N
BIN 2 ......LIMESTONE	A2 ......R
BIN 3 ......SAND	B1 ......AIR
BIN 4 ......5/8"	C1 ......CaCl²
BIN 5 ......1 1/2"	D1 ......NON Cl ACC
	D2 ......SUPER P

	PRODUCT CODE	QUANTITY	UNITS	DESCRIPTION	UNIT PRICE	EXTENDED PRICE
17	4525381	4.00	yd	4.5 SK 25% FA 3/		
17	8104	1.00	ea	ENVIRONMENTAL WASTE CHAR		
17						
17						
					TAX	
					TOTAL	

CHARGE ☐ CASH ☐

WATER ADDED ON JOB AT CUSTOMER'S REQUEST Ø Gal. Received By

BLDG 24

Truck	Driver	User	Disp Ticket Num	Ticket ID	Time	Date
0426	616866	user 2	8900526	51293	9:10	12/18/

Load Size	Mix Code	Returned	Qty	Mix Age	Seq	Load ID
4.00 CYDS	4525381				D	52469

Material	Design Qty	Required	Batched	% Var	% Moisture	Actual Wat
CEMENT	318.0 lb	1272.0 lb	1410.0 lb	› 10.85%		
FLYASHF	106.0 lb	424.0 lb	440.0 lb	3.77%		
SAND	1468 lb	6283 lb	6260 lb	-0.37%	7.00% M	49 gl
3/8"RR	1800 lb	7236 lb	7240 lb	0.06%	0.50% M	4 gl
WATER	30.0 gl	52.4 gl	53.3 gl	1.71%		53.3 gl
HRWR	16.96 oz	67.84 oz	68.00 oz	0.24%		

Actual Num Batches: 1 Slump: 7.00 in @ Load Total: 15799 lb
Design W/C: 0.590 Water/Cement: 0.481 A Design Water: 120.0 gl Actual Water: 106.7 gl

Water in Truck: 0.0 gl Adjust Water: 0.0 / Load Trim Water: 1 -3.5 gl / CYDS
To Add: 13.3 gl Manual 9:10:15

Figure B-3: Specimen 1 Wall Section and Dead-End Anchor Block Batch Ticket

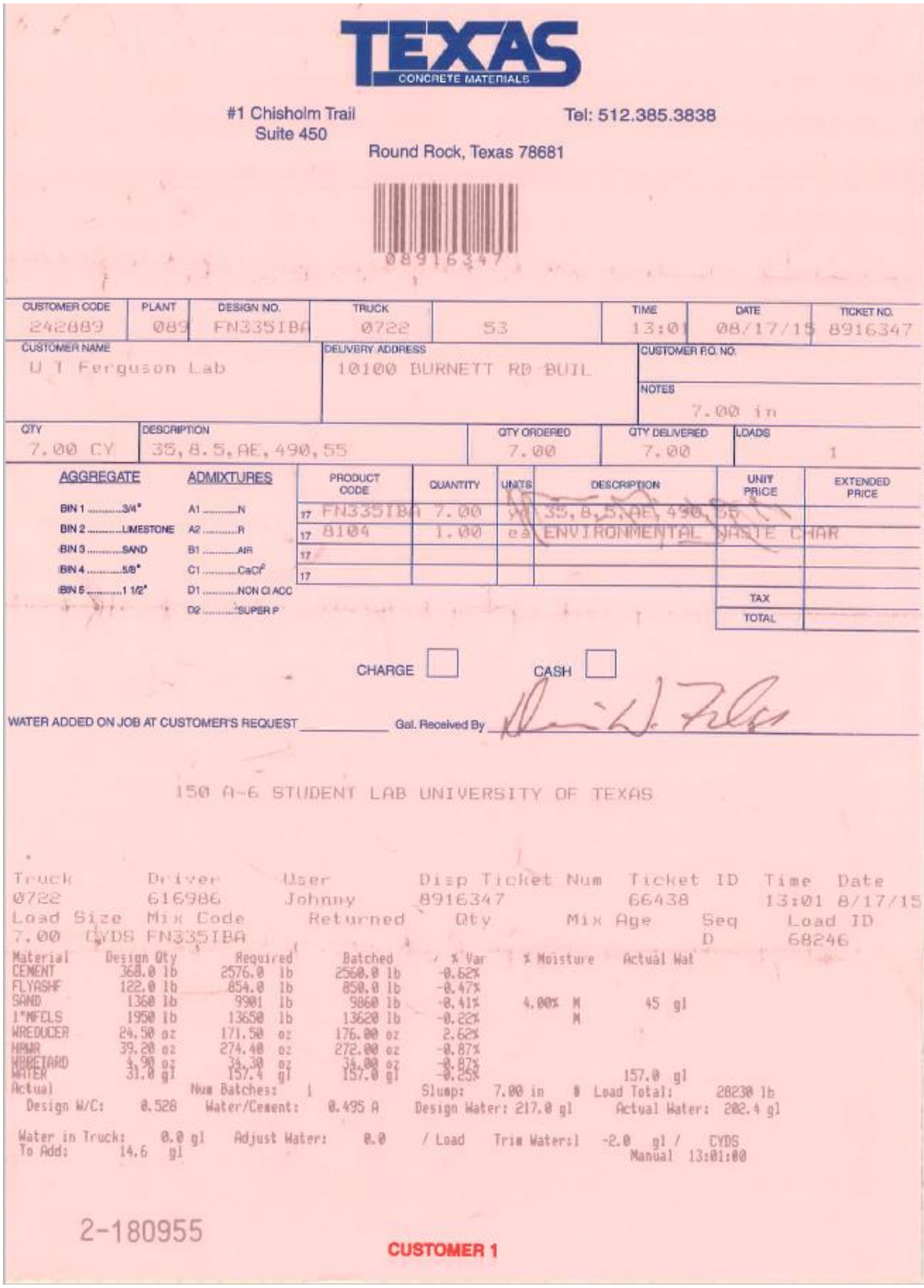

TEXAS CONCRETE MATERIALS

#1 Chisholm Trail
Suite 450
Round Rock, Texas 78681
Tel: 512.385.3838

08916347

CUSTOMER CODE	PLANT	DESIGN NO.	TRUCK		TIME	DATE	TICKET NO.
242089	089	FN335IBA	0722	53	13:01	08/17/15	8916347

CUSTOMER NAME: U T Ferguson Lab
DELIVERY ADDRESS: 10100 BURNETT RD BUIL
CUSTOMER P.O. NO.:
NOTES: 7.00 in

QTY	DESCRIPTION	QTY ORDERED	QTY DELIVERED	LOADS
7.00 CY	35,8.5,AE,490,55	7.00	7.00	1

AGGREGATE	ADMIXTURES
BIN 1 ......3/4"	A1 ......N
BIN 2 ......LIMESTONE	A2 ......R
BIN 3 ......SAND	B1 ......AIR
BIN 4 ......5/8"	C1 ......CaCl²
BIN 5 ......1 1/2"	D1 ......NON Cl ACC
	D2 ......SUPER P

	PRODUCT CODE	QUANTITY	UNITS	DESCRIPTION	UNIT PRICE	EXTENDED PRICE
17	FN335IBA	7.00	yd	35,8.5,AE,490,55		
17	8104	1.00	ea	ENVIRONMENTAL WASTE CHAR		
17						
17						
					TAX	
					TOTAL	

CHARGE ☐ CASH ☐

WATER ADDED ON JOB AT CUSTOMER'S REQUEST ________ Gal. Received By

150 A-6 STUDENT LAB UNIVERSITY OF TEXAS

Truck	Driver	User	Disp Ticket Num	Ticket ID	Time	Date
0722	616986	Johnny	8916347	66438	13:01	8/17/15

Load Size	Mix Code	Returned	Qty	Mix Age	Seq	Load ID
7.00 CYDS	FN335IBA				D	68246

Material	Design Qty	Required	Batched	% Var	% Moisture	Actual Wat
CEMENT	368.0 lb	2576.0 lb	2560.0 lb	-0.62%		
FLYASHF	122.0 lb	854.0 lb	850.0 lb	-0.47%		
SAND	1360 lb	9901 lb	9860 lb	-0.41%	4.00% M	45 gl
1"MFCLS	1950 lb	13650 lb	13620 lb	-0.22%	M	
WREDUCER	24.50 oz	171.50 oz	176.00 oz	2.62%		
HRWR	39.20 oz	274.40 oz	272.00 oz	-0.87%		
WRRETARD	4.90 oz	34.30 oz	34.00 oz	-0.87%		
WATER	31.0 gl	157.4 gl	157.0 gl	-0.25%		157.0 gl

Actual Num Batches: 1 Slump: 7.00 in # Load Total: 28230 lb
Design W/C: 0.528 Water/Cement: 0.495 A Design Water: 217.0 gl Actual Water: 202.4 gl

Water in Truck: 0.0 gl Adjust Water: 0.0 / Load Trim Water:1 -2.0 gl / CYDS
To Add: 14.6 gl Manual 13:01:00

2-180955

CUSTOMER 1

Figure B-4: Specimen 2 Live-End Anchor Block Batch Ticket

TEXAS CONCRETE MATERIALS
apac Safety First Always
a division of the Southwest Group of Oldcastle Materials

NRMCA MEMBER

Concrete Mix Design Submittal

Date Issued : 07/25/2016

Customer:
Project:
Plant:
Mix Code: **Mix Code must be used when ordering concrete.**
Mix Description:
Internal ID:

Material Type	Description	ASTM	SG	Weight
Cement	TYPE I/II	C-150	3.15	**362 lb**
Fly Ash	CLASS F	C-618	2.30	**155 lb**
Water	WATER	C-1602	1.00	**31 gal**
Admixture	WATER REDUCER	C-494 A/F	1.10	**5 /cwt**
Admixture	WATER REDUCER/RETARDER	C-494 B/D	1.20	**1 /cwt**
Fine Aggregate	NATURAL SAND	C-33 F	2.62	**1301 lb**
Coarse Aggregate	3/8" RIVER GRAVEL	C-33	2.60	**1850 lb**
			Total	**3929 lb**

Slump: 6.0 +/- 1.5" Unit Weight: 145.5 lb/ft3
Air: 2 % Designed W/C Ratio: 0.50

Draft

Data enclosed represents the potential of the mix when sampled, cured and tested per the appropriate, current ACI and ASTM standards. Chemical admixtures are added in accordance with the manufacturer's recommendation Texas Concrete Materials reserves the right to adjust these dosages to meet changes in jobsite conditions and/or demand up to and including substitution of equivalent products. Texas Concrete Materials has no knowledge or authority regarding where this mix is to be placed, therefore it is the responsibility of the project architect/engineer, and/or the contractor to ensure that the above designed mix parameter of compressive strength, water/cement ratio, cement content, and air content are appropriate for the anticipated environmental conditions (i.e. ACI 318, ACI 301 and the local Building Codes). Aggregate weights may change depending on gradations or specific gravity of material. Mix Design Proportions and specifications are confidential and proprietary trade secrets of Texas Concrete Materials any use or dissemination without permission is a violation of federal criminal law.

Prepared By :

____

Figure B-5: Concrete Mixture Design Properties for Specimen 2 Wall Section and Dead-End Anchor Block

TEXAS CONCRETE MATERIALS

#1 Chisholm Trail
Suite 450

Round Rock, Texas 78681

Tel: 512.385.3838

Left plant 8:34
Arrive: 9:16

08926241

CUSTOMER CODE	PLANT	DESIGN NO.	TRUCK		TIME	DATE	TICKET NO.
242889	089	P3030324	0435	9	8:22	12/16/15	8926241

CUSTOMER NAME: U T Ferguson Lab

DELIVERY ADDRESS: 10100 BURNET RD BLDG

CUSTOMER P.O. NO.:

NOTES: 6.00 in AU495L

QTY	DESCRIPTION	QTY ORDERED	QTY DELIVERED	LOADS
9.00 CY	3500 PG	9.00	9.00	1

AGGREGATE
- BIN 1 ....3/4"
- BIN 2 ....LIMESTONE
- BIN 3 ....SAND
- BIN 4 ....5/8"
- BIN 5 ....1 1/2"

ADMIXTURES
- A1 ....N
- A2 ....R
- B1 ....AIR
- C1 ....CaCl²
- D1 ....NON Cl ACC
- D2 ....SUPER P

	PRODUCT CODE	QUANTITY	UNITS	DESCRIPTION	UNIT PRICE	EXTENDED PRICE
17	P3030324	9.00	yd	3500 PG		
17	8104	1.00	ea	ENVIRONMENTAL WASTE CHAR		
17						
17						
					TAX	
					TOTAL	

CHARGE ☐ CASH ☐

WATER ADDED ON JOB AT CUSTOMER'S REQUEST Ø Gal. Received By [signature]

AU495L

Truck	Driver	User	Disp Ticket Num	Ticket ID	Time	Date
0435	617065	jacoby	8926241	76000	8:22	12/16/1

Load Size	Mix Code	Returned	Qty	Mix Age	Seq'	Load ID
9.00 CYDS	P3030324				D	78105

Material	Design Qty	Required	Batched	% Var	% Moisture	Actual Wat
CEMENT	362.0 lb	3258.0 lb	3230.0 lb	-0.86%		
FLYASHF	155.0 lb	1395.0 lb	1420.0 lb	+ 1.79%		
SAND	1301 lb	12294 lb	12240 lb	-0.44%	5.00% M	70 gl
3/8"RR	1850 lb	16692 lb	16620 lb	-0.43%	0.25% M	5 gl
WATER	31.0 gl	185.9 gl	185.1 gl	-0.38%		185.1 gl
WREDUCER	25.85 oz	232.65 oz	232.00 oz	-0.28%		
WRRETARD	5.17 oz	46.53 oz	47.00 oz	1.01%		

Actual Num Batches: 1 Slump: 6.00 in Load Total: 35072 lb
Design W/C: 0.500 Water/Cement: 0.467 A Design Water: 279.0 gl Actual Water: 260.0 gl

Water in Truck: 0.0 gl Adjust Water: 0.0 / Load Trim Water:1 -2.0 gl / CYDS
To Add: 19.0 gl Manual 8:22:55

2-189689 **CUSTOMER 1**

Figure B-6: Specimen 2 Wall Section and Dead-End Anchor Block Batch Ticket

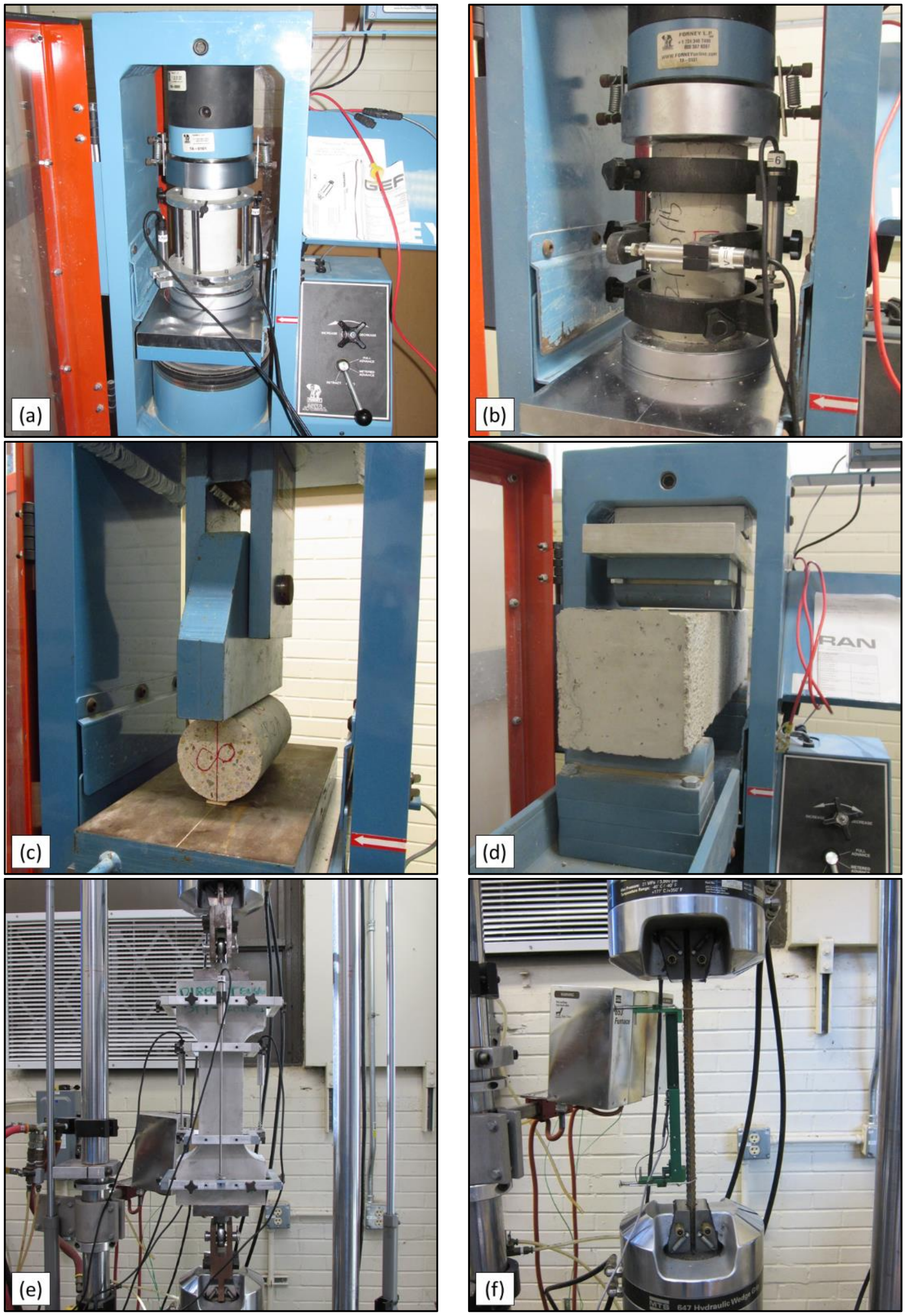

Figure B-7: Testing of Material Properties Showing: (a) Compressive Strength Test, (b) Modulus of Elasticity and Poisson's Ratio Test, (c) Splitting Tensile Strength Test, (d) Modulus of Rupture Test, (e) Direct Tension Test, (f) Reinforcing Bar Tension Test

Table B-1: Specimen 1 Live-End Anchor Block Concrete Compressive Strength Data

Age (days)	Date	Curing Method	Max. Load (kips)	Strength, f_c' (ksi)
7	8/4/14	Water	27.92	2.22
7	8/4/14	Water	27.33	2.18
15	8/12/14	Water	36.62	2.89
15	8/12/14	Water	37.81	2.98
28	8/25/14	Water	47.13	3.71
28	8/25/14	Water	48.88	3.84
28	8/25/14	Water	42.00	3.30
28	8/25/14	Water	46.49	3.66
28	8/25/14	Air	35.20	2.77
28	8/25/14	Air	33.93	2.68
28	8/25/14	Air	33.65	2.65

Table B-2: Specimen 1 Wall Section and Dead-End Block Concrete Compressive Strength Data

Age (days)	Date	Curing Method	Max. Load (kips)	Strength, f_c' (ksi)
28	1/15/15	Air	33.34	2.64
28	1/15/15	Air	33.07	2.62
28	1/15/15	Water	21.91	1.73
28	1/15/15	Water	21.52	1.70
28	1/15/15	Water	22.10	1.75
104	4/1/15	Air	39.62	3.13
104	4/1/15	Air	37.19	2.94
126	4/23/15	Air	37.98	3.00
126	4/23/15	Air	38.07	3.02
126	4/23/15	Air	38.08	3.02
127	4/24/15	Air	37.97	3.00
127	4/24/15	Air	38.92	3.08
127	4/24/15	Air	36.93	2.93
127	4/24/15	Air	37.94	3.01
127	4/24/15	Air	37.99	3.00

Table B-3: Specimen 2 Live-End Anchor Block Concrete Compressive Strength Data

Age (days)	Date	Curing Method	Max. Load (kips)	Strength, f_c'(ksi)
28	9/14/15	Air	83.52	6.65
28	9/14/15	Air	93.48	7.44
28	9/14/15	Air	91.01	7.24
28	9/14/15	Water	94.18	7.49
28	9/14/15	Water	105.73	8.41
28	9/14/15	Water	97.12	7.73

Table B-4: Specimen 2 Wall Section Concrete Core Sample Compressive Strength Data

Age (days)	Date	Curing Method	Max. Load (kips)	Strength, f_c'(ksi)
146	5/10/16	Core	81.17	6.46
146	5/10/16	Core	88.47	7.04
146	5/10/16	Core	87.34	6.95

Table B-5: Specimen 2 Wall Section and Dead-End Anchor Block Air Cured Concrete Compressive Strength Data

Age (days)	Date	Curing Method	Max. Load (kips)	Strength, f_c'(ksi)
1	12/17/15	Air	13.32	1.06
1	12/17/15	Air	13.82	1.10
1	12/17/15	Air	12.44	0.99
5	12/21/15	Air	36.89	2.94
5	12/21/15	Air	38.25	3.04
5	12/21/15	Air	38.22	3.04
7	12/23/15	Air	44.07	3.51
7	12/23/15	Air	42.61	3.39
7	12/23/15	Air	44.41	3.53
14	12/30/15	Air	56.85	4.52
14	12/30/15	Air	57.98	4.61
14	12/30/15	Air	57.91	4.61
28	1/13/16	Air	66.54	5.27
28	1/13/16	Air	60.53	4.80
28	1/13/16	Air	63.68	5.05
28	1/13/16	Air	62.76	4.97
28	1/13/16	Air	63.11	5.00
28	1/13/16	Air	63.32	5.01
28	1/13/16	Air	66.83	5.30
56	2/10/16	Air	64.21	5.11
56	2/10/16	Air	61.07	4.86
56	2/10/16	Air	65.72	5.23
132	4/26/16	Air	59.57	4.72
132	4/26/16	Air	52.90	4.19
132	4/26/16	Air	55.22	4.38
135	4/29/16	Air	53.98	4.28
135	4/29/16	Air	58.33	4.62
135	4/29/16	Air	58.20	4.61

Table B-6: Specimen 2 Wall Section and Dead-End Anchor Block Water Cured Concrete Compressive Strength Data

Age (days)	Date	Curing Method	Max. Load (kips)	Strength, f_c'(ksi)
5	12/21/15	Water	35.16	2.80
5	12/21/15	Water	35.67	2.84
5	12/21/15	Water	33.28	2.65
7	12/23/15	Water	36.86	2.93
7	12/23/15	Water	37.60	2.99
7	12/23/15	Water	39.56	3.15
14	12/30/15	Water	49.87	3.97
14	12/30/15	Water	50.30	4.00
14	12/30/15	Water	51.43	4.09
28	1/13/16	Water	58.69	4.64
28	1/13/16	Water	58.91	4.66
28	1/13/16	Water	56.59	4.48
28	1/13/16	Water	60.33	4.77
28	1/13/16	Water	59.3	4.69
28	1/13/16	Water	57.04	4.51
56	2/10/16	Water	70.75	5.63
56	2/10/16	Water	64.34	5.12
56	2/10/16	Water	67.86	5.40
135	4/26/16	Water	83.57	6.61
135	4/26/16	Water	86.40	6.82
135	4/26/16	Water	87.05	6.88
135	4/29/16	Water	86.74	6.85
135	4/29/16	Water	85.84	6.79
135	4/29/16	Water	89.49	7.07

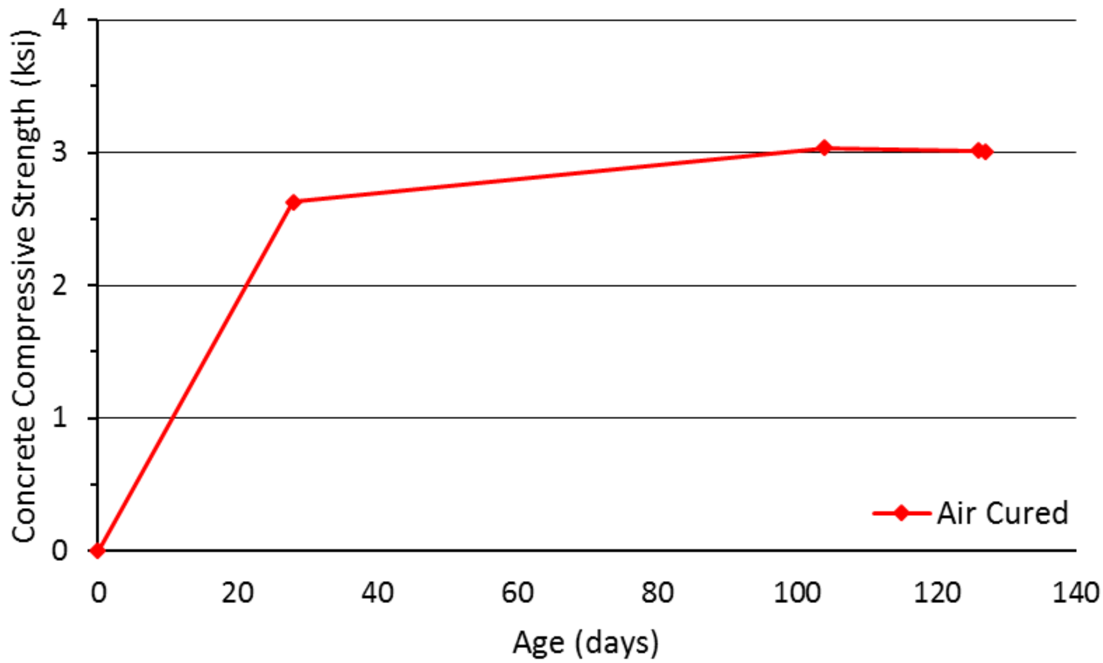

Figure B-8: Specimen 1 Wall Section and Dead-End Anchor Block Concrete Compressive Strength Development

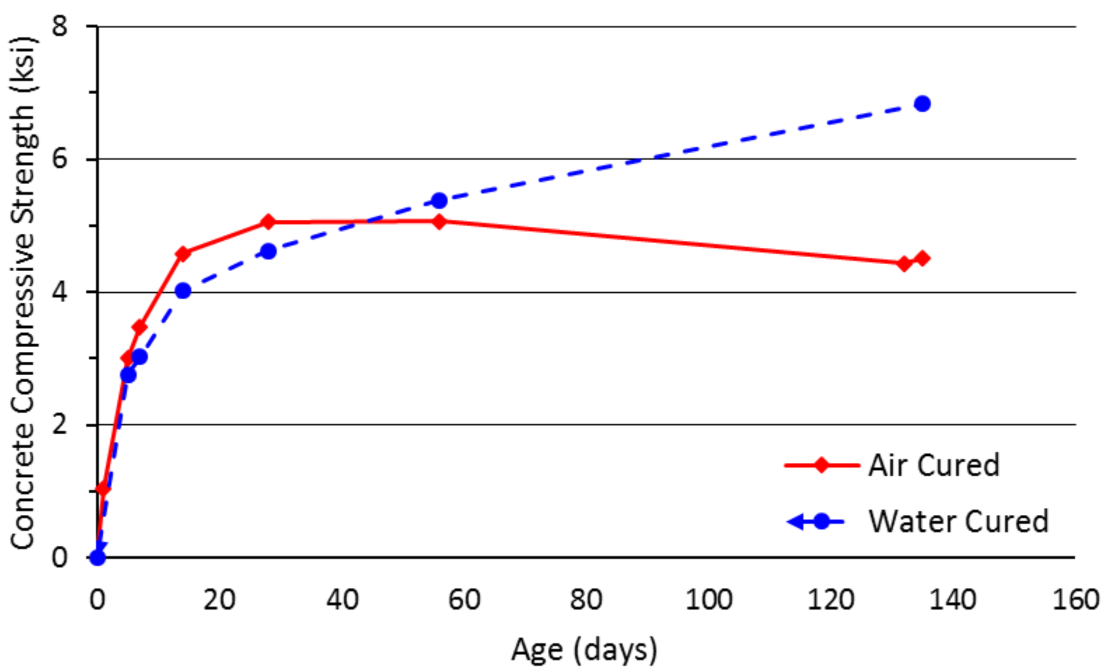

Figure B-9: Specimen 2 Wall Section and Dead-End Anchor Block Concrete Compressive Strength Development

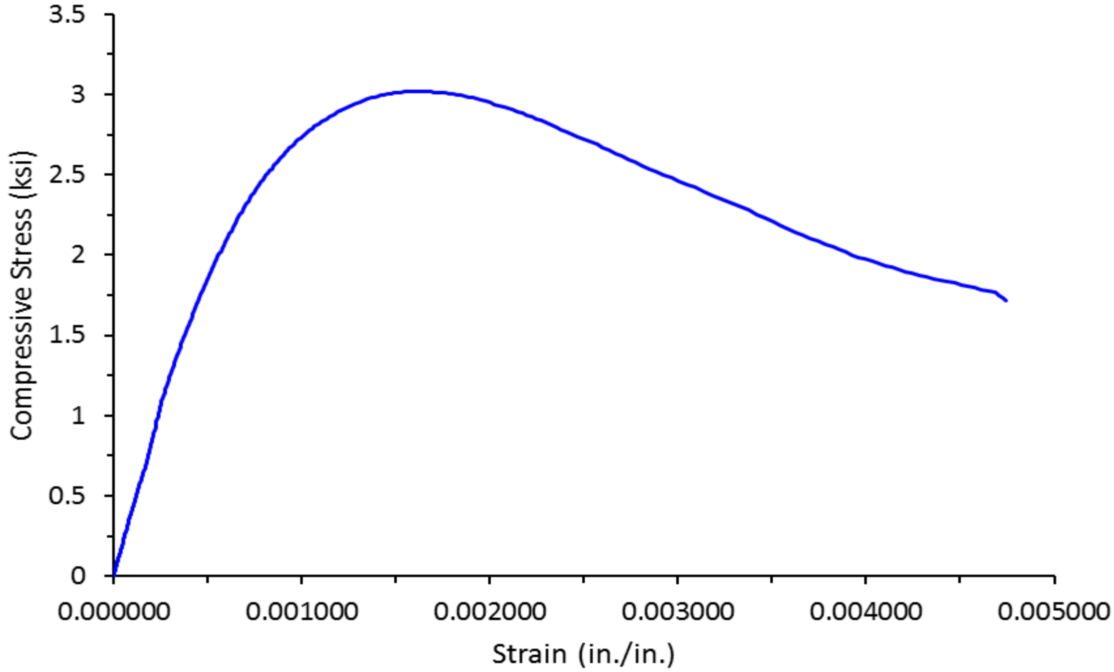

Figure B-10: Typical Concrete Compressive Strength Test Stress versus Strain Plot

Table B-7: Specimen 1 Wall Section and Dead-End Anchor Block Concrete Modulus of Elasticity and Poisson's Ratio Data

Age (days)	Date	Curing Method	Elastic Modulus, E_c (ksi)	Poisson's Ratio, ν
28	1/15/15	Water	3,949	N/A
28	1/15/15	Water	3,953	N/A
28	1/15/15	Water	3,988	N/A
127	4/24/15	Air	3,457	0.176
127	4/24/15	Air	3,630	0.174
127	4/24/15	Air	3,641	0.177

Table B-8: Specimen 2 Wall Section and Dead-End Anchor Block Concrete Modulus of Elasticity and Poisson's Ratio Data

Age (days)	Date	Curing Method	Elastic Modulus, E_c (ksi)	Poisson's Ratio, ν
5	12/21/15	Air	3,588	N/A
5	12/21/15	Air	3,625	N/A
5	12/21/15	Air	3,913	N/A
5	12/21/15	Water	4,831	N/A
5	12/21/15	Water	4,880	N/A
5	12/21/15	Water	6,638	N/A
7	12/23/15	Air	4,472	N/A
7	12/23/15	Air	4,260	N/A
7	12/23/15	Air	6,550	N/A
7	12/23/15	Water	3,306	N/A
7	12/23/15	Water	3,140	N/A
7	12/23/15	Water	4,374	N/A
28	1/13/16	Air	4,573	0.200
28	1/13/16	Air	4,157	0.175
28	1/13/16	Air	4,185	0.177
28	1/13/16	Water	4,407	0.207
28	1/13/16	Water	4,712	0.215
28	1/13/16	Water	4,669	0.219
135	4/29/16	Air	4,543	0.178
135	4/29/16	Air	5,588	0.224
135	4/29/16	Air	4,603	0.189
135	4/29/16	Water	6,140	0.169
135	4/29/16	Water	5,761	0.193
135	4/29/16	Water	5,609	0.199

Table B-9: Specimen 1 Wall Section and Dead-End Anchor Block Concrete Splitting Tensile Strength Test Data

Age (days)	Date	Curing Method	Max. Load (kips)	Strength, f_{sp} (psi)
28	1/15/15	Water	10.76	220
28	1/15/15	Water	10.40	212
28	1/15/15	Water	12.13	246
127	4/24/15	Air	19.78	406
127	4/24/15	Air	18.54	381
127	4/24/15	Air	18.39	373
127	4/24/15	Air	18.90	381
127	4/24/15	Air	17.49	357

Table B-10: Specimen 2 Wall Section and Dead-End Anchor Block Concrete Splitting Tensile Strength Test Data

Age (days)	Date	Curing Method	Max. Load (kips)	Strength, f_{sp} (psi)
28	1/13/16	Air	29.71	595
28	1/13/16	Air	26.79	544
28	1/13/16	Air	26.87	544
28	1/13/16	Water	26.56	536
28	1/13/16	Water	25.50	514
28	1/13/16	Water	27.50	552
135	4/29/16	Air	23.90	481
135	4/29/16	Air	24.64	495
135	4/29/16	Air	24.77	499
135	4/29/16	Water	32.65	653
135	4/29/16	Water	26.56	535
135	4/29/16	Water	30.02	604

Table B-11: Specimen 1 Wall Section and Dead-End Anchor Block Concrete Modulus of Rupture Test Data

Age (days)	Date	Curing Method	Max. Load (kips)	Strength, f_r (psi)
127	4/24/15	Air	7.68	619
127	4/24/15	Air	7.96	642
127	4/24/15	Air	9.11	722
127	4/24/15	Air	7.89	635
127	4/24/15	Air	7.24	575
127	4/24/15	Air	7.98	641

Table B-12: Specimen 2 Wall Section and Dead-End Anchor Block Concrete Modulus of Rupture Test Data

Age (days)	Date	Curing Method	Max. Load (kips)	Strength, f_r (psi)
28	1/13/16	Air	8.07	638
28	1/13/16	Air	7.72	597
28	1/13/16	Air	7.50	608
28	1/13/16	Water	8.16	679
28	1/13/16	Water	7.71	636
28	1/13/16	Water	8.41	699
135	4/29/16	Air	10.75	852
135	4/29/16	Air	10.75	845
135	4/29/16	Air	10.20	780

Table B-13: Specimen 1 Wall Section and Dead-End Anchor Block Concrete Direct Tension Test Data

Age (days)	Date	Curing Method	Max. Load (kips)	Strength, f_t’ (psi)
134	5/1/15	Air	2.87	176
134	5/1/15	Air	3.65	223
134	5/1/15	Air	3.85	237

Table B-14: Specimen 2 Wall Section and Dead-End Anchor Block Concrete Direct Tension Test Data

Age (days)	Date	Curing Method	Max. Load (kips)	Strength, f_t' (psi)
28	1/13/16	Air	7.08	419
28	1/13/16	Air	6.67	412
28	1/13/16	Air	6.71	412
28	1/13/16	Water	6.33	398
28	1/13/16	Water	7.10	431
28	1/13/16	Water	7.27	435
28	1/13/16	Water	7.16	444
135	4/29/16	Air	7.67	450
135	4/29/16	Air	7.92	480
135	4/29/16	Air	6.52	399
135	4/29/16	Air	7.06	434

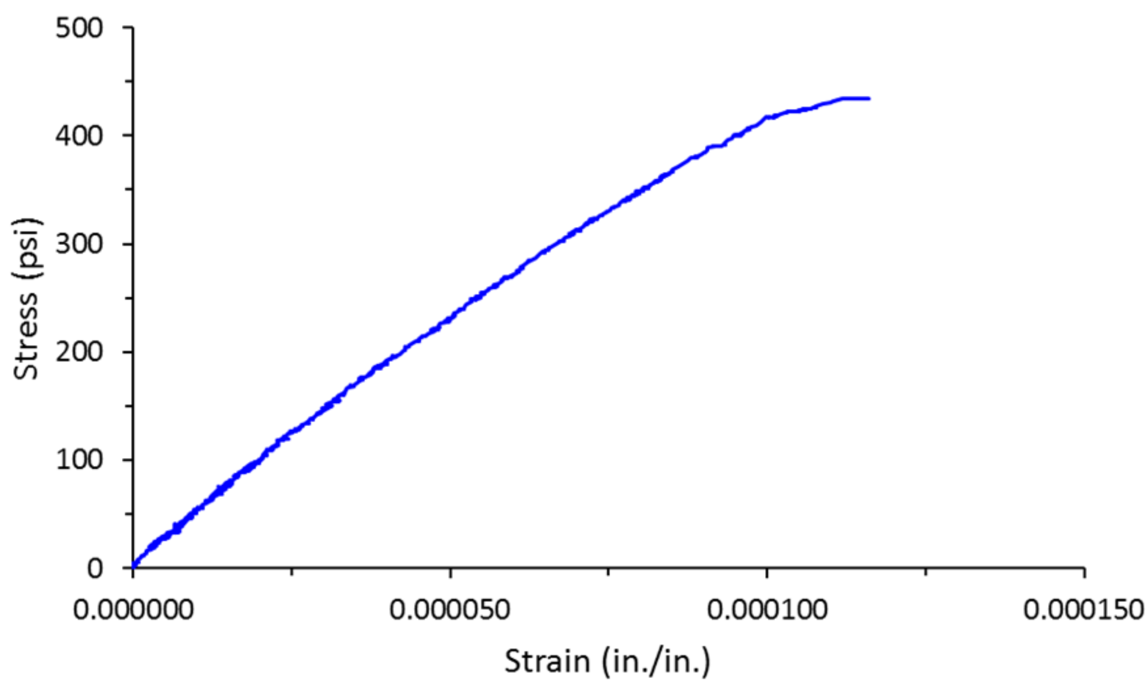

Figure B-11: Typical Concrete Direct Tension Test Stress versus Strain Plot

Mill Certification Details

Customer: Ambassador Steel Corporation
Bill of Lading #: 667972-NTX
Chief Metallurgist:
Heat #: JW14102995
Product: Rebar ASTM A615/A615M-12 GR 60[420] AASHTO M31-07
10/#3 Rebar
Grade: A61560
Comments:

Date: 4/5/2014
Tag #: JW1411079403
Mill: Nucor Jewett
Size: 10/#3 Rebar
Division: TX

Chemical Properties - Wt.%

Mn	C	Cu	Si	Cr	Ni	Mo	S	P	V	Nb	Pb	Sn	Ti	N	Ca	Al	B	Ceq
.950	.360	.250	.160	.150	.120	.037	.032	.009	.004	.001	.000	.000	.000	.000	.000	.000	.000	.550

Carbon Equivalent= 0.55

Physical Properties

Imperial = psi

Tensile: 109,200
Yield: 68,600
Elongation (in 8 inches): 14.00
Elongation (in 2 inches):

Bend Test: OK

The testing was conducted in accordance with the requirements of this specification. All melting and manufacturing processes were performed in the United States of America.

For Internal Use Only

Chief Metallurgist

Figure B-12: Specimen 1 Steel Mill Certification Test Report for No. 3 Reinforcing Bars Used in the Curved Wall Section

Mill Certification Details

Customer: Ambassador Steel Corporation
Bill of Lading #: 653174-NTX
Chief Metallurgist:
Heat #: JW13107986
Product: Rebar ASTM A615/A615M-12 GR 60[420] AASHTO M31-07 13/#4 Rebar
Grade: A61560
Comments:

Date: 9/10/2013
Tag #: JW1311242070
Mill: Nucor Jewett
Size: 13/#4 Rebar
Division: - TX

Chemical Properties - Wt.%

Mn	Cu	C	Cr	Si	Ni	Mo	S	P	V	Nb	Pb	Sn	Ti	N	Ca	Al	B	Ceq
.960	.380	.380	.180	.180	.140	.036	.029	.014	.003	.001	.000	.000	.000	.000	.000	.000	.000	.580

Carbon Equivalent= 0.58

Physical Properties

Imperial = psi

Tensile: 99,200
Yield: 62,900
Elongation (in 8 inches): 16.00
Elongation (in 2 inches):

Bend Test: OK

The testing was conducted in accordance with the requirements of this specification. All melting and manufacturing processes were performed in the United States of America.

For Internal Use Only

Chief Metallurgist

Figure B-13: Specimen 1 Steel Mill Certification Test Report for No. 4 Reinforcing Bars Used in the Curved Wall Section

NUCOR
NUCOR CORPORATION
NUCOR STEEL TEXAS

Mill Certification
6/16/2015

MTR #: 0000105518
8812 Hwy 79 W
Jewett, TX 75846
(903) 626-4461
Fax: (903) 626-6290

Sold To: HARRIS REBAR NUFAB LLC
PO BOX 627
AUBURN, IN 46706
(936) 258-8221
Fax: (936) 258-9837

Ship To: HARRIS-SAN ANTONIO-CARRIER
N/A
NEW BRAUNFELS, TX 78130
(830) 387-2910

Customer P.O.	0000162608	Sales Order	219898.1
Product Group	Rebar	Part Number	900000137204200
Grade	ASTM A615/A615M-14 GR 60[420] AASHTO M31-07	Lot #	JW1510310902
Size	13/#4 Rebar	Heat #	JW15103109
Product	13/#4 Rebar 60' A615M GR420 (Gr60)	B.L. Number	J1-707462
Description	A615M GR 420 (Gr60)	Load Number	J1-310031
Customer Spec		Customer Part #	

I hereby certify that the material described herein has been manufactured in accordance with the specifications and standards listed above and that it satisfies those requirements.

Roll Date: 5/14/2015 Melt Date: 5/11/2015 Qty Shipped LBS: 6,012 Qty Shipped Pcs: 150

C	Mn	P	S	Si	Cu	Ni	Cr	Mo	V	Cb
0.38%	1.03%	0.012%	0.035%	0.19%	0.32%	0.14%	0.17%	0.044%	0.0038%	0.001%

Yield 1: 65,200psi Tensile 1: 101,900psi Elongation: 13% in 8"(% in 203.3mm)
Bend OK

Specification Comments:

Comments: E-mail: websales@nstexas.com

1. All manufacturing processes of the steel, including melting, have been performed in the U.S.A.
2. Mercury in any form has not been used in the production or testing of this product.
3. Welding or weld repair was not perfomed on this material.
4. This material conforms to the specifications described on this document and may not be reproduced, except in full, without written approval of Nucor Corporation.
5. Results reported for ASTM E45 (Inclusion content) and ASTM E381 (Macro-etch) are provided as interpretation of ASTM procedures.

Bhargava R Vantari
Bhargava R Vantari
Division Metallurgist

NSMG-10 January 1, 2012

Page 2 of 2

Figure B-14: Specimen 2 Steel Mill Certification Test Report for No. 4 Reinforcing Bars Used in the Curved Wall Section

Table B-15: Specimen 1 Reinforcing Bar Tensile Testing Data

Bar Designation	Yield Strength, f_y (ksi)	Tensile Strength, f_u (ksi)	Elastic Modulus, E_s (ksi)	Elongation at Fracture (%)
#3	67.27	108.98	30,747	14.74
#3	67.53	109.37	30,615	14.92
#3	67.16	109.18	30,561	14.55
#4	74.32	100.81	29,965	11.51
#4	72.50	100.75	30,443	14.64
#4	71.70	100.72	26,971	12.92
#4	75.30	100.56	30,891	13.24
#4	79.00	99.67	26,713	13.92
#4	70.40	99.37	31,052	14.78

Table B-16: Specimen 2 Reinforcing Bar Tensile Testing Data

Bar Designation	Yield Strength, f_y (ksi)	Tensile Strength, f_u (ksi)	Elastic Modulus, E_s (ksi)	Elongation at Fracture (%)
#4	60.09	95.29	27,974	14.84
#4	64.32	99.76	28,923	15.09
#4	59.25	95.22	29,868	15.02
#4	59.28	95.33	27,741	15.09

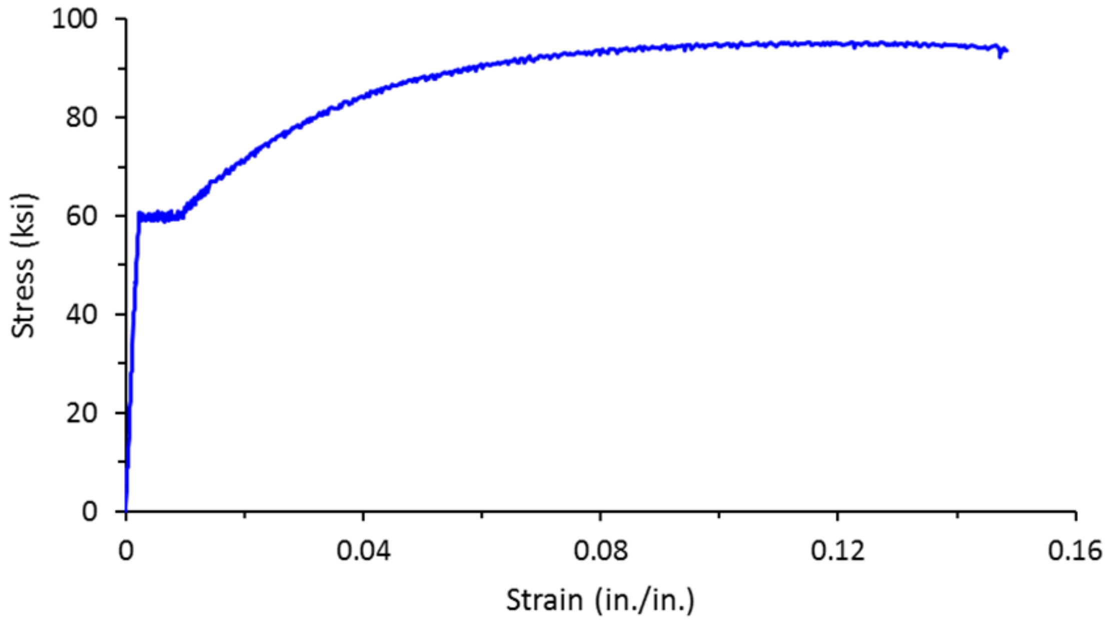

Figure B-15: Typical Reinforcing Bar Tensile Test Stress versus Strain Plot

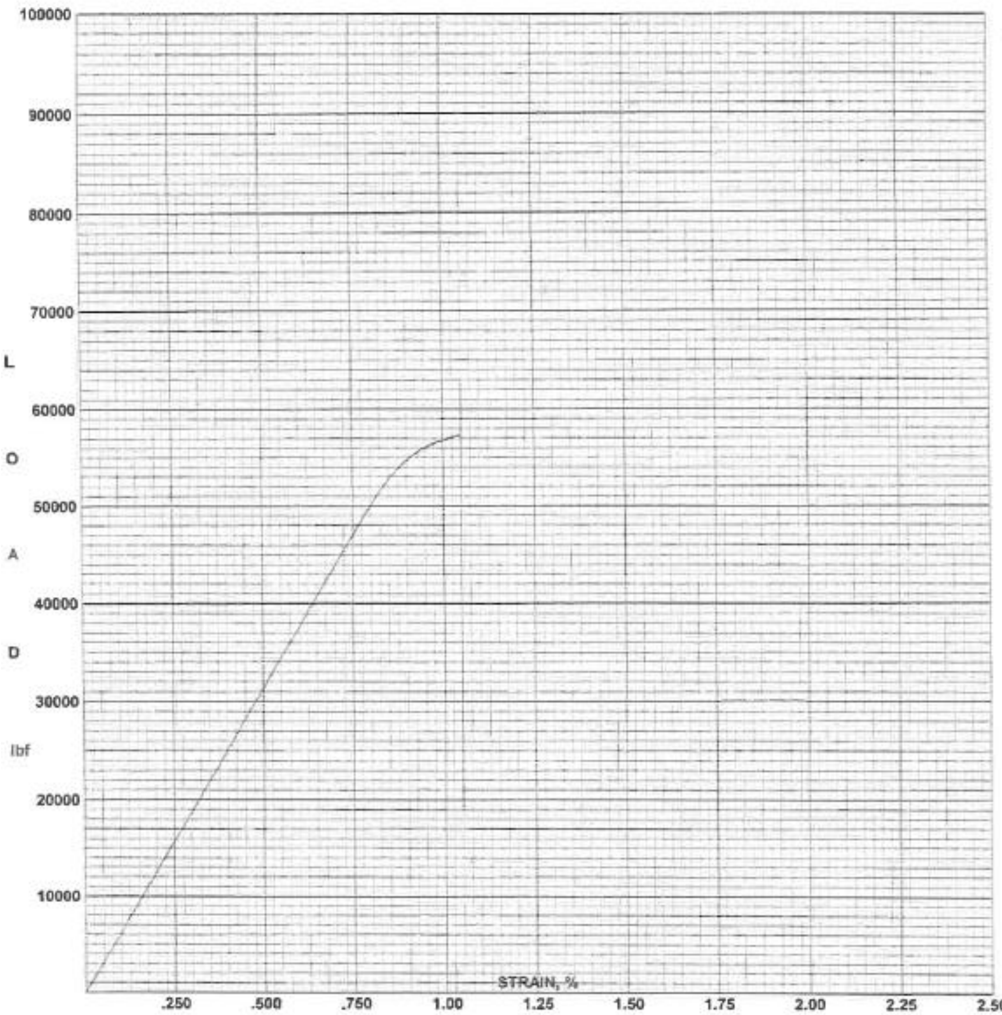

American Spring Wire
11020 Tanner Road
Houston, TX 77041

7-Strand Wire

Customer	University of Texas
Order No.	58130
Item	.600" 270K LR Strand
Lot No.	610623
Quantity	1
PAK(1)	930572208
PAK(2)	-
PAK(3)	-
PAK(4)	-
Comment	P/O# 2014A05523

CS Area, in²:	**0.2217**
CS Area, mm²:	**143.06**
EUL #2, kN:	**252.51**
EUL #2, lbf:	**56769**
Ultimate, lbf:	**62715**
Ultimate, kN:	**278.96**
TE (Man), %:	**7.77**
Modulus, Mpsi:	**28.3**
Modulus, MPa:	**194890**
PAK NUMBER:	**930572208**

This strand was manufactured in the United States of America from domestically produced materials and conforms with the Buy American Regulations. American Spring Wire Corp. certifies that the results listed above comply with the requirements of ASTM A416 (Latest Revision). Testing of prestressing strand at independent laboratories and at a PCI certified prestressing manufacturing facility have shown that ASW's strand will bond to concrete of a normal strength and consistency in conformance with the equations for transfer and development length given in the ACI/AASHTO specifications.

Signed Julio Torres Date 10-31-13

7 Strand Cable - Chart Data
Oct 31, 2013 7:05:52 AM

BR 9/30/2004 QC100012LFRM REV. 002

Figure B-16: Strand Mechanical Properties Data Report for Specimen 1

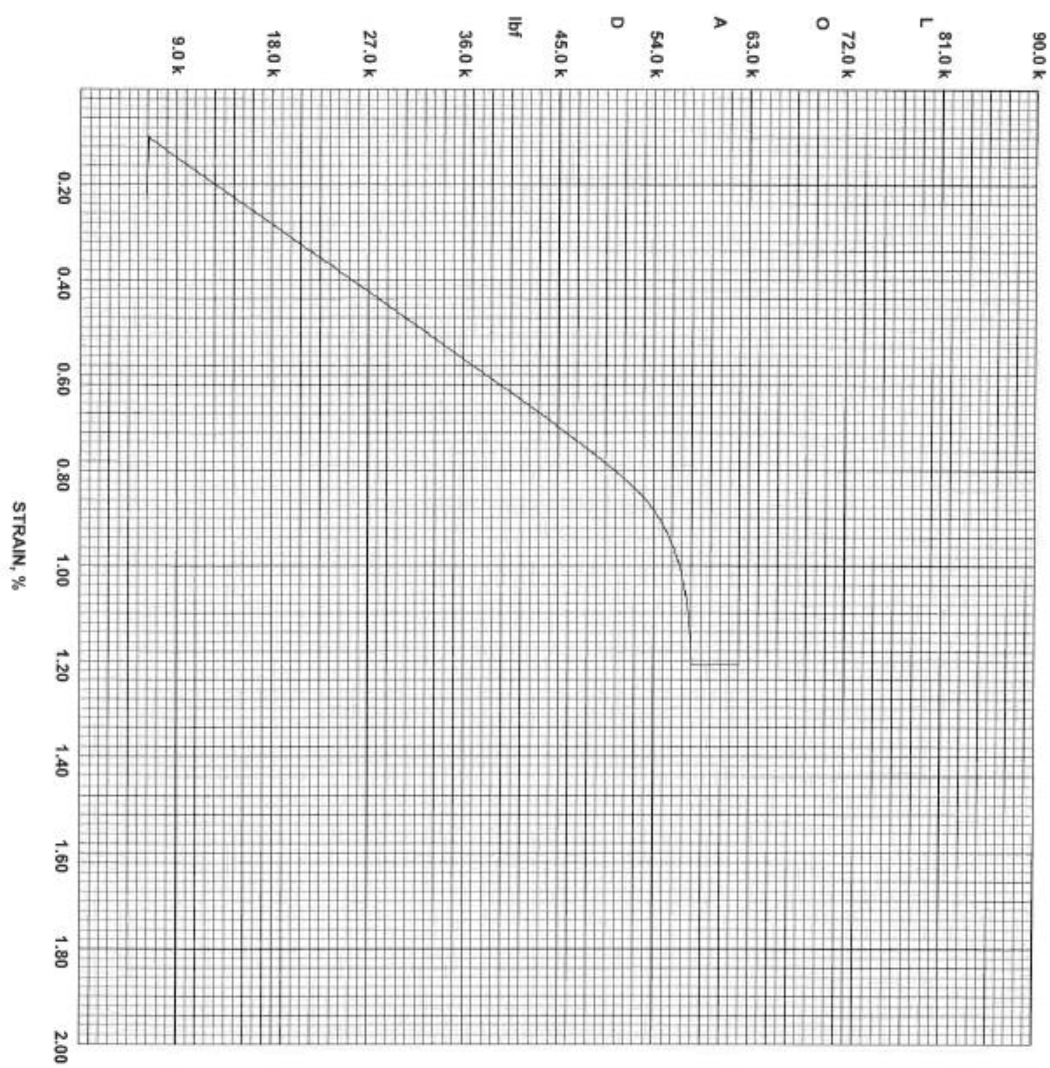

Insteel Wire Products
Prestressed Concrete Strand

.600" 270 7W LOW RELAXATION

Test Number:	202588
Tested By:	JT
Ultimate Breaking Strength, lbf:	62128
Ultimate Breaking Strength, kN:	276
Load @ 1% Extension, lbf:	56471
Load @ 1% Extension, kN:	251
Ultimate Elongation, %:	7.77
Rep. Area, in²:	0.218
Rep. Area, mm²:	140.6
Actual Area, in²:	.2199
Actual Area, mm²:	142
Avg Modulus of Elasticity, Mpsi:	29.0
Avg Modulus of Elasticity, MPa:	199947.6
Reference:	

Jul 28, 2015 10:36:00 AM
SN: 321315 V7.02.11

Figure B-17: Strand Mechanical Properties Data Report for Specimen 2

PROLAMSA
60 AÑOS
www.prolamsausa.com

CERTIFICADO DE CALIDAD / MILL TEST REPORT

CLIENTE / SOLD TO	DESTINATARIO/SHIP TO	FACTURA/INVOICE
Triple S Steel Supply Co. PO Box 21119 Houston TX C.P.77226	Triple S - Irvington Whs 8411 Irvington Houstop TX C.P. 77022	1200047973 FECHA/DATE 04/24/2014

O.C./ P.O.	PEDIDO/ ORDER	ROLLO/ COIL	LOTE/ PACKAGE	CODIGO/ CODE	DESCRIPCIÓN DEL MATERIAL/ MATERIAL DESCRIPTION	LONGITUD/ LENGTH	ANALISIS %C	%Mn	%P	%S
HOU-158456	30029315-200	0008802906	0009178886	300551	SQR 3.000 0.2500 HBC STK 20.00	20.000 Feet	0.0949	0.33	0.0193	0.0094
HOU-158456	30029315-200	0008802906	0009178908	300551	SQR 3.000 0.2500 HBC STK 20.00	20.000 Feet	0.0949	0.3348	0.0193	0.0094
HOU-158456	30029315-200	0008802913	0009176614	300551	SQR 3.000 0.2500 HBC STK 20.00	20.000 Feet	0.0878	0.3473	0.0179	0.0114
HOU-158456	30029315-200	0008802906	0009178939	300551	SQR 3.000 0.2500 HBC STK 20.00	20.000 Feet	0.0949	0.3348	0.0193	0.0094
HOU-158456	30029315-280	0009025044	0009166785	308039	ROUN 2.000 0.0747 HCQ 20.00	20.000 Feet	0.0762	0.5755	0.0125	0.0094
HOU-158456	30029315-280	0009025044	0009166823	308039	ROUN 2.000 0.0747 HCQ 20.00	20.000 Feet	0.0762	0.5755	0.0125	0.0094
HOU-158456	30029315-280	0009025044	0009166867	308039	ROUN 2.000 0.0747 HCQ 20.00	20.000 Feet	0.0762	0.5755	0.0125	0.0094
HOU-158456	30029315-280	0009025044	0009166458	308039	ROUN 2.000 0.0747 HCQ 20.00	20.000 Feet	0.0762	0.5755	0.0125	0.0094
HOU-158456	30029315-280	0009025044	0009166719	308039	ROUN 2.000 0.0747 HCQ 20.00	20.000 Feet	0.0762	0.5755	0.0125	0.0094
HOU-158456	30029315-280	0009025044	0009166490	308039	ROUN 2.000 0.0747 HCQ 20.00	20.000 Feet	0.0762	0.5755	0.0125	0.0094
HOU-158456	30029315-280	0009025044	0009166892	308039	ROUN 2.000 0.0747 HCQ 20.00	20.000 Feet	0.0762	0.5755	0.0125	0.0094
HOU-158456	30029315-280	0009025044	0009167234	308039	ROUN 2.000 0.0747 HCQ 20.00	20.000 Feet	0.0762	0.5755	0.0125	0.0094
HOU-158456	30029315-280	0009025044	0009166728	308039	ROUN 2.000 0.0747 HCQ 20.00	20.000 Feet	0.0762	0.5755	0.0125	0.0094
HOU-158456	30029315-280	0009025044	0009167508	308039	ROUN 2.000 0.0747 HCQ 20.00	20.000 Feet	0.0762	0.5755	0.0125	0.0094

O.C./ P.O.	PEDIDO/ ORDER	ROLLO/ COIL	LOTE/ PACKAGE	PROPIEDADES FISICAS/ MECHANICAL PROPERTIES DUREZA/ (HRB)	TENSION/ TENSILE (ksi)	CEDENCIA/ YIELD (ksi)	ELONGACION/ ELONGATION(%)	ESTANDAR/ STANDAR	COLADA/ HEAT	HECHO/ MADE
HOU-158456	30029315-200	0008802906	0009178886	79	65	55	29	A500 HRGrade BC	136292	Made in Mexico
HOU-158456	30029315-200	0008802906	0009178908	79	65	55	29	A500 HRGrade BC	136292	Made in Mexico
HOU-158456	30029315-200	0008802913	0009176614	79	65	55	29	A500 HRGrade BC	241072	Made in Mexico
HOU-158456	30029315-200	0008802906	0009178939	79	65	55	29	A500 HRGrade BC	136292	Made in Mexico
HOU-158456	30029315-280	0009025044	0009166785	50	45	33	24	A513	440243	Made in Mexico
HOU-158456	30029315-280	0009025044	0009166823	50	45	33	24	A513	440243	Made in Mexico
HOU-158456	30029315-280	0009025044	0009166867	50	45	33	24	A513	440243	Made in Mexico
HOU-158456	30029315-280	0009025044	0009166458	50	45	33	24	A513	440243	Made in Mexico
HOU-158456	30029315-280	0009025044	0009166719	50	45	33	24	A513	440243	Made in Mexico
HOU-158456	30029315-280	0009025044	0009166490	50	45	33	24	A513	440243	Made in Mexico
HOU-158456	30029315-280	0009025044	0009166892	50	45	33	24	A513	440243	Made in Mexico
HOU-158456	30029315-280	0009025044	0009167234	50	45	33	24	A513	440243	Made in Mexico
HOU-158456	30029315-280	0009025044	0009166728	50	45	33	24	A513	440243	Made in Mexico
HOU-158456	30029315-280	0009025044	0009167508	50	45	33	24	A513	440243	Made in Mexico

Imprimió/Printed by: Info. Prolamsa 04/24/2014 23:31:21 Pág:1/ 2

Emitted by: Luis de Alvarado
Coord. De Laboratorio

Figure B-18: Steel Mill Certification Test Report for Specimen 1 Ducts

WEBCO INDUSTRIES

MATERIAL TEST REPORT

Sold To: 414000 **TUBULAR STEEL INC.** **1031 EXECUTIVE PKWY DR.** **ST. LOUIS MO 63141-6351**	**Ship To: 63027** **TUBULAR STEEL/LORAIN** **7440 DEER TRAIL LANE** **LORAIN OH 44053**

Purchase Order: 049860
Part Number: LINE 5
Sales Order: 193122
Material: A695400009507405 ASTM A513-5 4000OD 38100ID Tubular Steel
Delivery / File Nbr: 80324776

Description: ASTM A513-5-15 DOM GRADE C1026

Test: NDT ELECTRIC TESTED TO ASTM A450 OR A1016 & APPLICABLE TEST METHOD E309 OR E426. SRA. . MATERIAL HAS NO CONTAMINATION BY
MERCURY, LEAD, ASBESTOS, AND NO REPAIR BY WELDING.

Heat Number:		GA69834	WA404087
		%	%
CARBON	LDL	0.240	0.250
MANGANESE	LDL	0.690	0.710
PHOSPHORUS	LDL	0.010	0.007
SULFUR	LDL	0.002	0.002
SILICON	LDL	0.020	0.020
NICKEL	LDL	0.050	0.040
CHROMIUM	LDL	0.060	0.070
MOLYBDENUM	LDL	0.020	0.010
COPPER	LDL	0.090	0.090
ALUMINUM	LDL	0.034	0.033
BORON	LDL	0.0001	0.0001
CALCIUM	LDL	0.002	0.003
COLUMBIUM	LDL	0.002	0.002
NITROGEN	LDL	0.008	0.009
TIN	LDL	0.007	0.005
TITANIUM	LDL	0.002	0.001
VANADIUM	LDL	0.001	0.002
Ultimate	**(PSI)**	92,848 / 92,848	92,870 / 92,870
Yield	**(PSI)**	79,965 / 79,965	80,712 / 80,712
Elongation (%)		21 / 21	17 / 17
Hardness	**(RB)**	91 / 92	90 / 92
Origin of Melt		USA	USA
Manufactured in		USA	USA

Webco Industries, Inc. certifies that the material described was manufactured and tested and/or inspected in accordance with the specification and fulfills requirements in such respect.
This document conforms to the requirements of Specification EN 10204 Inspection Document Type 3.1.
This document was prepared by means of electronic processing and is valid without signature.

Date: 09/22/2015

Tony Stubblefield
Quality Manager
tstubblefield@webcoindustries.com

Webco Industries | 9101 W 21st Street | Sand Springs, OK 74063 USA | (918)245-2211

Figure B-19: Steel Mill Certification Test Report for Specimen 2 Ducts

Appendix C: Experimental Results

Appendix C presents additional results from the structural testing for both of the curved wall specimens. The information is presented as follows:

- Snapshots of the delamination failures and additional images of the failed curved wall specimens.
- Circumferential reinforcing bar data for the 45° and 75° locations of both specimens.
- Embedded strain gauge data showing through-thickness strains for Specimen 1 at the 45° location and for Specimen 2 at the 15° location.
- Concrete surface strain gauge data showing through-thickness strains measured at the top of both specimens.
- NDI Optotrak Certus system data showing the global movement of Specimen 2 from the top view and side view.

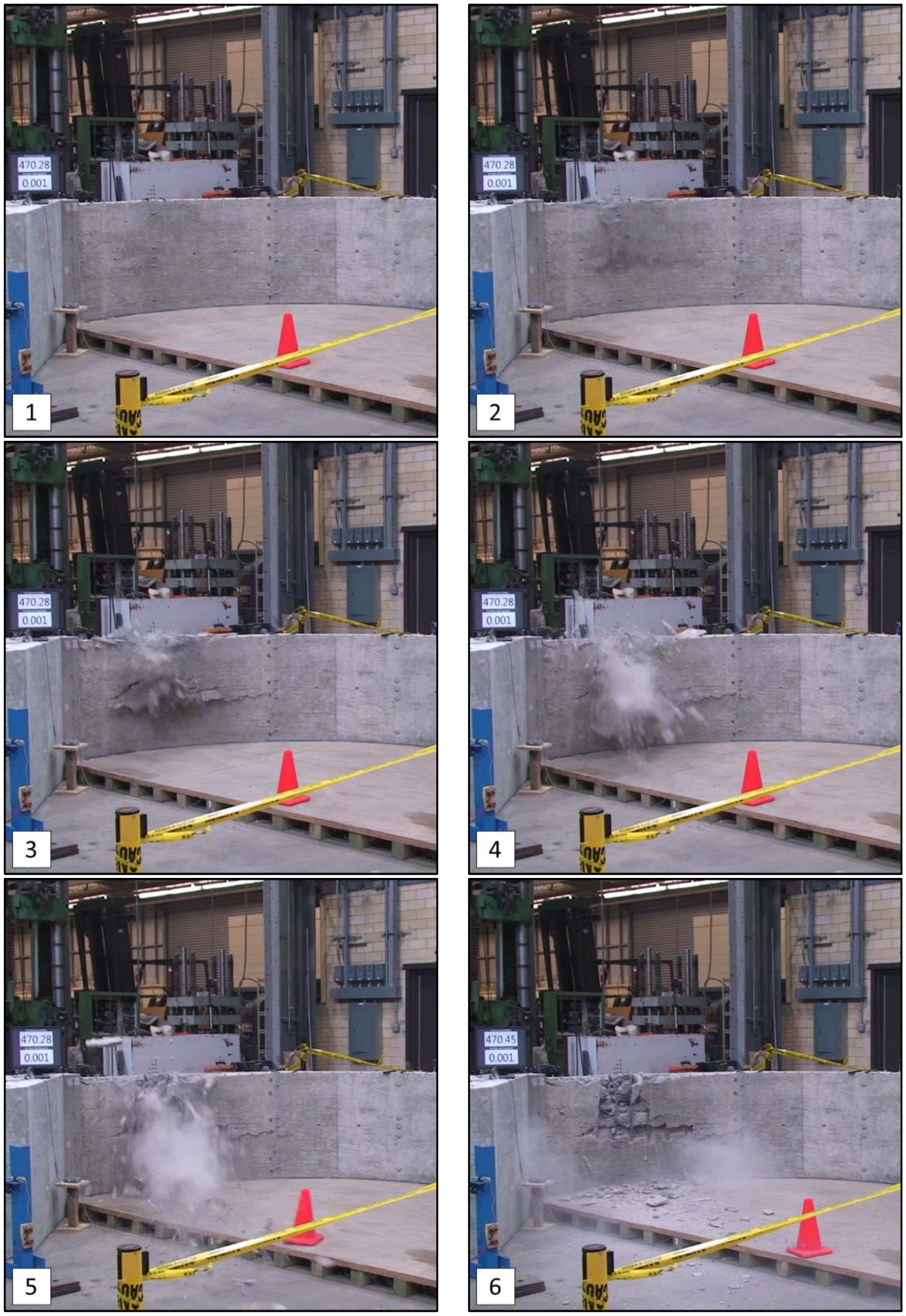

Figure C-1: Snapshots of the Delamination Failure of Specimen 1 at the 15° Location from the Front

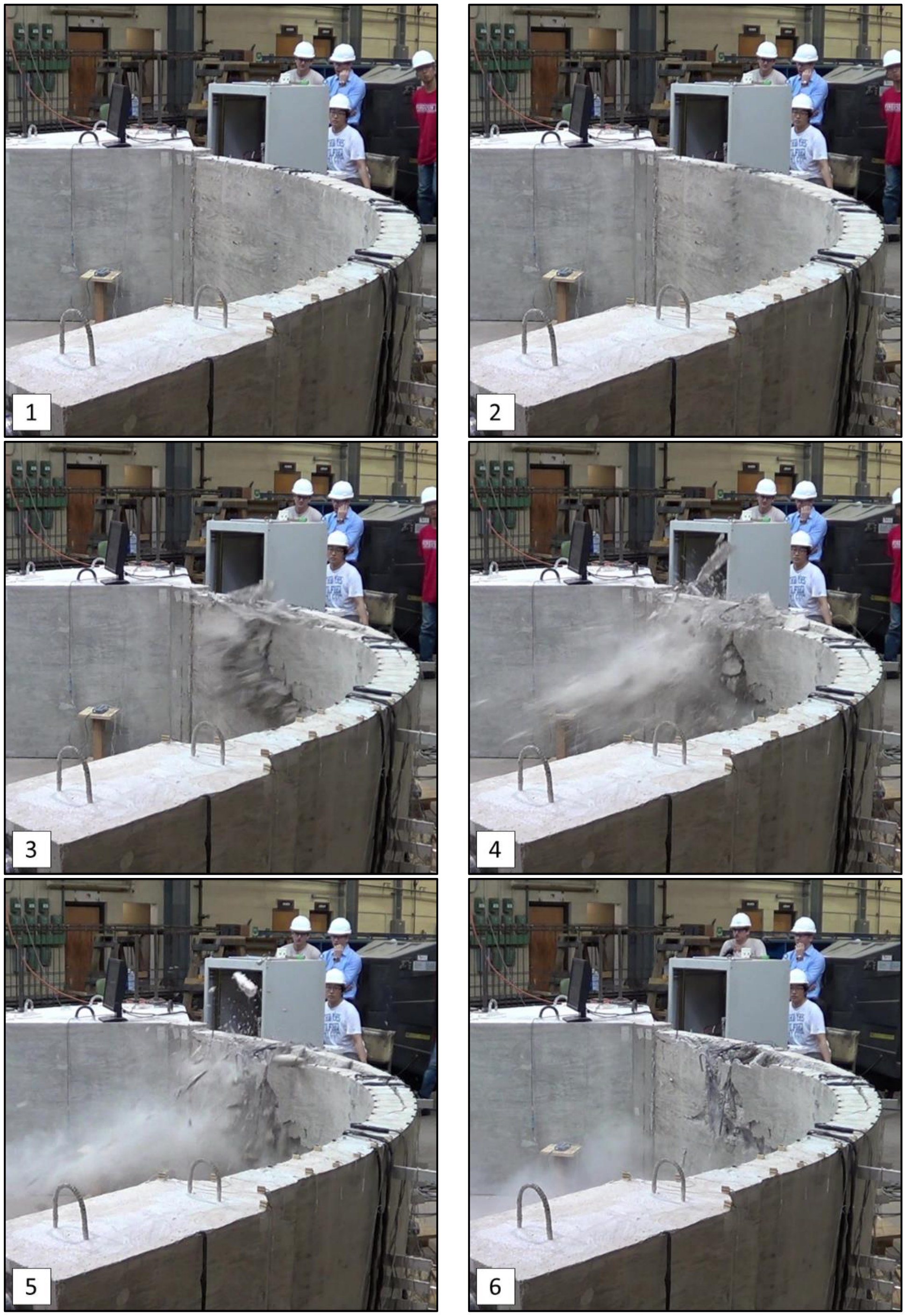

Figure C-2: Snapshots of the Delamination Failure of Specimen 1 at the 15° Location from the Side

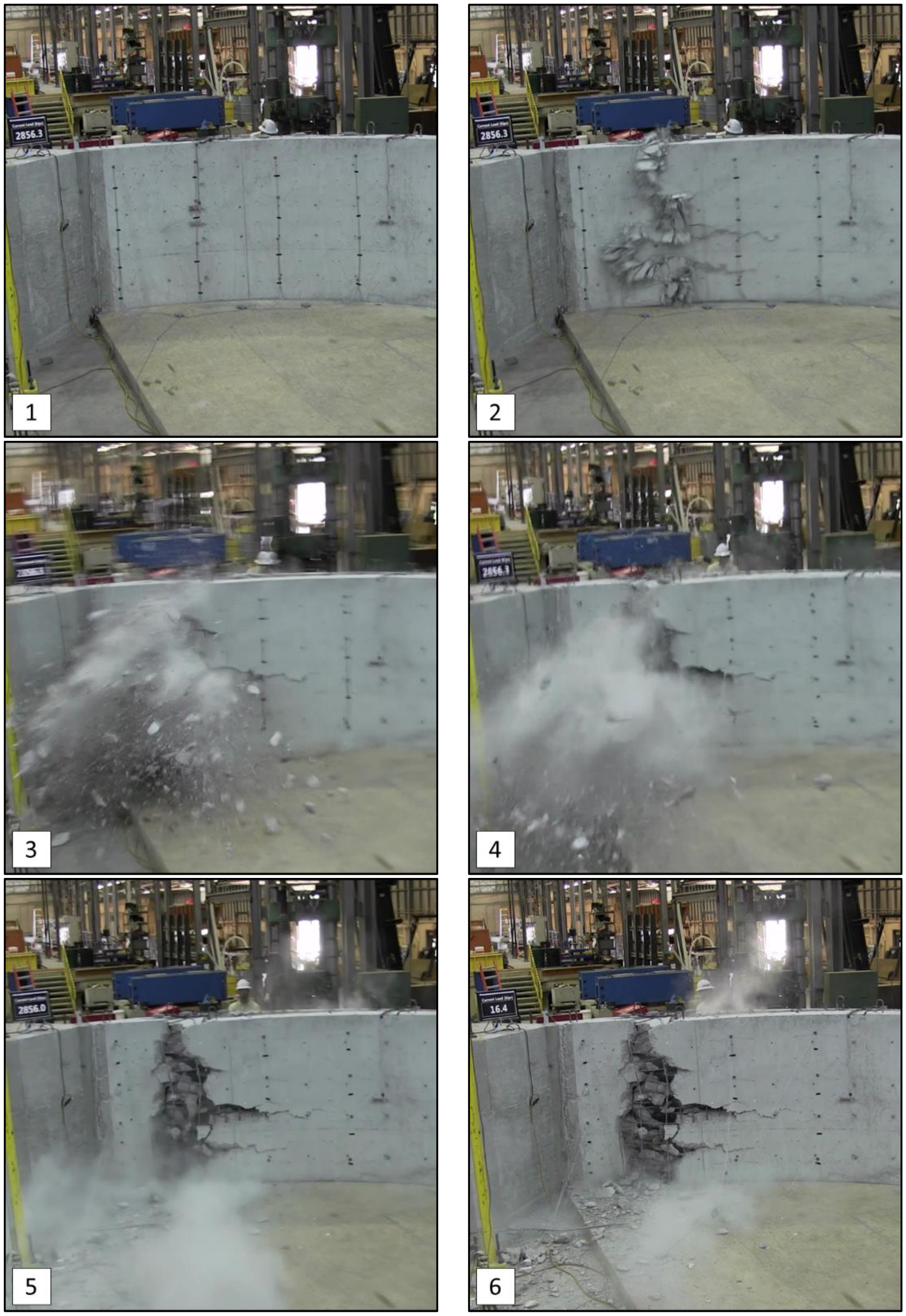

Figure C-3: Snapshots of the Delamination Failure of Specimen 2 at the 15° Location from the Front

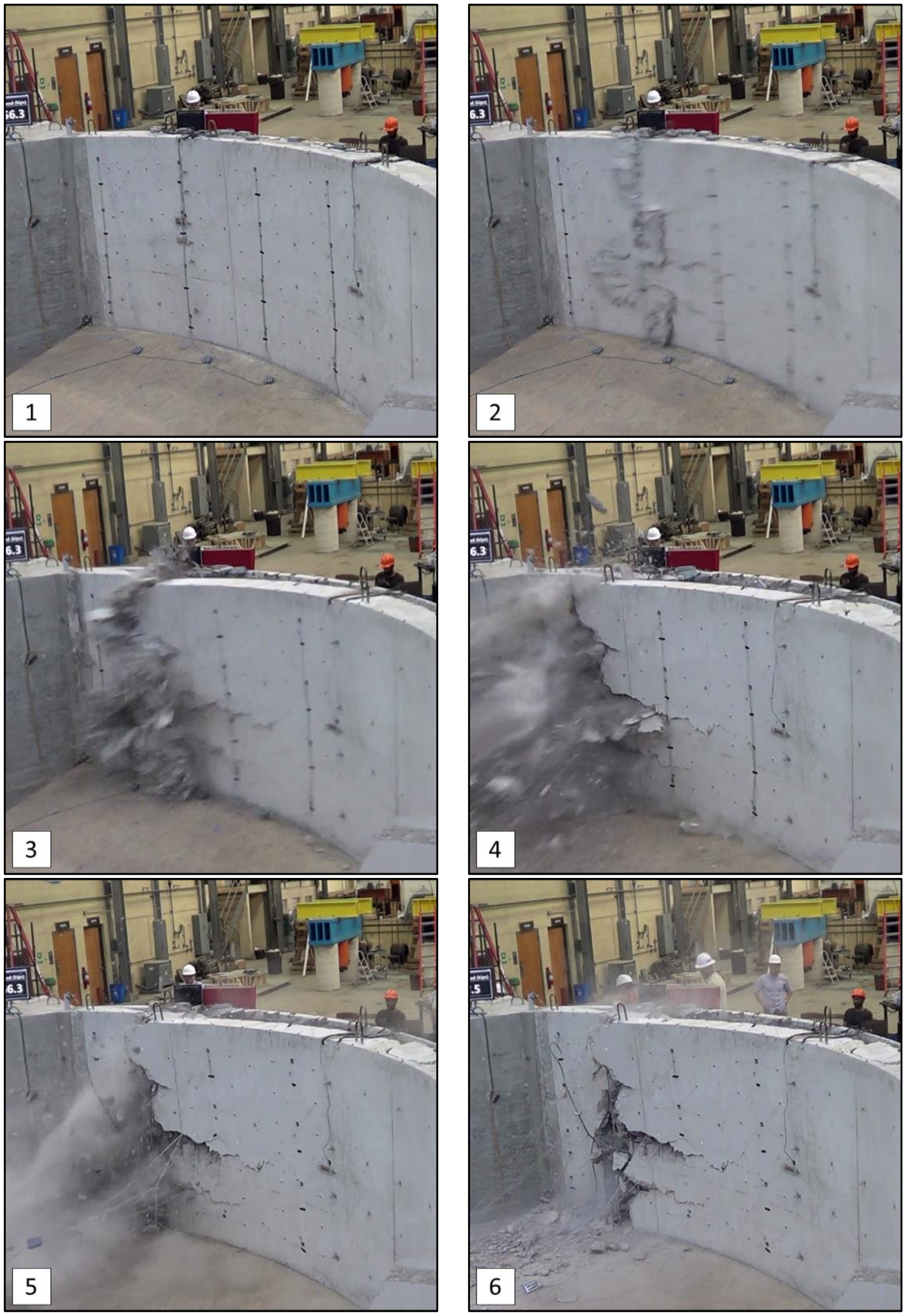

Figure C-4: Snapshots of the Delamination Failure of Specimen 2 at the 15° Location from the Side

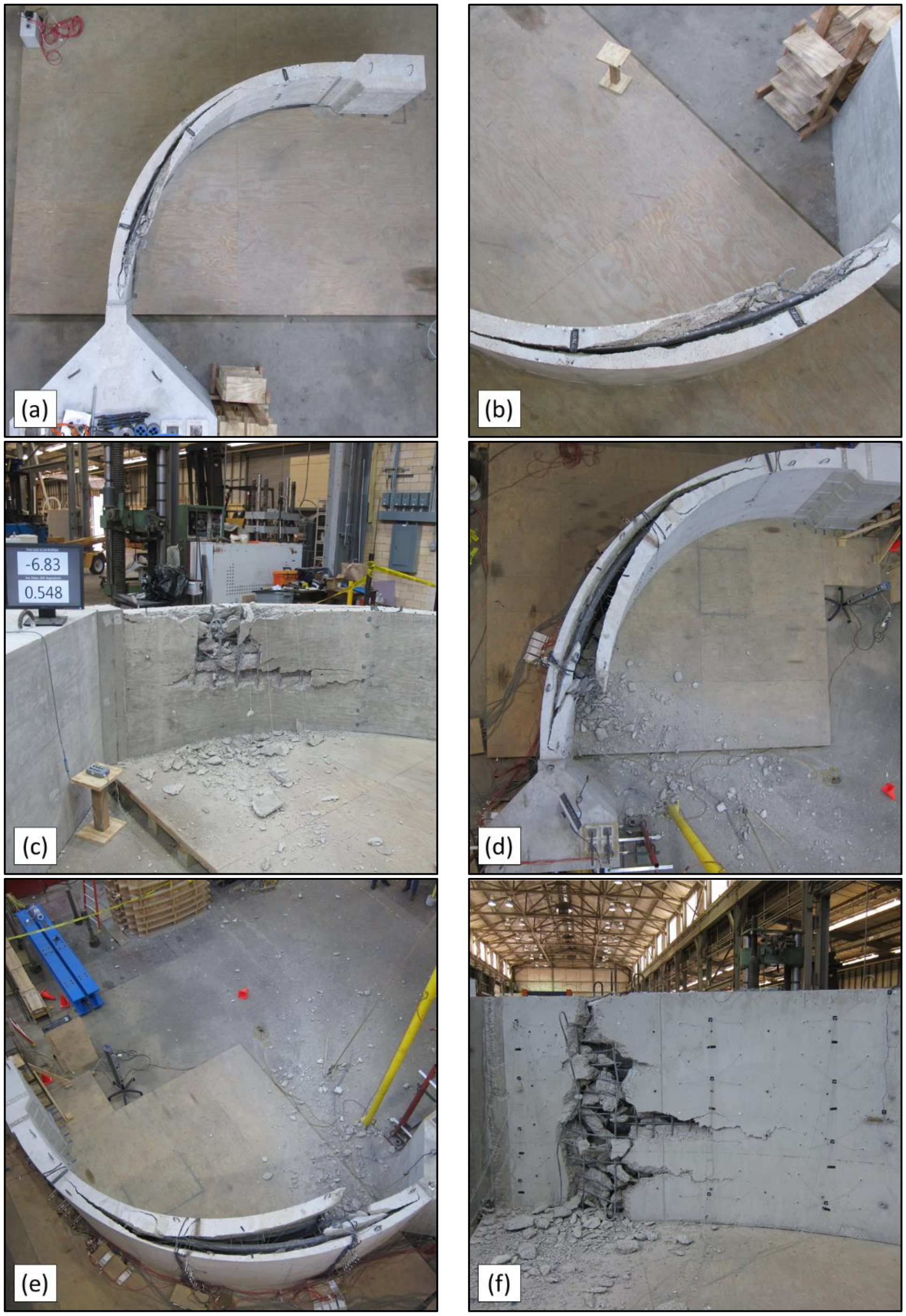

Figure C-5: Images of the Failed Test Specimens Showing: (a) Top of Specimen 1, (b) Back of Specimen 1, (c) Front of Specimen 1, (d) Top of Specimen 2, (e) Back of Specimen 2, (f) Front of Specimen 2

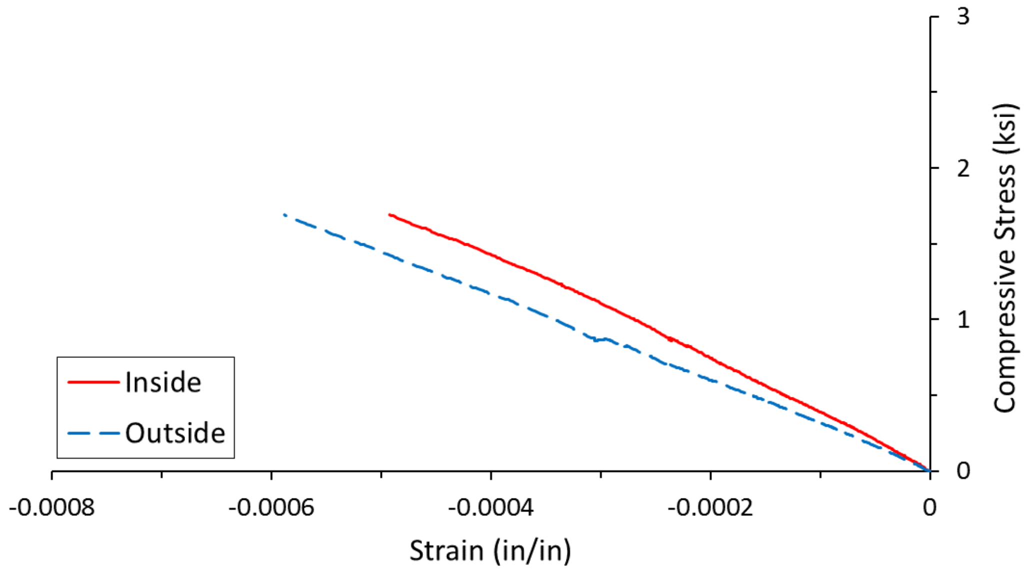

Figure C-6: Compressive Stress versus Average Strain of the Circumferential Rebar at the 45° Location of Specimen 1

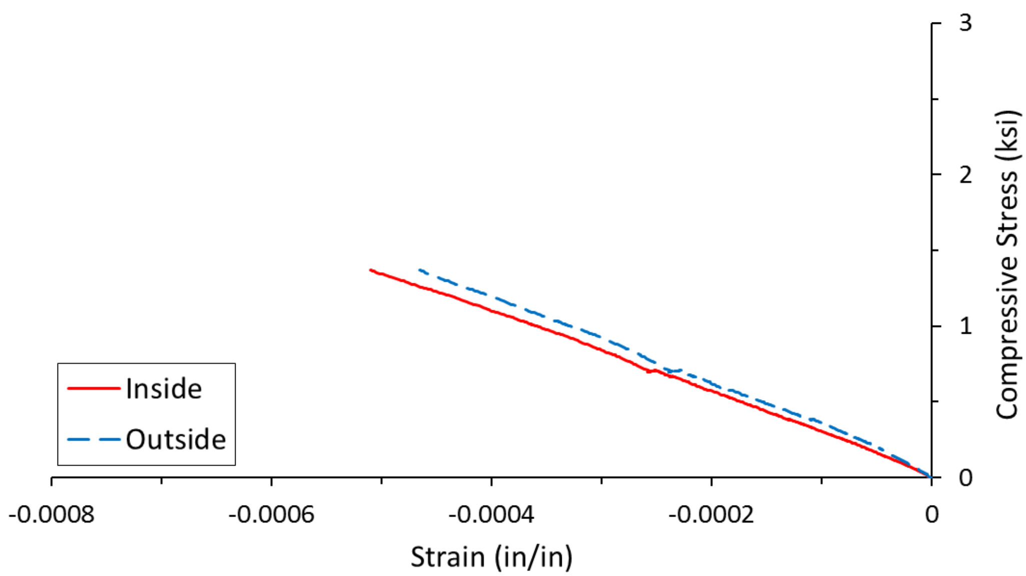

Figure C-7: Compressive Stress versus Average Strain of the Circumferential Rebar at the 75° Location of Specimen 1

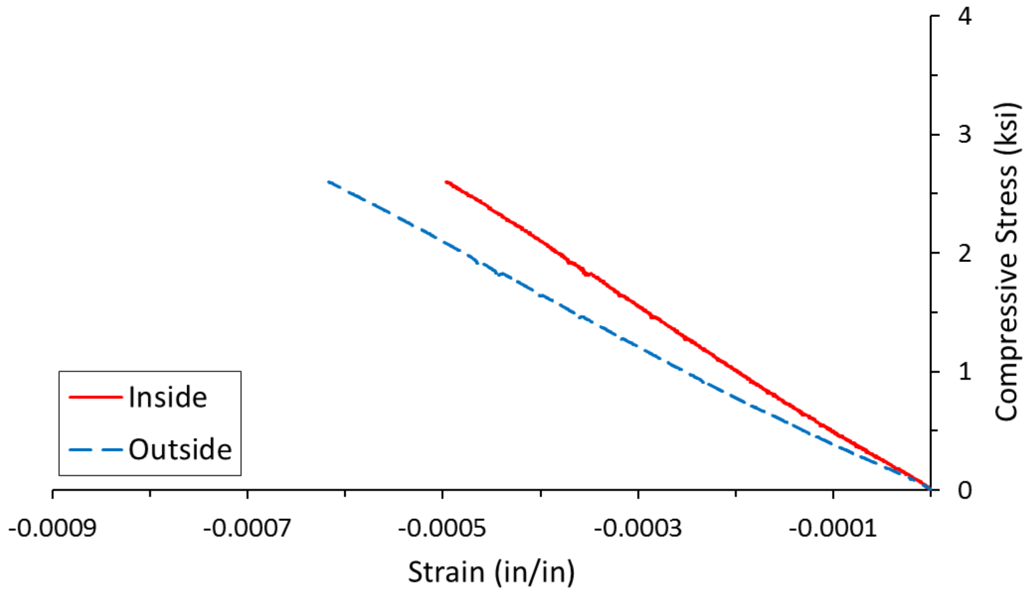

Figure C-8: Compressive Stress versus Average Strain of the Circumferential Rebar at the 45° Location of Specimen 2

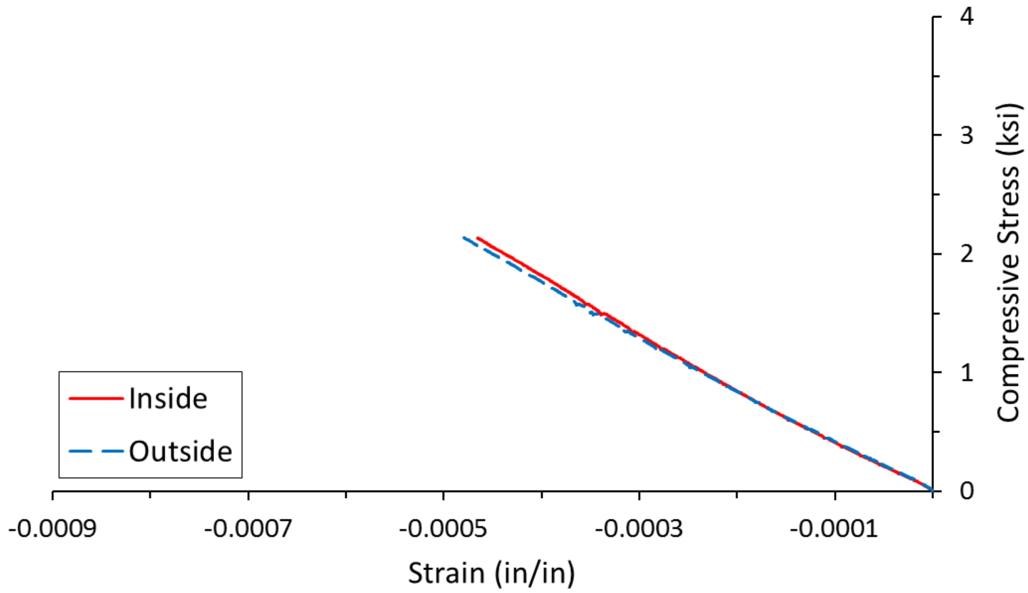

Figure C-9: Compressive Stress versus Average Strain of the Circumferential Rebar at the 75° Location of Specimen 2

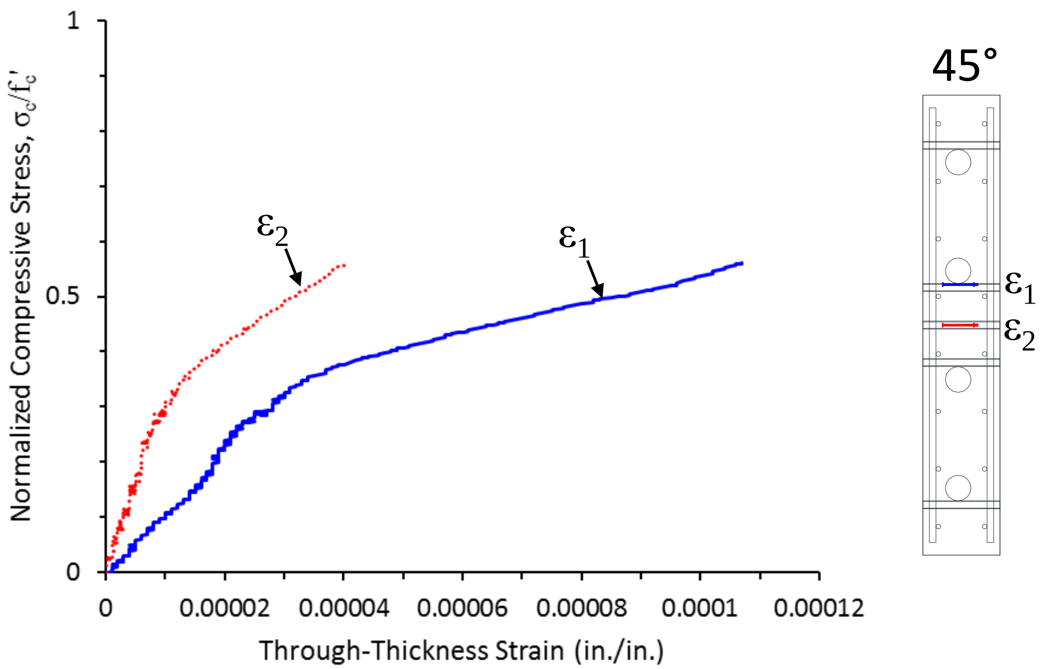

Figure C-10: Through-Thickness Strains versus Normalized Compressive Stresses at the 45° Location of Specimen 1 Measured by Embedded Strain Gauges

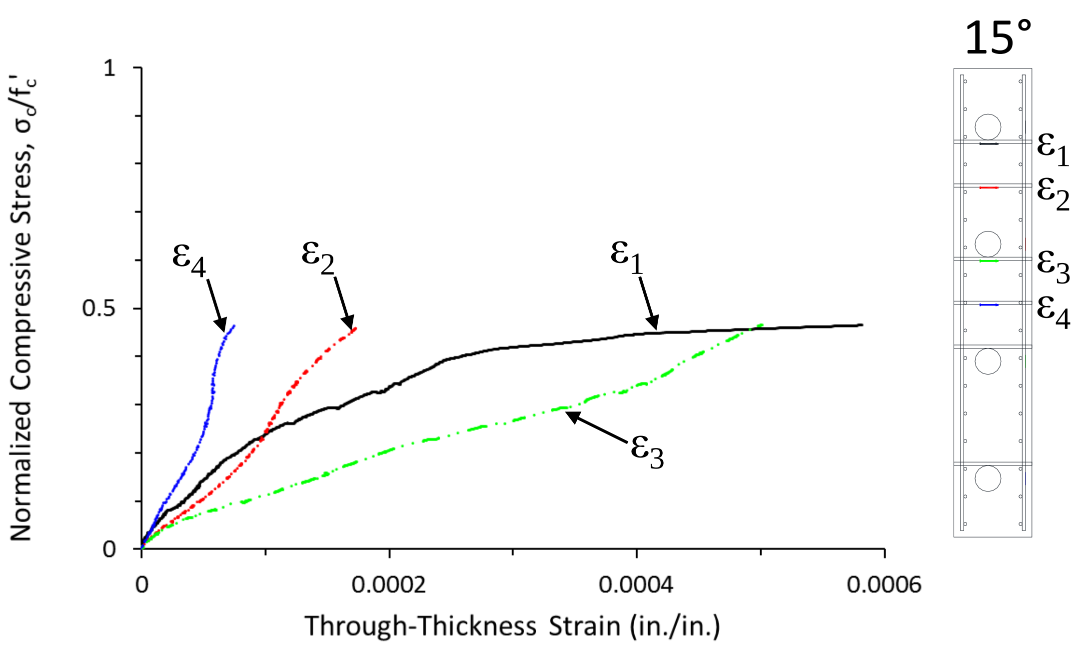

Figure C-11: Through-Thickness Strains versus Normalized Compressive Stresses at the 15° Location of Specimen 2 Measured by Embedded Strain Gauges

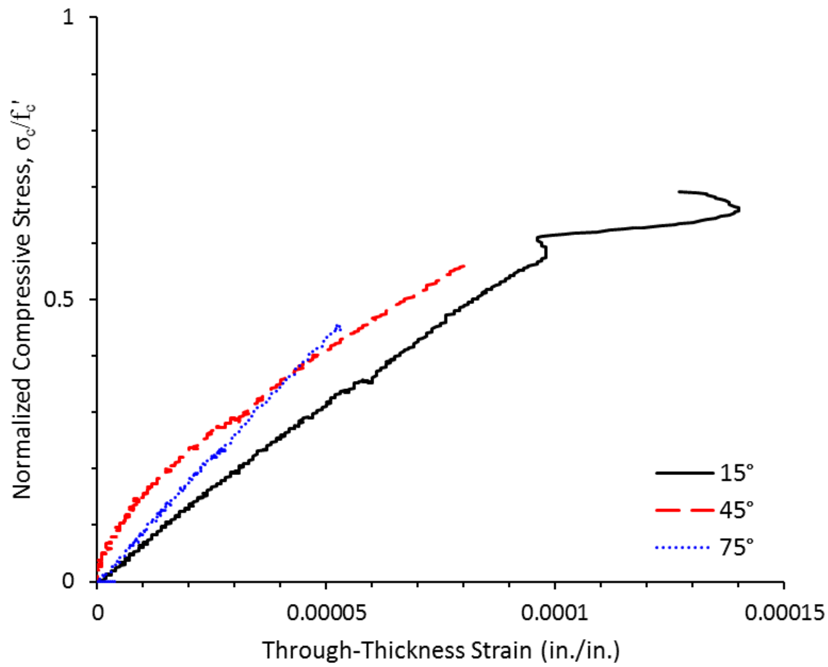

Figure C-12: Top Surface Through-Thickness Strains versus Normalized Compressive Stresses of Specimen 1 Measured by Surface Strain Gauges

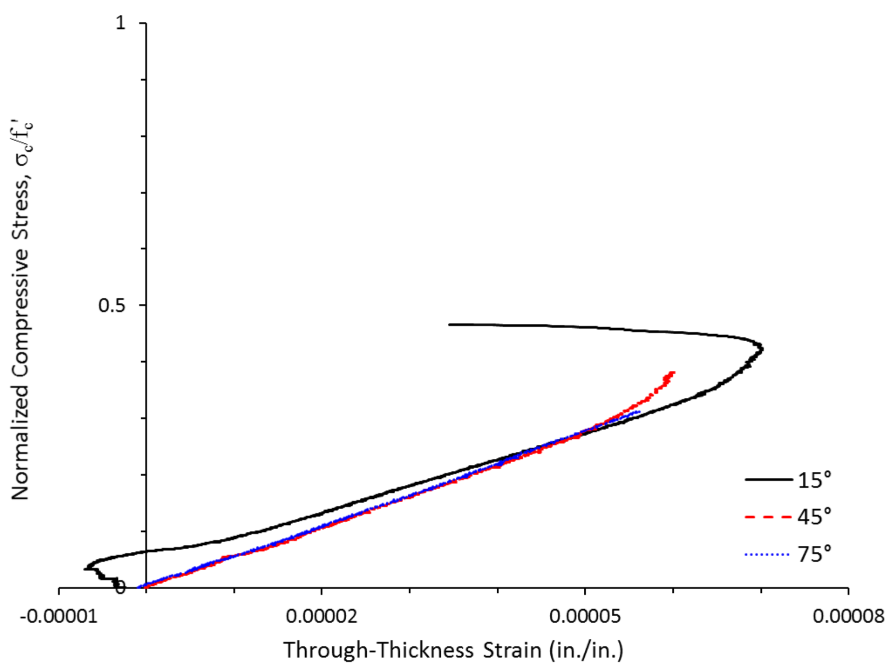

Figure C-13: Average Top Surface Through-Thickness Strains versus Normalized Compressive Stresses of Specimen 2 Measured by Surface Strain Gauges

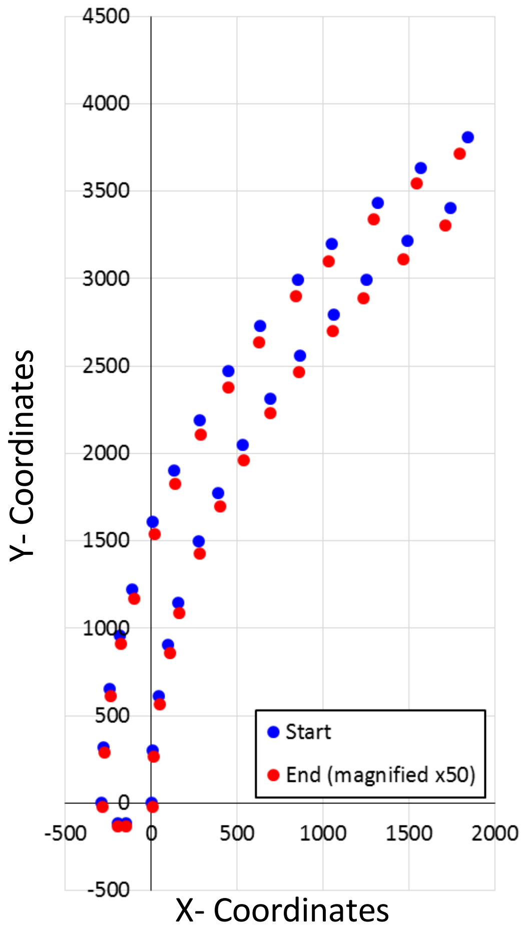

Figure C-14: NDI Optotrak Certus System Data Showing the Global Movement of Specimen 2 from the Top

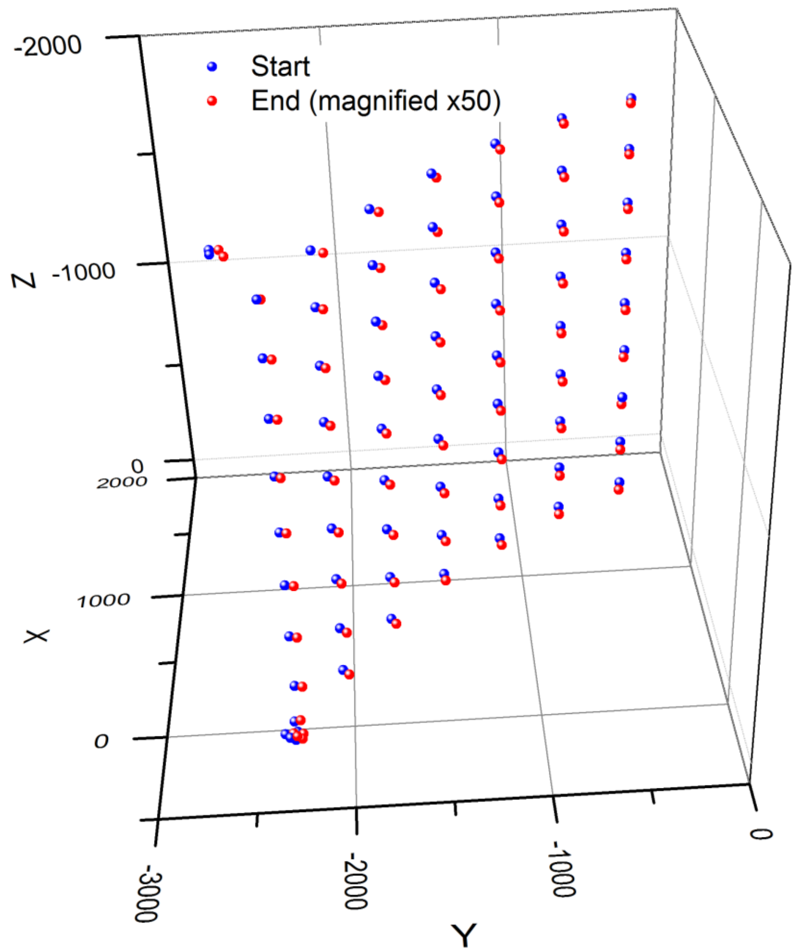

Figure C-15: NDI Optotrak Certus System Data Showing the Global Movement of Specimen 2 from the Side

References

Acharya, Sourav, and Devdas Menon. 2003. "Prediction of Radial Stresses due to Prestressing in PSC Shells." *Nuclear Engineering and Design* 225 (1): 109–25. DOI: 10.1016/S0029-5493(03)00135-3.

ACI Committee 318. 2014. *Building Code Requirements for Structural Concrete (ACI 318-14) and Commentary (ACI 318R-14)*. Farmington Hills, MI: American Concrete Institute.

ACI-ASCE Committee 343. 1995. *Analysis and Design of Reinforced Concrete Bridge Structures (ACI 343R-95)*. Farmington Hills, MI: American Concrete Institute.

ACI-ASCE Committee 359. 2015. *ASME Boiler and Pressure Vessel Code Section III - Rules for Construction of Nuclear Facility Components - Division 2 - Code for Concrete Containments*. New York, NY: ASME International.

Ashar, H., and D. J. Naus. 1983. "Overview of the Use of Prestressed Concrete in US Nuclear Power Plants." *Nuclear Engineering and Design* 75 (3): 425–437.

ASTM A370. 2016. *Standard Test Methods and Definitions for Mechanical Testing of Steel Products*. West Conshohocken, PA: ASTM International.

ASTM A416/A416M. 2016. *Standard Specification for Low-Relaxation, Seven-Wire Steel Strand for Prestressed Concrete*. West Conshohocken, PA: ASTM International.

ASTM A513/A513M. 2015. *Standard Specification for Electric-Resistance-Welded Carbon and Alloy Steel Mechanical Tubing*. West Conshohocken, PA: ASTM International.

ASTM A615/A615M. 2016. *Standard Specification for Deformed and Plain Carbon-Steel Bars for Concrete Reinforcement*. West Conshohocken, PA: ASTM International.

ASTM C39/C39M. 2016. *Standard Test Method for Compressive Strength of Cylindrical Concrete Specimens*. West Conshohocken, PA: ASTM International.

ASTM C78/C78M. 2016. *Standard Test Method for Flexural Strength of Concrete (Using Simple Beam with Third-Point Loading)*. West Conshohocken, PA: ASTM International.

ASTM C469/C469M. 2014. *Standard Test Method for Static Modulus of Elasticity and Poisson's Ratio of Concrete in Compression*. West Conshohocken, PA: ASTM International.

ASTM C496/C496M. 2011. *Standard Test Method for Splitting Tensile Strength of Cylindrical Concrete Specimens*. West Conshohocken, PA: ASTM International.

Bae, Sungjin. 2013. *Radial Tension Induced by Prestressing Forces and Moments*. SMiRT-22. San Francisco, CA: IASMiRT.

Basu, Prabir C., Vijay N. Gupchup, and L. R. Bishnoi. 2001. *Containment Dome Delamination*. SMiRT-16. Washington DC: IASMiRT.

Florida Power and Light Company. 1970. "Containment Dome Report Turkey Point Unit 3." Docket No. 50-250.

Johnston, David West, and ACI Committee 347. 2014. *ACI SP-4: Formwork for Concrete*. 8thed. Farmington Hills, MI: American Concrete Institute.

Moreadith, Frederick L., and Richard E. Pages. 1983. "Delaminated Prestressed Concrete Dome: Investigation and Repair." *Journal of Structural Engineering* 109 (5): 1235–1249.

Penn, Ivan. 2013. "Duke Energy Announces Closing of Crystal River Nuclear Power Plant." *Tampa Bay Times*, February 5. http://www.tampabay.com/news/business/energy/duke-energy-announces-closing-of-crystal-river-nuclear-power-plant/1273794.

Progress Energy. 2010. "Crystal River Unit #3 Containment Investigation and Repair." June 30. http://www.nrc.gov/docs/ML1019/ML101940524.pdf.

Progress Energy. 2011. "Crystal River Nuclear Plant Status Update." June 28. https://www.progress-energy.com/assets/www/docs/company/062811.pdf.

Ragunath, S. S., N. Rajagopalan, and K. Ramamurthy. 2001. *Influence of Prestressing on Radial Stresses in Nuclear Containment Domes*. SMiRT-16. Washington DC: IASMiRT.

Schultz, D.M., J.T. Julien, and H.G. Russell. 1984. "Tension Tests of Concrete Containment Wall Elements." *Nuclear Engineering and Design* 77 (3): 381–91.

Van Landuyt, Dean W. 1991. "The Effect of Duct Arrangement on Breakout of Internal Post-Tensioning Tendons in Horizontally Curved Concrete Box Girder Webs." Master's Thesis, Austin, TX: The University of Texas at Austin.